ANCHOR TENANT APPROACHES IN PROCESS INTEGRATION AND DESIGN

A Dissertation

by

KEVIN JACOB TOPOLSKI

Submitted to the Office of Graduate and Professional Studies of
Texas A&M University
in partial fulfillment of the requirements for the degree of

DOCTOR OF PHILOSOPHY

Chair of Committee,	Mahmoud El-Halwagi
Committee Members,	Fadwa T. Eljack
	Nimir Elbashir
	M. M. Faruque Hasan
Head of Department,	M. Nazmul Karim

May 2019

Major Subject: Chemical Engineering

ABSTRACT

Global chemical demand is growing at a significant rate as it is driven by population growth. This growth entails the increased usage of resources and environmental stress if a business as usual approach is taken. Economic gains and the mitigation of these growth effects could be achieved through the adoption of Eco-Industrial Park (EIP) practices where intermediate and waste streams from one manufacturing plant are exchanged with another. It is of interest to develop methodological approaches to facilitate the design of EIPs that will enable increased production efficiency. A subset class of EIPs, Carbon-Hydrogen-Oxygen SYmbiosis Networks (CHOSYNs), and their design is focused upon. The concept of CHOSYNs leverages the foundation of the hydrocarbon processing industry by utilizing material streams containing carbon, hydrogen and oxygen atoms to create synergies among participating facilities.

It is important to account for the various relationships between the EIP participants when synthesizing a new CHOSYN or retrofitting an existing system. The Anchor-Tenant model is adopted to account for these relationships in the synthesis of CHOSYNs. “Anchors” are first invited as key participants that provide the foundation within the EIP. “Tenants” are potential plants that could be developed and integrated with existing “Anchor(s)” thus creating a genesis of an EIP.

Multiscale optimization approaches are developed to identify and screen the tenants and to determine performance benchmarks for individual plants and for the whole

EIP. An approach is initially developed to synthesize CHOSYNs while considering the material throughputs of the anchors and tenants. Next, this approach is extended to include an additional tenant screening step that considers the transfer of energy between EIP participants. A case study is solved to illustrate the application of these methods.

DEDICATION

To my father who passed away in June 2016.

ACKNOWLEDGEMENTS

I am a firm believer in the statement: “I am not the sole victor of my victories and the sole victim of my defeats”. That being said, I am indebted to a multitude of family, friends and colleagues. This section will thank those whom have had a large impact on my life to date.

To my mother and father, Anne Tommaso and Joseph Topolski, thank you for your support and in shaping how I am today. I thank my step-father, Raymond Hinske, who I have had frequent discussions on research and chemical engineering and who has held me to the professional standard of an ExxonMobil distinguished engineer. My sisters, Sarah and Mackenzie, have and are a great support we all grew up, especially through difficult times.

I am extremely grateful of my advisor, Mahmoud El-Halwagi, for providing me with the privilege to study and develop myself under his tutelage. It is during my stay in his research group where I was able to learn how to perform research and mentor my peers effectively. I will cherish these skills dearly. I would also like to thank those in my committee, Dr. Fadwa Eljack, Dr. Nimir Elbashir, Dr. M. M. Faruque Hasan and Dr. M. Sam Mannan, for their teaching and guidance during the pursuit of my doctorate.

My thanks extend to my friends that I have made while at Texas A&M University. This includes but is not limited to Erfika Edelia, Debalina Sengupta, Cassio Ahumada, Michele Tacchi, Bob Browne, Jon Raftery, Pritishma Lakhe, Pilar Suarez, Edna Mendez,

Luis Camacho, Stefany Angarita and Patrick Lathrop. Having all these people around and more made my experience at graduate school all the more enjoyable.

The recommendations that Dr. Theresa Carvajal, Dr. Bryan Boudouris and Dr. Carl Laird were instrumental for me to be in my current position. It was Dr. Carvajal and Dr. Boudouris who provided me an introduction to academic and materials science research. It was Dr. Laird who kindled my interest in process optimization and graduate research. To these three, I am grateful for having worked with and learned from you. It would be remiss of me not to mention Dr. Stephen Beaudoin, Robert Davis and Linda Davis whom has had interest in my development and would not hesitate to help me if I asked.

Finally, I would like to thank Malcolm Chisholm for being a second father to me in times of distress. He was the one who taught me how to be a better person and later, employed me. I do have good memories working for him where I was driven to continually improve myself with each day, physically and mentally.

CONTRIBUTORS AND FUNDING SOURCES

Contributors

This work was supervised by a thesis committee consisting of Professor El-Halwagi, Professor Hasan and Professor Elbashir of the Texas A&M University Department of Chemical Engineering and Professor Eljack of the Qatar University Department of Chemical Engineering.

The case study of Chapter II was provided by Professor Mahmoud El-Halwagi. The energy stream data associated to the case study in Chapter III was collected by both the student and Marc Panu of the Department of Chemical Engineering. The mathematical model and associated optimization code were provided by Professor Luis Fernando Lira-Barragán and Professor José María Ponce-Ortega of the Universidád Michoacana de San Nicolás de Hidalgo Department of Chemical Engineering.

All other work conducted for the thesis (or) dissertation was completed by the student independently.

Funding Sources

This work was made possible in part by Qatar Foundation under NPRP Grant Number 6-678-2-280. Its contents are solely the responsibility of the authors and do not necessarily represent the official views of the Qatar National Research Fund.

Graduate study also was supported by the Texas A&M University Graduate Teaching Fellowship for Fall 2018.

TABLE OF CONTENTS

Page

LIST OF FIGURES

Page

LIST OF TABLES

Page

1. INTRODUCTION

The challenges that human population growth causes necessitate the need for sustainability in future development. Such challenges include but are not limited to: an increasing lack of natural resources, increased pollution and a continuing drive for economic prosperity. Unfortunately, the aforementioned challenges are not mutually attainable and so sustainable development that provides a balance in meeting these challenges are favorable. Sustainable development is defined as "development that meets the needs of the present without compromising the ability of future generations to meet their own needs" (Brundtland, 1987). As this pertains to the manufacturing industry, future development should be resource efficient, minimally polluting and maintain positive economic growth. Industrial Symbiosis and its physical manifestation, Eco-Industrial Parks (EIPs), are seen as a means to achieve sustainable development in manufacturing (Doyle et. al, 1996).

Industrial Symbiosis is defined as the engagement of "traditionally separate entities in a collective approach to competitive advantage by the involving physical exchange of materials, energy, water, and by-products" (Chertow, 2000). The benefits entailed by the adopting Industrial Symbiosis and in turn, constructing EIPs are the economic and environmental gains from utilizing a byproduct and/or waste from one plant as a raw material for another. Whereas these benefits attracted interest in the formation of EIPs, attempts in the planned synthesis of EIPs have not been successful. A key difficulty in the planned synthesis of EIPs is cited as the scale and complexity involved with creating economic exchanges between EIP participants (Gibbs and Deutz, 2005). Despite this,

multiple examples of EIPs have been identified around the world and have developed spontaneously (Gibbs and Deutz, 2007), (Chertow and Ehrenfeld, 2012). Several qualitative approaches for synthesis of EIPs was identified by Chertow and Ehrenfeld (2012), of which include the Anchor Tenant model. A successful approach for the planned synthesis of EIPs is one that captures the synergistic and competitive interactions between EIP participants. The significance of this study is the proposition of several approaches for the grassroot synthesis of Carbon-Hydrogen-Oxygen Symbiosis Networks (CHOSYNs), a subset of EIPs within the hydrocarbon industry that are based on the exchange of material streams containing Carbon, Hydrogen and Oxygen atoms (Noureldin and El-Halwagi, 2015).

Chapter II introduces an approach inspired by the Anchor Tenant model for the grassroots synthesis of CHOSYNs. The Anchor Tenant model defines existing, "first-to-build" or foundational plants as Anchors whereas the plants invited for construction and integration are termed as Tenants. This approach decomposes the EIP synthesis task into several mass integration targeting techniques to screen ideal Tenants to complement the Anchors. The application of these techniques highlights significant interactions between different CHOSYN participants while utilizing fundamental chemical processing information.

Chapter III extends upon the approach introduced by Chapter II by including interaction between CHOSYN participants through the exchange of energy streams. This extension accounts for enhanced energy integration opportunities by determining ideal streams to reserve upon the Tenant heat integration for the latter EIP energy integration.

The application of this extended approach highlights how different EIP participants may benefit from different aspects of the proposed approach. This indicates how Tenants that rely heavily on energy for operation might be precluded from screening for invitation.

1.1. References

Brundtland, G. (1987). Our common future: Report of the 1987 World Commission on Environment and Development. United Nations, Oslo, 1, 59.

Chertow, M. R. (2000). Industrial symbiosis: literature and taxonomy. Annual review of energy and the environment, 25(1), 313-337.

Chertow, M., & Ehrenfeld, J. (2012). Organizing Self-Organizing Systems. Journal of Industrial Ecology, 16(1), 13-27.

Doyle, B., Lowe, E. A., Moran, S. R., & Holmes, D. B. (1996). Fieldbook for the Development of Eco-Industrial Parks.

Gibbs, D., & Deutz, P. (2005). Implementing industrial ecology? Planning for eco-industrial parks in the USA. Geoforum, 36, 452-464. doi:10.1016/j.geoforum.2004.07.009

Gibbs, D., & Deutz, P. (2007). Reflections on implementing industrial ecology through eco-industrial park development. Journal of Cleaner Production, 15, 1683-1695. doi:10.1016/j.jclepro.2007.02.003

Noureldin, M. M., & El-Halwagi, M. M. (2015). Synthesis of C-H-O Symbiosis Networks. AIChE Journal, 61(4), 1242-1262.

2. AN ANCHOR-TENANT APPROACH TO THE SYNTHESIS OF CARBON-HYDROGEN-OXYGEN SYMBIOSIS NETWORKS*

2.1. Introduction

Industrial symbiosis is aimed at enhancing the competitive advantage of multiple industrial facilities through synergistic integration of mass, energy, information, and services (Chertow, 2000). An effective implementation for industrial symbiosis is through the establishment of eco-industrial parks (EIPs). An EIP is a special type of an economic zone in which multiple industries, businesses, and services are integrated to facilitate exchange of materials (e.g., intermediates, byproducts, water, and wastes) and energy with the objective of creating synergistic opportunities and enhancing the overall economic and environmental performance of the participating entities and the impacted communities. The benefits of developing EIPs include reduced raw material input while maintaining product output, reduced environmental consequences and reduced capital expenses by sharing unit processes (Lowe, 2001). Multiple examples of EIPs can be found around the world including those of public and private enterprises (Gibbs and Duetz, 2007).

Process systems engineering approaches have been proposed for the design of EIPs. A source-sink framework was proposed by Spriggs et al. (2004) to enable mass integration among multiple plants using the material-recovery pinch analysis developed by El-Halwagi et al. (2003). Optimization approaches for water integration in an EIP were

developed to enhance water conservation and cost effectiveness (e.g., Chew et al., 2008; Lovelady and El-Halwagi, 2009; Bandyopadhyay et al., 2010; Aviso et al., 2011; Rubio-Castro et al., 2012; Bishnu et al., 2014; López-Díaz et al., 20115; Alnouri et al., 2016). Integration frameworks were also proposed for the synthesis of EIPs handling hydrocarbons such as syngas, fuel gas, and carbon dioxide (e.g., Hasan et al., 2011; Roddy, 2013; Kantor et al., 2015; Al-Mohannadi and Linke, 2016). A survey of literature on optimization of EIPs was reported by Boix et al. (2015).

Recently, a multiscale mass integration approach was introduced by Noureldin and El-Halwagi (2015) to synthesize carbon-hydrogen-oxygen symbiosis networks (CHOSYN). According to this approach, atomic-based targets can be set for the integration of multiple plants within an EIP. Next, multi-scale optimization can be used to attain the targets and to detail the design of the integrated infrastructure and connections for streams, species, and units. A shortcut targeting approach utilizing fundamental atomic and stoichiometric information for the development of CHOSYN soon followed (El-Halwagi, 2017). The developed techniques for the targeting, design, and optimization of CHOSYNs have focused on the retrofitting of a cluster of adjacent plants, industrial city, or an EIP with the purpose of integrating a set of existing plants. Most of the EIPs have grown organically through a "bottom-up" approach whereby individual opportunities have been retrospectively identified for existing plants. Although such approaches have yielded clear benefits, a more profound impact can be achieved if industrial symbiosis is incorporated in the design of new parks and industrial cities involving multiple processing facilities. This is particularly true for the construction of massive infrastructures that are

associated with abundant supplies of certain feedstocks. For instance, with the recent discovery and production of substantial quantities of shale gas, significant infrastructures are being established (e.g., Al-Douri et al., 2017; Hasaneen and El-Halwagi, 2017; Marano et al., 2015; Siirola, 2014). In such cases, a grass-root approach is needed to deliberately construct a well-integrated EIP. First, a limited number of principal plants (referred to as "anchors") are invited based on feedstock availability, product demands, market suitability, and regional benefits. The rest of the EIP is to be populated by supporting plants (referred to as "tenants") that can create synergistic opportunities with the anchors and with other tenants and the region.

The purpose of this work is to develop a systematic approach for the targeting, design, and integration of grass-root EIPs with known anchors but unknown tenants. A multi-scale atomic based framework is developed to answer the following key questions:

- Which tenants should be invited to participate in the EIP? What is the type and size of each tenant?
- What new infrastructure is to be constructed to induce industrial symbiosis?
- How should the feedstocks, byproducts, products, and wastes be integrated?
- How to reconcile the conflicting objectives of the multiple plants?
- How to include collective constraints on available resources and permitted waste discharges?

In this work, a multi-scale systems approach is proposed. First, preliminary targeting techniques are introduced for the selection of tenant plants based on fundamental atomic, stoichiometric, and economic information. The intention is to discard tenant plants that exhibit unfavorable results before more detailed modeling is carried out. Next, a superstructure formulation is developed to account for the various potentials configurations integrating the participating plants and the newly added infrastructure. A case study that demonstrates the approach is described and accompanied with a discussion of the results.

2.2. Problem Statement

The problem of developing a grass-root CHOSYN may be stated as follows. Given is a set $ANCHORS = \{r \mid r = 1,2,..., N_{anchors}\}$ of anchor plants to be installed in EIP. Given also is a set $SOURCES = \{i \mid i = 1,2,..., N_{source}\}$ which defines inlet streams to be integrated into the industrial park expansion. This set is divided into subsets for external, anchor byproduct and anchor waste streams. The subset $EXTERNAL\_SOURCE = \{i \mid i = 1,2,..., N_{external}\}$ represents external feedstock streams that are available for purchase. The subset $ANCHOR\_BYPRODUCTS = \{i \mid i = N_{external+1}, N_{external+2},..., N_{byproducts}\}$ consists of byproducts and other exchangeable streams coming from anchor plants. These streams have monetary value that is based on heating value and/or market prices. The subset $ANCHOR\_WASTES = \{i \mid i = N_{byproducts+1}, N_{byproducts+2},..., N_{source}\}$ is comprised of waste streams from the anchor plants (e.g., wastewater, gaseous emissions, solids) that can be

given away freely or can be acquired on a discounted cost (positive or negative) for utilization or effluent treatment. Each source i is described with a flowrate F_i^{Source}, temperature T_i^{Source}, pressure P_i^{Source} and composition $x_{i,c}$. The streams contain various chemical species specified by the set $COMPONENT = \{c|c = 1, 2, \dots, N_{component}\}$. In turn, these chemical species are composed of atoms which are represented with the set $ATOM = \{a|a = 1, 2, \dots, N_{atom}\}$.

The set $TENANT = \{k|k = 1, 2, \dots, N_{tenant}\}$ represents facilities, termed as prospective tenant plants, to be considered for possible addition to the EIP. Each candidate tenant k has process inlets and outlets given by the sets $TENANT\ INLET_k = \{v_k^{in}|v_k^{in} = 1, 2, \dots, N_{Sink\ Inlet,k}\}$ and $TENANT\ OUTLETS_k = \{v_k^{out}|v_k^{out} = 1, 2, \dots, N_{Sink\ Outlet,k}\}$, respectively. Distinction is made for the tenant outlet emitting product streams and recyclable streams which are respectively represented by the subsets: $PRODUCT_k = \left[v_k^{out}\middle|v_k^{out} = 1, 2, \dots, N_{Product,k}\right]$ and $RECYCLE_k = \{v_k^{out}|v_k^{out} = N_{Product,k} + 1, N_{Product,k} + 2, \dots, N_{Recycle,k}\}$.

The shared unit operations and processes that exchange, separate, mix, split and chemically convert material streams constitute the set $INTERCEPTOR = \{j|j = 1, 2, \dots, N_{Inteceptors}\}$. Similar to tenants, each interceptor j possesses inlets and outlets which are respectively represented by the sets $INTERCEPTOR\ INLET_j = \{u_j^{in}|u_j^{in} = 1, 2, \dots, N_{Interceptor\ Inlets,j}\}$ and $INTERCEPTOR\ OUTLET_j = \{u_j^{out}|u_j^{out} = 1, 2, \dots, N_{Interceptor\ Outlets,j}\}$.

The aim of the design task is to develop a systematic approach for the multi-scale targeting, integration, and optimization of the grassroots EIP. The specific outcomes of the approach involve the screening and selection of the types and sizes of the tenants, conceptual design of the infrastructure to be added, integration of streams, species, and units among the available feedstocks, byproducts, products, and wastes from the anchors and tenants, the surrounding environment, and relevant markets.

2.3. Synthesis Approach

As shown by Figure 2.1, a source-interceptor-sink framework is utilized as a basis superstructure for integrating tenants with anchors. The sources include the external feedstocks as well as the byproducts, products, and wastes from the anchor plants. The interceptors refer to physical and chemical units that conditions the streams prior to integration. These include compressors, pumps, heat exchangers, separators, reactors, etc. Their selection and sizing are yet to be determined. The tenants include the candidate plants that are considered for integration into the EIP. Again, their types and sizes are to be determined through optimization. The streams leaving the tenants are given the options of exiting the EIP in the form of products or terminal wastes or being recycled to be further integrated with the rest of the EIP. The potentially recyclable streams are represented through a set $RECYCLE_k = \{v_k^{out} | v_k^{out} = N_{Product,k} + 1, N_{Product,k} + 2, \dots, N_{Recycle,k}\}$.

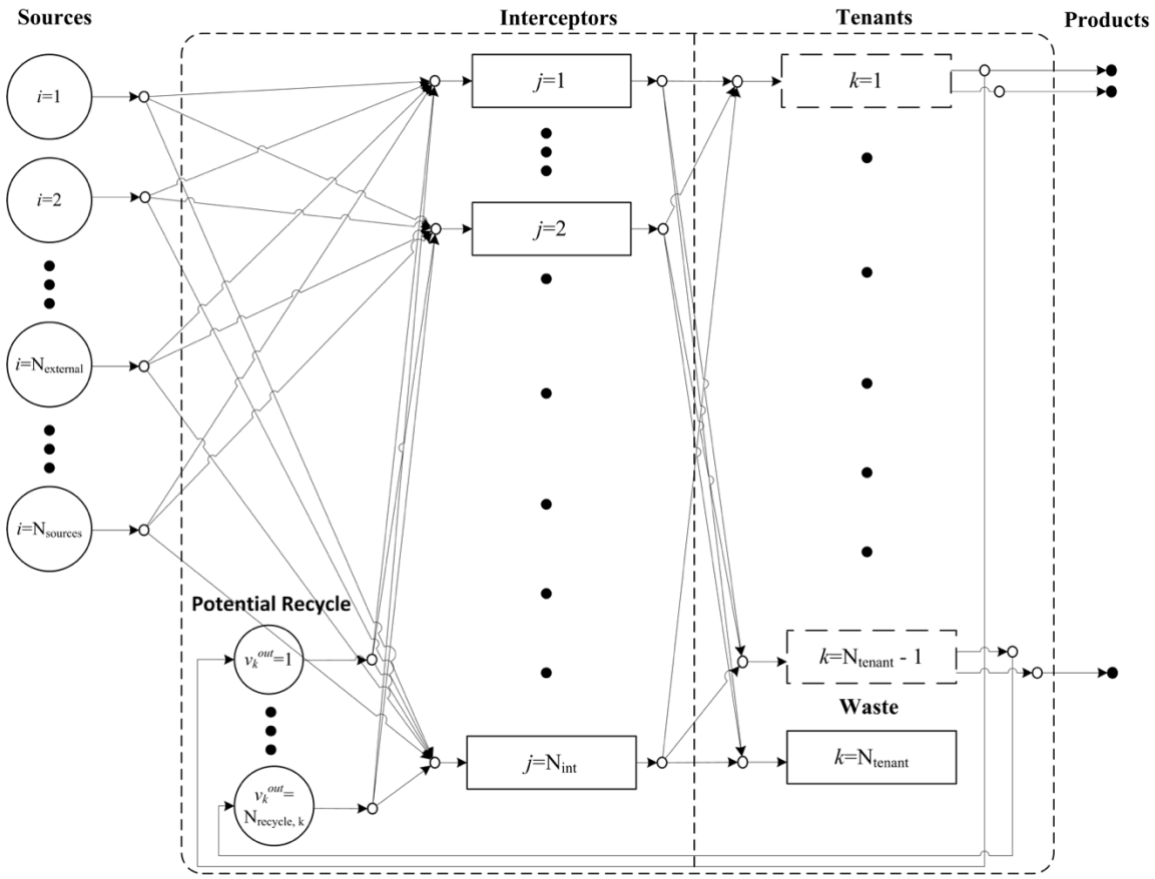

Figure 2.1: A Source-Interceptor-Sink Framework for the Anchor-Tenant Approach

Streams emitted by anchor plants as byproducts and wastes as well as raw material streams are termed as sources. These sources are split and allocated accordingly to interceptors. Interceptors are unit operations or processes that can modify material streams so that they meet the inlet requirements of a tenant or another interceptor. The sinks in the source-interceptor-sink framework represent the tenants and waste facilities. This framework is modified such that the sinks representing the tenant plants can receive streams as well as emit streams that may be sold for profit or recycled internally within the CHOSYN.

The proposed formulation details a process synthesis framework to represent many feasible configurations of the added facilities and integration network. It is of interest to consider a large collection of technologies as tenants to determine quality network configurations. However, this leads to significant expenses in modeling and difficulties in solving the formulated optimization problem. To mitigate these challenges, it is proposed that screening targeting steps are first undertaken to exclude suboptimal network configurations prior to the detailed modelling for the superstructure. The steps of the proposed approach are described in the following sections along with the generic superstructure formulation.

2.3.1. Superstructure Formulation

The following are constraints that define the material stream allocation, the performance of the interceptors and the throughputs of the tenants.

Mole Balance over Source Streams. Each interceptor, j, possesses a set of inlet ports and outlet ports which are identified by the respective indices, u_j^{in} and u_j^{out}. Each source, i, is divided into streams directed to each interceptor inlet port, u_j^{in}. The flowrates of these streams are termed $F_{i,u_j^{in}}^{Split}$. The mole balance for source splitting stated as

$$F_i^{source} = \sum_j \sum_{u_j^{in}} F_{i,u_j^{in}}^{Split} \qquad \forall i \tag{1}$$

Overall and Component Balances over Interceptor Inlet Ports. Each interceptor port u_j^{in} receives a stream that is aggregate of source stream fractions and tenant recycle streams. designated for recycle. The mole and component balances are given

$$W_{u_j^{in}}^{In} = \sum_i F_{i,u_j^{in}}^{Split} + \sum_k \sum_{v_k^{out}} F_{v_k^{out},u_j^{in}}^{Recycle} \qquad \forall j, \forall u_j^{in} \tag{2}$$

$$W_{u_j^{in}}^{in} y_{u_j^{in},c}^{In} = \sum_i F_{i,u_j^{in}}^{Split} x_{i,c} + \sum_k \sum_{v_k^{out} \in Recycle_k} F_{v_k^{out},u_j^{in}}^{Recycle} z_{v_k^{out},c}^{Out} \qquad \forall c, \forall j, \forall u_j^{in} \quad (3)$$

where $W_{u_j^{in}}^{in}$ and $y_{u_j^{in},c}^{In}$ represent the inlet flowrate and the cth mole fraction of the stream inputted to port u_j^{in}. $F_{v_k^{out},u_j^{in}}^{Recycle}$ and $z_{v_k^{out},c}^{Out}$ represent the recycle stream flowrate connecting tenant outlet port v_k^{out} to interceptor inlet port u_j^{in} and the cth mole fraction of the stream emitted by port v_k^{out}.

Interceptor Unit Modeling Equations and Constraints. The model for interceptor unit j is described by the vector set of equations, Φ_j, which is given as

$$\Phi_j \left(W_{u_j^{out}}^{out}, y_{u_j^{out},c}^{out}, W_{u_j^{in}}^{in}, y_{u_j^{in},c}^{In}, D_j^{int}, O_j^{int}, S_j^{int} \right) = 0 \qquad \forall j \quad (4)$$

where $W_{u_j^{out}}^{out}$ and $y_{u_j^{out},c}^{out}$ are the flowrate and cth mole fraction of the stream outlet port u_j^{out}. Also included are D_j^{int}, O_j^{int} and S_j^{int} which are variables that represent the design, operation and state of interceptor j, respectively. Φ_j is subject to a vector set of inequalities, Ξ_j, represent technology constraints of interceptor j. This follows as

$$\Xi_j(W_{u_j^{out}}^{out}, y_{u_j^{out},c}^{out}, W_{u_j^{in}}^{in}, y_{u_j^{in},c}^{In}, D_j^{int}, O_j^{int}, S_j^{int}) \geq 0 \quad \forall j \quad (5)$$

These modeling equation and constraints are presented generally as functions of design, operation, state, inlet streams and outlet stream variables. This is to highlight the flexibility in the level of detail provided by the modelling. These models might be based on fundamental relationships, empirical correlations or equations established by representative data. The flexibility in modeling allows for the use of the formulation to provide practical integration network designs with the appropriate level of detail.

Mole Balance over Interceptor Outlet Ports. The streams exiting each interceptor outlet u_j^{out} is fragmented into streams that are directed to each tenant inlet port, v_k^{in}. The flowrates of these fragment streams are termed as $H_{u_j^{out},v_k^{in}}^{Split}$. The mole balance over the outlet port is given

$$W_{u_j^{out}}^{out} = \sum_k \sum_{v_k^{in}} H_{u_j^{out},v_k^{in}}^{Split} \qquad \forall j, \forall u_j^{out} \tag{6}$$

Mole and Component Balances over Tenant Inlet Ports. The mole and component balances over the tenant inlet ports are given as follows

$$H_{v_k^{in}}^{in} = \sum_j \sum_{u_j^{out}} H_{u_j^{out},v_k^{in}}^{Split} \qquad \forall k, \forall v_k^{in} \tag{7}$$

$$H_{v_k^{in}}^{in} z_{v_k^{in},c}^{in} = \sum_j \sum_{u_j^{out}} H_{u_j{}^{out},v_k^{in}}^{Split} y_{u_j^{out},c}^{out} \qquad \forall k, \forall v_k^{in}, \forall c \tag{8}$$

where $H_{v_k^{in}}^{in}$ and $z_{v_k^{in},c}^{in}$ represent the flowrate and the cth mole fraction of the stream entering port v_k^{in}.

Tenant Unit Modeling Equations and Constraints. The modeling of tenant k is given by the vector set of equations Ψ_k. This is provided as

$$\Psi_k \left(H_{v_k^{out}}^{out}, z_{v_k^{out},c}^{out}, H_{v_k^{in}}^{in}, z_{v_k^{in},c}^{in}, D_k^{Tenant}, O_k^{Tenant}, S_k^{Tenant} \right) = 0 \qquad \forall k \tag{9}$$

where $H_{v_k^{out}}^{out}$ and $z_{v_k^{out},c}^{out}$ represent the flowrate and the cth mole fraction of the stream exiting tenant outlet port v_k^{out}. The D_k^{Tenant}, O_k^{Tenant} and S_k^{Tenant} variables represent the design, operation and state of tenant k, respectively. The tenant modeling also includes constraints on the design and operation of tenant k. The constraints tenant k are provided by the vector set Ω_k which is described as

$$\Omega_k \left(H_{v_k^{out}}^{out}, z_{v_k^{out},c}^{out}, H_{v_k^{in}}^{in}, z_{v_k^{in},c}^{in}, D_k^{Tenant}, O_k^{Tenant}, S_k^{Tenant} \right) \geq 0 \qquad \forall k \tag{10}$$

Mole Balance over Tenant Outlet Ports for Recycle. The streams emitted by tenant outlet ports in the set $Recycle_k$ can be further utilized within the integration network. These streams are split into streams directed to the interceptors. This is represented below

$$H_{v_k^{out}}^{out} = \sum_j \sum_{u_j^{in}} F_{v_k^{out},u_j^{in}}^{Recycle} \qquad \forall k, \forall v_k^{out} \in Recycle_k \tag{11}$$

Equations 1-11 are subject to optimization in accordance to what objective is being pursued. Such possible objectives could include the minimization of emissions, maximization of profit, or the minimization of external source usage. The solution to the superstructure formulation provides a network topography that incorporates selected tenant plants with anchor plants, provides technical details for modifying material streams from plant to plant and gives preliminary profit and cost estimates for implementing the network with plant additions.

It should be emphasized that this formulation may be utilized in multiple industrial symbiosis scenarios. As described before, this formulation is developed to determine and integrate additional plants into an EIP. This formulation is also applicable to the formation of industrial parks as well as simultaneous formation and expansion of industrial parks. This highlights the flexibility of this approach for various aspects of EIP development.

2.4. Preliminary Screening Using Targeting Techniques

The consideration of numerous alternatives of candidate tenants in the superstructure formulation can lead into difficulties in optimization and a significant effort in modeling. It is attractive to develop shortcut targeting techniques to screen out poorly

matched tenants for the park expansion by using fundamental system information. The use of targeting techniques also leads to insights to determine whether the results from screening warrant further design and analysis.

The proposed targeting technique determines promising products to manufacture while considering simple cost data, overall atomic balances, feedstocks and reactions. At this stage of screening, capital investment and non-feedstock operating costs are not considered. Tenants that fail to generate a positive gross margin (the difference between sales and cost of raw materials) are excluded from further analysis. Furthermore, tenants with highest gross margins are prioritized for subsequent and detailed optimization.

The problem addressed by this technique is posed as follows: given are a set of candidate feedstocks and a set of possible products, develop an initial target for the selection of products, raw materials and reaction. The previously defined components that are identified as salable products make a subset of $COMPONENT$ titled $PRODUCT = \left[c \middle| c = 1, 2, \dots, N_{product}\right]$. Also given are a set of reactions that are available for service that convert component c to component c'. This set labeled as $REACTION = \{r | r = 1, 2, \dots, N_{reaction}\}$. These reactions provide the fundamental basis for the tenant plants chosen in this approach.

The component flowrates entering the park expansion system, termed as $F_c^{Source\ Component}$, are given as

$$F_c^{Source\ Component} = \sum_i F_i^{Source} x_{i,c} \quad \forall c \tag{12}$$

The moles of atom a entering the system are termed as $Atom_a^{Source}$. The amount to atoms entering the park expansion system are accounted for with the following relation

$$Atom_a^{Source} = \sum_c Atom\ Set_{c,a} F_c^{Source\ Component} \quad \forall a \tag{13}$$

where the parameter $Atom\ Set_{c,a}$ is quantity of atoms a in component c.

The moles of atom a exiting the system as products or unutilized byproducts, respectively termed as $Atom_a^{Demand}$ and $Atom_a^{Leftover}$, are accounted for with the component flowrates for the products and byproducts exiting the park expansion system, represented by $F_c^{Product}$ and $F_c^{Unutilized}$. This is given

$$Atom_a^{Demand} = \sum_{c \in PRODUCT} Atom\ Set_{c,a} F_c^{Product} \quad \forall a \tag{14}$$

$$Atom_a^{Leftover} = \sum_c Atom\ Set_{c,a} F_c^{Unutilized} \quad \forall a \tag{15}$$

The defined system is subject to the conservation of atoms. This is provided as

$$Atom_a^{Source} - Atom_a^{Demand} - Atom_a^{Leftover} = 0 \quad \forall a \tag{16}$$

It is of interest to determine the overall change of moles of c to develop an overall reaction formula in the park expansion system. The overall change of component c is identified as an overall stoichiometric coefficient, termed as Θ_c. A negative value for this variable represents component c consumed as a reactant in the overall reaction. Conversely, a positive value represents component c created as a product. This is represented

$$F_c^{Product} + F_c^{Unutilized} - F_c^{Source\ Component} = \Theta_c \quad \forall c \tag{17}$$

The overall reaction is the sum of previously defined reactions as shown below

$$\Theta_c = \sum_r \alpha_{r,c} \xi_r \qquad \forall c \tag{18}$$

where ξ_r and $\alpha_{r,c}$ represents the extent of reaction of r and the stoichiometric coefficient associated to reaction r with component c.

The flowrate of the source stream i is bounded by an upper limit on supply, termed as F_i^{Supply}. This is given

$$F_i^{Source} \leq F_i^{Supply} \quad \forall i \tag{19}$$

The component flowrate of c created as a salable product is also constrained by the upper limit given for market demands, termed as F_c^{Demand}. This is provided as

$$F_c^{Product} \leq F_c^{Demand} \quad \forall c \in PRODUCT \tag{20}$$

Equations (12) to (20) are used in the product targeting technique along with a defined objective function. Possible objective functions for this formulation include the maximizing the sales margin (difference between sales and feedstock cost), minimizing waste, or minimizing fresh feedstock usage.

2.5. A Simplified Superstructure with Species Sorting-Reaction Stages

Another proposed approach is to simplify the aforementioned superstructure by considering multi-stage sharp separation of the involved species and allocation to a set of chemical reactions. This approach builds on the representation proposed by Bao et al. (2011) which was developed to target primary material flowrate allocation and reactions for a biorefinery. This technique simplifies modeling material stream allocation by representing conversion technologies as reaction nodes that emit products and byproducts with complete separation. Reaction nodes can accept and emit certain components identified in the sets: $COMPONENT\ IN_r = \left[c_r^{in} \middle| c_r^{in} = 1, 2, N_{component\ in_r}\right]$ and $COMPONENT\ OUT_r = \left[c_r^{out} \middle| c_r^{out} = 1, 2, N_{component\ out_r}\right]$. A set of candidate reactions: $REACTIONS = \{r\,|r = 1,2, \ldots, N_{reaction}\}$ is considered to convert the chemical reactants into products, byproducts, intermediates, and wastes. Figure 2.2 gives a

structural representation of the reaction path synthesis superstructure. This is an extended version of the representation introduced by Bao et al. (2011) which was developed for the design of biorefineries. The set of feedstocks, byproducts, and wastes are fed to a series of component sorting and reaction stages (Figure 2.2). The stages are represented with the set $STAGE = \{m|m = 1, 2, \dots, N_{stage}\}$. Each sorting cell corresponds to one of the chemical species involved in the network. The chemical constituents in each source are allocated to the $N_{component}$ cells representing all the considered chemical species. The chemical sorting cells are followed by a stage of $N_{reaction}$ cells which correspond to the candidate chemical reactions that convert these chemical species into products, byproducts, intermediates, and wastes. The stages are repeated through the chemical sorting followed by reaction arrangement.

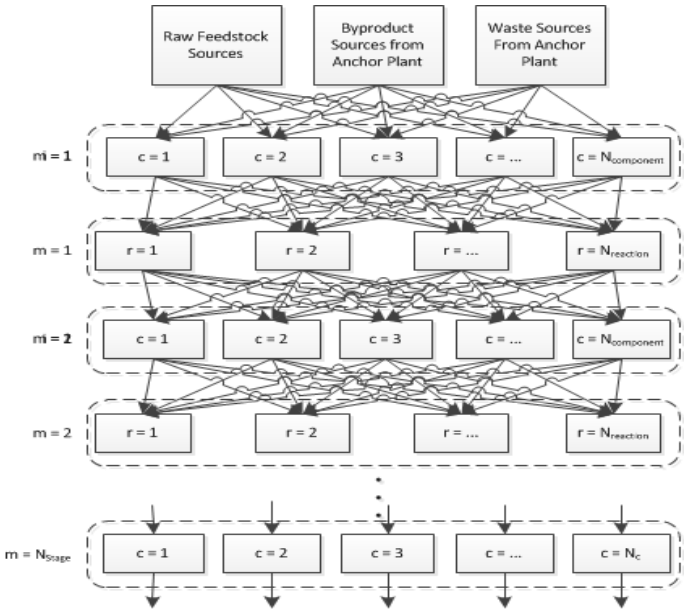

Figure 2.2: Structural Representation of Reaction Path Superstructure

The component flowrate of c entering the first stage of this structure is provided as

$$F_{c,1}^{Stage} = \sum_i F_i^{Source} x_{i,c} \qquad \forall c \tag{21}$$

where $F_{c,m}^{Stage}$ represents the component flowrate of c on stage m.

The component flowrate c on stage m is split up into multiple split component flowrates directed to each reaction node of r that can accept component c_r^{in}. These split flowrates are termed $F_{c_r^{in},m}^{in}$. This relation is shown below

$$F_{c,m}^{Stage} = \sum_r F_{c_r^{in},m}^{in} \quad \forall c, \forall m \tag{22}$$

There are multiple methods to implement the performance of plant process within this structural representation. The performance can be applied as input-output, fundamental or mechanistic models. This study uses an input-output mole balance with process yields included in the form of two equations for input and output. The equation for the input of the balance is given below

$$F_{c_r^{in},m}^{in} = \alpha_{r,c_r^{in}} R_{r,m} \quad \forall r, \forall c_r^{in}, \forall m \tag{23}$$

where $R_{r,m}$ is the extent of reaction for reaction r on stage m.

The equation for the output follows as

$$F_{c_r^{out},m}^{out} = Y_{r,c_r^{out}} \alpha_{r,c_r^{out}} R_{r,m} \quad \forall r, \forall c_r^{out} \tag{24}$$

where $Y_{r,c}$, and $F_{c,m}^{out}$ are the yield of component c of reaction r and the emitted component flowrate of c on stage m, respectively.

Following the conversion of components is the mixing of component c exiting the reaction r on the next stage. This is represented below

$$F_{c,m+1}^{Stage} = \sum_r F_{c_r^{out},m}^{out} \quad \forall c, \forall m \tag{25}$$

On the terminal stage, the component flowrate of c is allocated as a product or unutilized byproduct. This is given as

$$F_{c,N_{Stage}}^{Stage} = F_c^{Product} + F_c^{Unutilized} \quad \forall c \tag{26}$$

Equations (19) to (26) are optimized to an objective function. Like the component targeting, this formulation is optimized considering variety of criteria. In addition to the criteria mentioned in the product targeting technique, metrics for safety, reliability or sustainability could be introduced to optimize for those relevant factors.

The intended use of reaction targeting is to quickly screen and evaluate numerous plant processes that can be selected for invitation in to the park expansion system. The results of this targeting provide substance to the selection of plant processes and their respective capacities as well as simultaneously primary material allocation.

2.6. Case Study: Multiscale Targeting and Optimization of a CHOSYN with Two Anchors for the Production of Butadiene and Benzene from Shale Gas

Two anchor plants are to be established as the nucleus for a shale-gas monetization industrial city. The two plants are:

Anchor 1: Methane conversion to butadiene: The process is based on the following three primary reactions (Özinan and El-Halwagi, 2017):

Methane cracking to acetylene:

$2CH_4 \rightarrow C_2H_2 + 3H_2$

Hydrogenation of acetylene to ethylene:

$C_2H_2 + H_2 \rightarrow C_2H_4$

Dimerization of ethylene to butadiene:

$2C_2H_4 \rightarrow C_4H_6 + H_2$

Anchor 2: Methane aromatization to benzene: The process involves the following main reaction (Pérez-Uresti et al., 2017):

$6\ CH_4 \rightarrow C_6H_6 + 9\ H_2$

Naphthalene and hydrogen are the two major byproducts of the process.

Table 2.1 shows the data for the chemical species discharged from the two anchor plants. Available for purchase are three external sources: methane, oxygen, and steam.

Table 2.1: Flowrates (in kmol/h) of the Chemical Species Discharged from the Two Anchor Plants

Species	Butadiene Plant	Benzene Plant	Total
H_2	225	300	525
CO_2	160	40	200
C_2H_2	30	0	30
C_2H_4	25	0	25
C_4H_6	25	0	25
C_6H_6	0	25	25
$C_{10}H_8$	0	80	80

Table 2.2 summarizes the potential products for the tenants along with the basic chemical reactions for the proposed processes and their relevant cost data.

Table 2.2: Potential Products for the Tenants and Relevant Data

Reaction Index	Main Product	Basic Chemistry	Non-Feedstock Op. Cost ($/kmol product)	Annualized Fixed Cost ($/yr)*	Comments
1	Acetaldehyde	$C_2H_2 + H_2O \rightarrow CH_3CHO$	17.5	$6.8*10^5*P^{0.70}$	98% of maximum theoretical yield is obtained
2	Ethylene Oxide	$C_2H_4 + 0.5\ O_2 \rightarrow C_2H_4O$	11.1	$8.5*10^5*P^{0.65}$	95% of maximum theoretical yield is obtained
3	Methanol (via partial oxidation)	$CH_4 + ½\ O_2 \rightarrow CH_3OH$	7.6	$9.8*10^5*P^{0.60}$	90% of maximum theoretical yield is obtained
4	Methanol (via CO_2 hydrogenation)	$CO_2 + 3\ H_2 \rightarrow CH_3OH + H_2O$	13.9	$3.6*10^5*P^{0.63}$	85% of maximum theoretical yield is obtained
5	Propylene	$CH_3OH \rightarrow 1/3\ C_3H_6 + H_2O$	19.2	$1.7*10^5*P^{0.70}$	0.4 tonne of propylene and ethylene is produced per tonne of methanol.**
6	Phthalic Anhydride	$C_{10}H_8 + 4.5\ O_2 \rightarrow C_8H_4O_3 + 2\ CO_2 + 2\ H_2O$	41.3	$23.1*10^5*P^{0.60}$	93% of maximum theoretical yield is obtained
7	Styrene Butadiene Rubber	$C_6H_6 + C_2H_4 \rightarrow C_8H_{10}$ $C_8H_{10} \rightarrow C_8H_8 + H_2$ $C_4H_6 + C_8H_8 \rightarrow C_{12}H_{14}$	36.7	$17.6*10^5*P^{0.60}$	97% of maximum theoretical yield is obtained

*Based on a 10-year linear depreciation scheme with P being the flowrate of the main product in kmol/h
**Propylene and ethylene are assumed to be valued at the same price

Table 2.3, Table 2.4 and Table 2.5 respectively show the prices for purchasing the external (fresh) sources, the values of the species in the streams discharged from the anchor plants, and the selling prices of the main products from the tenants.

Table 2.3: External Source Price and Availability

Fresh Source	Purchased Price ($/kmol)	Maximum Available Supply (kmol/h)
CH4	2.1	300
O2	6.4	150
H2O (steam)	0.1	250

Table 2.4: Values* of Species in Streams Discharged from Anchor Plants

Species	Value ($/kmol)
H_2	0.35
CO_2	0.00
C_2H_2	0.20
C_2H_4	0.15
C_4H_6	0. 20
C_6H_6	0.30
$C_{10}H_8$	0.10

*The value of the species is also what another plant would pay to obtain the species from another plant

Table 2.5: Selling Prices for Main Products of Prospective Tenants

Potential Main Products for Tenants	Selling Price ($/kmol)	Maximum Market Demand (kmol/h)
Acetaldehyde CH_3CHO	43	150
Ethylene Oxide C_2H_4O	77	100
Methanol CH_3OH	39	450
Propylene C_3H_6	69	100
Phthalic Anhydride $C_8H_4O_3$	265	75
Styrene Butadiene Rubber $C_{12}H_{14}$	278	50

In order to ensure the economic viability of the participants, a minimum return on investment (ROI) of 10 yr^{-1}% is required for each tenant. A 10-year linear depreciation scheme with no salvage value is assumed. Additionally, the fixed capital investment is assumed to be 85% of the total capital investment.

The objective is to maximum the sum of the annual profits for all the tenants while satisfying the technical, economic, and environmental constraints. The carbon footprint for the whole EIP (anchors and tenants) is limited to a maximum CO_2 discharge of 150 kmol/h.

2.7. Results and Discussion

2.7.1. Targeting Approach

Product targeting was first applied to the case study to determine the optimal portfolio of products to manufacture and to elucidate the competitive and cooperative linkages when manufacturing multiple products. At this stage of screening, capital investment and non-feedstock operating costs are not considered and so the product portfolio is determined through maximizing the difference of product sales and feedstock cost subject to the constraint on carbon dioxide. Product targeting applied to the case study is implemented in GAMS as a linear program and solved using CPLEX (Brooke et al., 2006). Table 2.6, seen below, shows the maximized gross margin which is the difference of product sales and feedstock cost. The results obtained from the targeting step are summarized by Table 2.7 and Table 2.8 which respectively show the flowrates of the products as well as the utilized internal and external sources.

Table 2.6: Objective Function and Related Financial Information in Product Targeting

Item	$/hr
Product Sales	26,771
Feedstock Cost	1,726
Gross Margin	25,045

Table 2.7: Targeted Products and Produced Quantities in Product Targeting

Product Component	Flowrate (kmol/hr)
Acetaldehyde	30
Ethylene Oxide	0
Methanol	450
Propylene	0
Phthalic Anhydride	3.7
Styrene Butadiene Rubber	25

Table 2.8: Internal and External Sources Usage Quantities in Product Targeting

Internal Source Component	Flowrate (kmol/hr)
Hydrogen Gas	525
Carbon Dioxide	200
Acetylene	30
Ethylene	25
Butadiene	25
Benzene	25
Naphthalene	3.7
External Source Component	
Methane	266.7
Oxygen Gas	150
Water	0

Using the solution obtained from the targeting step, the flows of the various reactants and products are augmented to create the following overall reaction for the EIP:

$$525H_2 + 175.9CO_2 + 30C_2H_2 + 30C_2H_2 + 25C_2H_4 + 25C_4H_6 + 25C_6H_6 + 3.7C_{10}H_8 + 266.7CH_4 + 150O_2 \rightarrow 160.7H_2O + 30CH_3CHO + 450CH_3OH + 3.7C_8H_4O_3 + 25C_{12}H_{14}$$

In addition to the specific targets obtained by the benchmarking step, additional insights are also obtained. An example in this case study is observed at the oxygen atom balance. Oxygen gas is a limited resource and is required to manufacture ethylene oxide, methanol and phthalic anhydride. Before applying product targeting, Table 2.5 would indicate that the phthalic anhydride production is prioritized over methanol and ethylene oxide. Closer analysis on the oxygen gas component balance with an atomic perspective shows that the margin generated per atom of oxygen consumed is greater in methanol rather than in phthalic anhydride. Ethylene oxide manufacture is not considered here as the available ethylene is allocated to the production of styrene butadiene rubber, a more profitable product. Atomic perspective insights are also apparent in the analysis of the carbon atom balance. The optimal portfolio of products omits propylene manufacture as methanol is valued higher than propylene on a carbon atom basis. An analogous analysis on component values in Table 2.5 would show that the MTP route would give a negative margin and therefore, further consideration of this route is disregarded in this case study. It is expected from the case study product targeting that acetaldehyde is selected in the optimal product portfolio because there is an available byproduct stream of acetylene, water is generated as a byproduct in excess and the margin gained in acetaldehyde is positive. As water is available in excess as a byproduct from Reactions 4 and 6, 160.7

kmol/hr is emitted from the park expansion system. The carbon dioxide emitted from the park expansion systems is well below the limit imposed by the emissions constraint described in the case study. The remaining excess carbon dioxide that is emitted from the system highlights the complete use of byproduct hydrogen in the CO_2 hydrogenation reaction.

The results of product targeting are also analyzed from an atom economy point of view. This is significant as the chemical industry has placed increasing emphasis on atomic throughput and dematerialization. An additional metric is defined below.

$$Atomic\ Efficiency_a = \frac{\sum_c Atom\ Set_{c,a} F_c^{Product}}{\sum_c Atom\ Set_{c,a} F_c^{Unutilized}} * 100\% \quad (27)$$

The application of this metric to the results provides Table 2.9 which is shown below.

Table 2.9: Atomic Fluxes In and Out of Park Expansion System in Product Targeting (quantities in kmol/hr)

Atom	Feedstocks	Wastes	Products	Atomic Efficiency (%)
C	863.704	24.074	839.63	97.21
H	2606.296	321.481	2284.815	87.67
O	700	208.889	491.111	70.16

Emphasis is made on the high carbon efficiency for this system. The significance of the 97% carbon efficiency shows that the majority of feedstocks for the park expansion system are converted into salable products rather than exiting in the form of carbon dioxide emissions. Hydrogen and oxygen efficiencies are less as the main waste product leaving

the park expansion system is water. The oxygen efficiency tends to be lowest as less oxygen is supplied and oxygen atoms usually exit the chemical systems as waste products such as carbon dioxide and water.

2.7.2. Superstructure Approach

The next step is to synthesize a superstructure which shows the details of the interactions among the different entities in the EIP while accounting for the interception processes, the fixed cost of the system and the non-feedstock operating costs (in addition to the feedstock costs and values of sold products which were included in the targeting step). Results from the targeting step are used as initial guesses for the solution. The aforementioned superstructure representation and optimization formulation are used to a mixed-integer nonlinear program (MINLP) which was coded using GAMS and solved to global optimality using BARON with CPLEX and MINOS as the LP and NLP sub-solvers (Brooke et al., 2006; Tawarmalani & Sahinidis, 2005). This formulation contains 363 constraints and 497 variables, of which 7 are binary. This reaction targeting formulation could be applied as a mixed integer linear program (MILP) by discretizing the capital cost functions but this is not seen as necessary given the size of the formulation and solvers available for use. The solution time is 3 s using an Intel i5-6500 CPU at 3.2 GHz. In this program, the collective after-tax profits of all participating tenant were maximized subject to a carbon dioxide emissions constraint and a minimum ROI constraint for invited plants. The screened financial outputs and the flowsheet component allocation are provided below in Table 2.10 and Figure 2.3.

Table 2.10: Key Results from the Optimal Solution of the Case Study

Reaction Index	Production Capacity (kton/yr)	Annual After-Tax Profit (MM$/yr)	ROI (%)
1	0	0	0
2	0	0	0
3	66	43	14.2
4	44	24	23.8
5	0	0	0
6	5	6	10
7	34	37	26.7

As seen in Figure 2.3, much of the product and used resources obtained from the superstructure solution are close to the ones obtained from the targeting solution. A notable difference between the two solutions is the reaction and resource allocation for acetaldehyde manufacture. This is explained as the ROI earned by including acetaldehyde manufacture at the production capacity predicted by the product targeting did not meet the minimum 10% ROI held for invited plants. The inclusion of the annualized fixed cost and non-feedstock operating cost of acetaldehyde manufacture *are* significant enough to outweigh the benefit gained from acetaldehyde product sales despite having a competitive feedstock advantage.

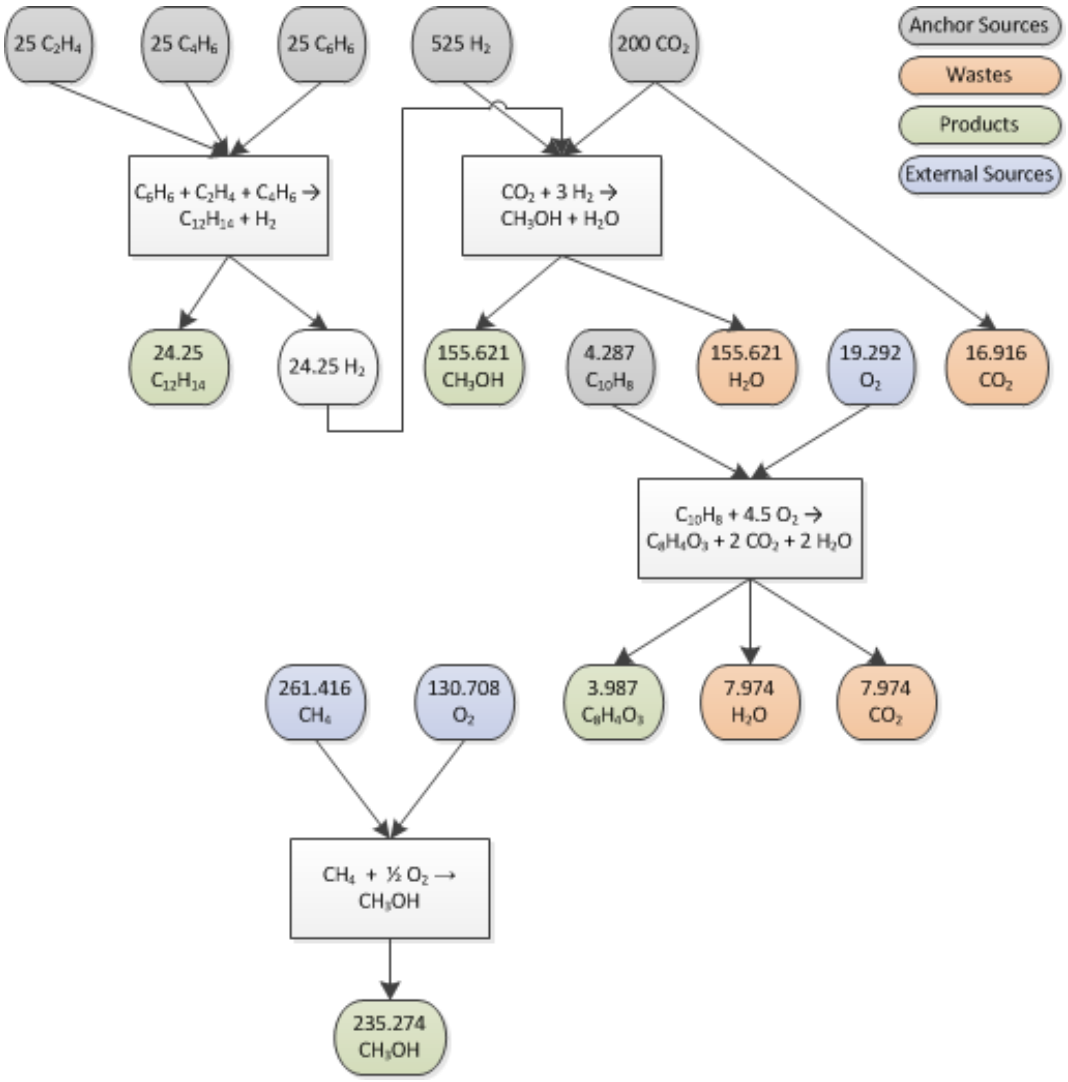

Figure 2.3: Superstructure Solution (all flows are in kmol/h)

It is significant to emphasize that the majority of tenants chosen to be added to the industrial park show a great deal of material exchange through anchor-tenant and/or tenant-tenant collaboration. This is seen with styrene-butadiene rubber, phthalic anhydride and a fraction of methanol manufacturing. The predicted hydrogen exchange from styrene-butadiene and methanol manufacturing elucidates a possibility for collaboration between

tenants in addition with that of anchors. In contrast to the cooperation between tenants is the competition between methanol and phthalic anhydride production made apparent in product targeting and exhibited again in reaction targeting. Implied in the results shown by reaction targeting, the priority for distributing oxygen gas is based on the after-tax profit gain per oxygen atom. Figure 2.3 indicates clearly that oxygen use for methanol production is prioritized over phthalic anhydride production but not much so that phthalic anhydride is excluded from the selection of tenants; the phthalic anhydride ROI in Table 10 implies that the incremental after-tax profit gained by allocating all oxygen resources to methanol production is less than what is gained from inviting phthalic anhydride production. Additional benefits accrue from industrial symbiosis. As shown in Table 2.11, the tenant participation in the EIP potentially avoids 64.2 kton/yr of fresh hydrocarbon use. Using byproducts and waste streams allows for the potential of saving 44.3 MM$ in feedstock costs. 70.6 kton/yr of carbon dioxide emissions are avoided as carbon dioxide could potentially be sequestered and utilized as a feedstock in the methanol production. This case study illustrates the benefits gained by the invited plants underline how waste-utilizing chemical facilities and downstream chemical facilities are suited for invitation and integration into a chemical industrial park.

Table 2.11: Potential Mitigated Impact with Park Integration

Reaction Index	Feedstock Cost Savings (MM$/yr)	Avoided Fresh Hydrocarbon Use (kton/yr)
1	0	0
2	0	0
3	0	0
4	6.3[1]	24.3
5	0	0
6	2.7[2]	4.8
7	34.3[2]	35.1

[1]Assuming product methanol is produced using CH4 and O2
[2]Taking market prices for ethylene, butadiene, benzene and naphthalene to be $0.17/lb, $0.8/lb, $2.2/gal and $552/ton, respectively

Atom economy is also employed at this stage of targeting. Table 2.12 shows the updated fluxes of carbon, hydrogen and oxygen atoms in reaction targeting. In comparison to Table 2.9, lesser efficiencies are observed. This is explained by the inclusion of reaction yields in the reaction targeting. Atoms that are introduced as feedstocks are lost to unaccounted byproducts at this stage of targeting. It still remains that a high efficiency is observed for carbon atoms while loses in oxygen and hydrogen are explained by the emission of water out of the park expansion system.

Table 2.12: Atomic Fluxes In and Out of Park Expansion System After Superstructure Optimization (quantities in kmol/hr)

	Feedstocks	Wastes	Products	Atomic Efficiency (%)
C	804.287	24.891	713.791	88.75
H	2529.961	327.19	1919.029	75.85
O	700	213.376	402.856	57.55

2.8. Conclusion

A new approach has been introduced for the grass-root design of CHOSYN with known anchors and candidate tenants. Three approaches have been proposed: a general superstructure, a simplified superstructure, and stoichiometric-economic targeting. The general superstructure uses a source-interceptor-sink representation, accounts for all configurations and interconnections of interest, and uses detailed modeling of the technologies and the associated capital and operating costs. The simplified superstructure approach uses a multi-stage sorting of species followed by reactions. The targeting approach uses atomic targeting and high-level economic data to eliminate losing tenants and to prioritize promising candidates. The use of the targeting technique is useful in providing valuable benchmarks and insights, narrowing down the search space, and offering an initial solution to the superstructure-based approaches. A case study for has been solved to illustrate the use of this approach and to demonstrate the gained insights.

2.9. References

Al-Mohannadi, D. M., & Linke, P. (2016). On the systematic carbon integration of industrial parks for climate footprint reduction. Journal of Cleaner Production, 112, Part 5, 4053-4064.

Alnouri, S. Y., Linke, P., & El-Halwagi, M. M. (2016). Synthesis of industrial park water reuse networks considering treatment systems and merged connectivity options. Computers & Chemical Engineering, 91, 289-306.

Aviso, K. B., Tan, R. R., Culaba, A. B., Foo, D.C.Y. and Hallale, N., Fuzzy Optimization Of Topologically Constrained Eco-Industrial Resource Conservation Networks With Incomplete Information Engineering Optimization. 43(3), 257-279 (2011)

Bandyopadhyay, S., G. C. Sahu, D. C. Y. Foo, and R. R. Tan. "Segregated targeting for multiple resource networks using decomposition algorithm." AIChE journal 56(5) 1235-1248 (2010)

Bao, B., Ng, D. K., Tay, D. H., Jiménez-Gutiérrez, A., & El-Halwagi, M. M. (2011). A shortcut method for the preliminary synthesis of process-technology pathways: An optimization approach and application for the conceptual design of integrated biorefineries. Computers & Chemical Engineering, 35, 1374-1383.

Bishnu, S. K., Linke, P., Alnouri, S. Y., & El-Halwagi, M. (2014). Multiperiod planning of optimal industrial city direct water reuse networks. Industrial and Engineering Chemistry Research, 53, 8844-8865.

Boix, M., Montastruc, L., Azzaro-Pantel, C., & Domenech, S. (2015). Optimization methods applied to the design of eco-industrial parks: A literature review. Journal of Cleaner Production, 87, 303-317.

Chertow, M. R. (2000). Industrial symbiosis: literature and taxonomy. Annual review of energy and the environment, 25, 313-337.

Chew I.M.L., Tan R., Ng D.K.S., Foo D.C.Y., Majozi T., Gouws J. Synthesis of Direct and Indirect Interplant Water Network. Industrial & Engineering Chemistry Research, 47(23):9485-9496 (2008)

El-Halwagi, M. M., F. Gabriel, and D. Harell, "Rigorous Graphical Targeting for Resource Conservation via Material Recycle/Reuse Networks", Ind. Eng. Chem. Res., 42, 4319-4328 (2003)

El-Halwagi, M. M. (2017). A Shortcut Approach to the Multi-scale Atomic Targeting and Design of C–H–O Symbiosis Networks. Process Integration and Optimization for Sustainability, 1-11.

Gibbs, D. and Deutz, P., 2007. Reflections on implementing industrial ecology through eco-industrial park development. Journal of Cleaner Production, 15(17), pp.1683-1695.

Hasan, M. M. F., I. A. Karimi, C. M. Avison, Preliminary Synthesis of Fuel Gas Networks to Conserve Energy & Preserve the Environment, Industrial & Engineering Chemistry Research 2011, 50(12), 7414–7427.

Hasaneen, R. and M. M. El-Halwagi, "Integrated Process and Microeconomic Analyses to Enable Effective Environmental Policy for Shale Gas in the United States", Clean Technologies and Environmental Policy, 19(6), 1775-1789 (2017)

Kantor, I., Betancourt, A., Elkamel, A., Fowler, M. and Almansoori, A., 2015. Generalized mixed-integer nonlinear programming modeling of eco-industrial networks to reduce cost and emissions. *Journal of Cleaner Production*, *99*, pp.160-176.

López-Díaz, D. C., Lira-Barragán, L. F., Rubio-Castro, E., Ponce-Ortega, J. M., & El-Halwagi, M. M. (2015). Synthesis of Eco-Industrial Parks Interacting with a Surrounding Watershed. ACS Sustainable Chemistry & Engineering, 3, 1564-1578.

Lovelady, E. M., & El-Halwagi, M. M. (2009). Design and integration of eco-industrial parks for managing water resources. Environmental Progress and Sustainable Energy, 28, 265-272.

Lowe E. A, "Eco-Industrial Park Handbook for Asian Developing Countries", A Report to Asian Development Bank. Indigo Development, Santa Rosa, California (2001)

Noureldin, M. M. B., & El-Halwagi, M. M. (2015). Synthesis of C-H-O Symbiosis Networks. AIChE Journal, 61, 1242-1262.

Pérez-Uresti, S., Adrián-Mendiola, J., El-Halwagi, M., & Jiménez-Gutiérrez, A. (2017). Techno-Economic Assessment of Benzene Production from Shale Gas. Processes, 5, 33.

Rubio-Castro, E., Ponce-Ortega, J. M., Serna-Gonzalez, M., Jimenez-Gutierrez, A., & El-Halwagi, M. M. (2011). A global optimal formulation for the water integration in eco-industrial parks considering multiple pollutants. Computers and Chemical Engineering, 35, 1558-1574.

Spriggs, H. D., E. A. Lowe, J. Watz, M. M. El-Halwagi, and E. M. Lovelady, "Design and Development of Eco-Industrial Parks", paper #109a, AIChE Spring Meeting, New Orleans, April, (2004)

3. INTEGRATING MASS AND ENERGY THROUGH THE ANCHOR-TENANT APPROACH FOR THE SYNTHESIS OF CARBON-HYDROGEN-OXYGEN SYMBIOSIS NETWORKS

3.1. Introduction

Future economic development in the petrochemical industries grows to be more difficult as time progresses. This attributed to present challenges such as resource scarcity, the use of unconventional and remote resources, a push to reduce emissions to limit global warming and combinations thereof. Often, a solution that meets one of the challenges may exacerbate others. A wholistic solution is necessary in addressing these challenges while maintaining lucrative economic development. Solutions that meets the aforementioned challenges could be attained through the application of industrial symbiosis practices such as the development and operation of Eco-Industrial Parks (EIPs).

Industrial symbiosis is defined as collection of disparate industries taking a collective approach to benefit themselves via the exchange of materials, energy, wastes and byproducts (Chertow, 2007). An EIP is a collection of separate businesses collocating in a central location that collaborate in the manufacture of goods and services through the exchange of material and energy streams to create synergistic opportunities that would improve economic and sustainable performance of its participants while reducing the environmental impact of the EIP on the surrounding communities. The benefits of participating in an EIP is the reduction of raw material cost, reduced environmental impact and an increase of capital productivity through the sharing of unit operating equipment

(Lowe, 2001). Examples of EIPs were initially identified in Kalundborg, Denmark (Ehrenfeld and Gertler, 1997), and subsequently around the world (Gibbs and Deutz, 2007).

Much of the initial EIP development is executed through self-organization rather than planned design (Chertow, 2007). However, there is much focus on developing methods that facilitate the design of EIPs to advantage economic and sustainable benefits of EIP participation. Chertow (2012) provides several qualitative models to synthesize Eco-Industrial parks. These models include the planned EIP model, the retrofit model, the self-organizing systems model, the circular economy model and the "build and recruit" or "Anchor-Tenant" model. Of these models, the Anchor Tenant will be discussed later in detail.

Quantitative models for EIP development have been established through multiple process systems engineering studies. Spriggs et al. (2004) proposed a source-sink representation of EIPs of which pinch analysis could be applied to determine minimum resource consumption targets (El-Halwagi et al., 2003). These process systems engineering models have approached the development of EIPs through the source-sink representation and its derivatives while considering applications to water, energy and material sharing networks, and combinations thereof. Applications to develop interplant water networks have been comprehensively addressed in the literature. Chew et al. (2008) introduced an optimization framework to synthesize direct and indirect interplant water integration schemes. Chew (2009) extended this study by incorporating a game theory approach into the decision making for designing the interplant water network among

multiple plants. Lovelady and El-Halwagi (2009) employed the source interceptor sink framework and optimized the design of EIP water sharing networks. Aviso et al. (2010a, 2010b) introduced fuzzy programming approaches into the design of interplant water network with and without the existence of a central park authority. Rubio-Castro et al. (2010) proposed a formulation to design an EIP water sharing network and an approach to solve it to global optimality. This study was followed by an extension including the effects of multiple pollutants in the water network design (Rubio-Castro et al., 2011). The effect of considering multiple objectives in the interplant water network design was investigated by Boix et al (2012). Very few studies on the design of interplant material sharing networks exist outside of water sharing networks. However, there are studies that exist on the material sharing of a chemical species or group of chemical species among a group of processes. Alves and Towler (2002) presented a method for developing hydrogen sharing networks. Roddy (2013) proposed opportunities to reduce carbon footprint by suggesting the development of a syngas network. Hasan et al. (2011) developed a superstructure for the design of fuel gas networks.

Another field of EIP development is through energy integration, but through the terminology of "Total Site" which is defined as a collection of plants or processes in a given area. Dhole and Linnhoff (1993) applied energy integration across multiple plants by establishing the concept of "Total Site" and developing a procedure for energy targeting. Hu and Ahmad (1994) applied pinch and exergy analysis to design the central utility system among multiple plants. This was followed up by Klemes et al. (1997), which presented a methodology for the simultaneous optimization of the production heat

exchanger networks and the utility generation system. Concerns on the practicality of total site heat integration was addressed through the development of approaches that led the design of direct and indirect heat exchanger networks, and multi-purpose heat exchanger networks that allowed for dependent and independent operation of the participating plants (Rodera & Bagajewicz, 1999, 2001), (Bagajewicz and Rodera, 2000, 2002). Other consideration such as the effect of distances between plants (Stijepovic and Linke, 2011) and non-uniform minimum approach temperatures (Varbanov et al., 2012) across plants were considered in previous total site heat integration studies. Wang et al. (2015) consolidated approaches developed by Bagajewicz and Rodera (2000) for the design of direct and indirect heat exchanger networks into a combined approach while also considering the effect of distance. Opportunities for enhancing heat integration between multiple plants was investigated by Song et al. (2016) where plant heat exchanger networks are modified to obtain higher grade heating and cooling without compromising the plant's heat recovery. A screening algorithm and optimization model was developed to decompose the heat integration of a site of *n* plants into smaller heat exchanger networks involving pairs and triplets of plant (Song et al., 2017a, 2017b).

Previous EIP literature developed methods to design EIPs where material streams are shared among multiple plants. These methods establish material sharing networks where material streams containing a component or group of similar components are transferred between plants after intermediate processing. This intermediate processing includes services such as mixing, splitting, separation and exchange of material streams.

Recently, the novel problem of designing Carbon-Hydrogen-Oxygen SYmbiosis Networks (CHOSYNs) was introduced (Noureldin and El-Halwagi, 2015) with the following unique characteristics:

- It focuses on hydrocarbon processing plants
- In addition to exchanging species, CHOSYN extend these services to include the chemical conversion of components containing C, H and O atoms and transforming them to intermediates, final products, and wastes
- It determines a maximum resource efficiency through atomic level analysis prior to performing the detailed process flowsheet design. Minimum resource targets are determined through performing an atomic balance around C, H, and O atoms over the process design system and achieved through the detailed network design methods that include reactive processes
- It uses multi-scale targeting and optimization to generate integrated schemes among the participating plants with different levels of details

Several contributions have been made in the area of systematizing the design of CHOSYNs. Noureldin and El-Halwagi (2015) developed a multi-scale optimization approach to the targeting and implementation of CHOSYNs. El-Halwagi (2017) introduced an algebraic approach for utilizing atomic information to benchmark the performance of a CHOSYN and to generate alternate pathways. The problem of handling flexible operations in the design of CHOSYNs to meet seasonal variations of product demand and source availability was approached by Al-Fadhli et al. (2018). Mukherjee and

El-Halwagi (2018) addressed the problem of designing CHOSYNs under uncertainty of source streams. Disjunctive programming techniques were used in the targeting and design of CHOSYNs (Juárez-García, 2018). In addition to integrating existing plants, it is also beneficial to consider the grassroots design of a new CHOSYN. Recently, Topolski et al. (2018) developed an optimization approach to address the grassroots synthesis of CHOSYNs through an anchor-tenant model. The anchor-tenant model recognizes that the plants that exist or are "first-to-build" are foundational to the growth of the EIP and thus termed as "anchors". The plants that are to be invited for construction and integration around these anchors are termed as "tenants". This anchor-tenant model addressed the selection of tenants through a multiscale approach that first addresses the screening of products to manufacture and then the screening of tenants before the detailed design of the material sharing network within the CHOSYN. Product and tenant screening is accomplished through the use of techniques that incorporate fundamental chemical processing information. These techniques are applied prior to the detailed design of the material sharing network to reduce design problem size by eliminating potential sub-optimal solutions.

Notwithstanding the value of the aforementioned contributions, there is a limitation in these research efforts: focus was limited to integrating mass among the participating plants. In addition to the value of integrating mass, substantial benefits can accrue as a result of integrating energy as well. The objective of this work is to introduce a systematic approach for the grassroots design of CHOSYNs while accounting for both mass and energy integration among the participating facilities. In addition to atomic

benchmarking and multi-scale mass integration, intra- and inter-plant heat and power integration are considered.

The organization of this chapter is as follows: First, the statement of inviting tenant facilities while considering their respective material and energy throughputs is presented. This is followed by the description of the proposed methodology that decomposes this problem into techniques to reduce the search space of tenants to invite. A case study that illustrates a growth opportunity to build a CHOSYN around existing anchor plants is presented. This is followed by the result and discussion from the application of the proposed approach and the conclusion.

3.2. Problem Statement

This study considers a group of manufacturing facilities collocated in a general area to form an CHOSYN. Each facility is represented by the set $PLANT = \{p|p = 1, 2, \dots, N_{Plant}\}$ which is divided into the following subsets $ANCHOR = \{p|p = 1, 2, \dots, N_{Anchor}\}$, $TENANT = \{p|p = N_{Anchor} + 1, N_{Anchor} + 2, \dots, N_{Tenant}\}$, and $UTILITY = \{p|p = N_{Tenant} + 1, N_{Tenant} + 2, \dots, N_{Plant}$. Anchor facilities are either existing or the "first to build" plants that will provide byproduct material and energy streams that tenant facilities could supplement their operation with. Utility facilities are those that provide material and energy streams at a cost.

A set $SOURCE_p = \{s_p|s_p = 1, 2, \dots, N_{Source_p}\}$ is defined to represent the group of external raw material, byproduct and waste streams from plant p that are available for service. These three streams are differentiated by the subsets defined as $EXTERNAL\ SOURCE_p = \{s_p|s_p = 1, 2, \dots, N_{p_{External}}\}$, $ANCHOR\ BYPRODUCT_p =$

$\{s_p | s_p = N_{p_{External}} + 1, N_{p_{External}} + 2, \dots, N_{p_{Byproduct}}\}$ and $ANCHOR\ WASTE_p = \{s_p | s_p = N_{p_{Byproduct}} + 1, N_{p_{Byproduct}} + 2, \dots, N_{p_{Source}}\}$. Each of these source streams are described by their flowrate F_{s_p} and composition $x_{s_p,c}$. The set $COMPONENT = \{c | c = 1, 2, \dots, N_{Component}\}$ is defined to represent the components that the source streams are composed of. In turn, these components are composed of atoms which are represented by the set $ATOM$ $\{a | a = 1, 2, \dots, N_{Atom}\}$. It is worth noting that $EXTERNAL\ SOURCE_p$ and $ANCHOR\ BYPRODUCT_p$ represents purchasable material streams originating from the external utility and anchor, respectively. $ANCHOR\ WASTE_p$ represents waste streams from anchor plants that are given away for free or at a negative cost.

These plants may designate additional process streams to provide heating and cooling to supplement their utility needs. Such streams are defined with the sets $HS_p = \{i_p | i_p = 1, 2, \dots, N_{Hot\ Stream_p}\}$ for hot streams and $CS_p = \{j_p | j_p = 1, 2, \dots, N_{Cold\ Stream_p}\}$ for cold streams. These streams are characterized by their target temperatures and supply temperatures which are represented for hot streams, $T_{i_p}^{In}$ and $T_{i_p}^{Out}$, and for cold streams, $T_{j_p}^{In}$ and $T_{j_p}^{Out}$, respectively. Furthermore, these streams possess a heat capacity flowrate FCp_{i_p} for hot streams and FCp_{j_p} for cold streams. Streams that entail latent heat effects are included for consideration where the enthalpy as approximated as the heat capacity with a degree difference in temperature. The heat capacity flowrates are known for anchors and are to be determined for tenants as part of the design and optimization.

Combined heat, power and refrigeration is also considered in addition to mass and heat integration. A Steam Rankine Cycle (SRC), an Organic Rankine Cycle (ORC) and an Absorption Refrigeration (AR) cycle are available technologies for integration. The SRC and ORC are defined systems that can accept process heat as their energy sources and convert it into electricity at an efficiency μ. Residual heat from the SRC and low-grade heat from the CHOSYN plants can be directed to the ORC to produce additional electricity or to an Absorption Refrigeration (AR) cycle to produce sub-ambient cooling. The AR cycle is defined as a single effect cycle and with a coefficient of performance (COP).

The aim of this study to develop a systematic approach that considers mass and energy integration for the multi-scale targeting, design and optimization of the grassroots EIP. The specific outcomes of this approach include the optimized selection of tenants and stream allocation for their respective material and energy needs. Conceptual flowsheets detailing the flow of mass and energy among anchor, tenants and utilities are developed as a result of this approach. The sizing and costing of facilities to build in the grassroots EIP are also determined.

3.3. Synthesis Approach

The problem of synthesizing an CHOSYN is decomposed and solved in a multiscale sequential optimization approach. This approach is developed to aid in the synthesis of a CHOSYN by recommending tenant plants to build and integrate into the CHOSYN while considering their material and energy stream characteristics. The sequential approach addresses the topic of CHOSYN design by screening candidate tenant

plants through mass integration principles and then follows with reinforcing the tenant screening with energy integration. Figure 3.1 illustrates this approach in a stepwise manner.

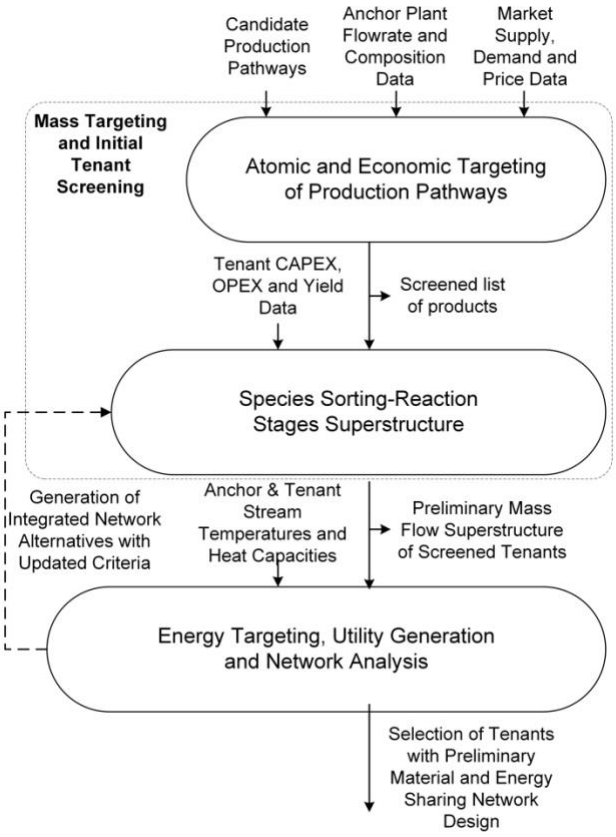

Figure 3.1: High-level Overview of the Proposed Approach

The outcome of this proposed approach is a selection of sized tenant facilities, a preliminary material sharing network and a shared heat exchanger network integrated with a centralized utility system. These details are subject to further scrutiny prior to the detailed CHOSYN design phase. If the tenant selection and material and energy sharing network are deemed unsatisfactory, design alternatives can be generated through looping

back to the Species Sorting-Reaction Stages (SSRS) superstructure step with updated design criteria. The detailed descriptions of the techniques that make up this approach are provided in the following subsections.

3.3.1. Mass Targeting and Initial Tenant Screening

The procedure to target products and screen tenants is illustrated in Figure 3.1 as the first two steps in this approach. The decision to apply mass integration principles to select tenants before energy integration is made knowing that raw material costs are typically the largest contributor to the total cost of production. Therefore, it is assumed that raw material allocation will have the dominant influence when determining ideal tenant plants to invite.

Material streams from anchor plants are identified for participation in the CHOSYN synthesis. The material stream flowrates and compositions are analyzed to determine the quantities of C, H and O atoms that are entering the CHOSYN design system. Likewise, externalities such as raw materials and potential products are analyzed for their supply/demand, prices and atomic composition. Potential production pathways are surveyed for consideration in the CHOSYN development. The data concerning raw materials, products, anchor streams and potential production pathways serve as inputs to the Atomic and Economic Targeting of Production Pathways (AETPP) targeting step to obtain a screened list of products for the CHOSYN. This becomes an input along with the capital expenditures (CAPEX), operating expenses (OPEX) and yield data relating to the aforementioned production pathways for the SSRS superstructure technique as seen in

Figure 1. The result of the SSRS superstructure technique is a network of the screened tenant plants where component flowrates are transferred between plants.

3.3.1.1. Atomic and Economic Targeting of Production Pathways (AETPP)

The scope of the AETPP technique is to determine attractive production pathways while considering economic data, stoichiometric conversion of chemical species and other additional constraints of interest. An outcome of this technique is a prioritized list of products and tenants that provides the optimal result of the objective pursued. The result is an overall stoichiometric reaction for the CHOSYN design system that illustrates the conversion of the system starting materials into end products and that could be decomposed into sub-reactions that elucidate the utilized production pathways.

The technique to address this problem is stated as follows: Given the sets of sources, products and the characteristic reactions representing the tenants, develop an optimal target that determines ideal products to pursue, the starting materials to purchase and the tenants to facilitate the production of those products. Chemical species that could be sold outside of the design system are identified in subset of $COMPONENT$, $PRODUCT = \{c|c = 1, 2, \dots, N_{Product}\}$. The subset of $TENANT$ is also utilized in this technique where the members in the set $TENANT$ are correlated to a characteristic reaction that represents the throughput of each tenant being considered.

The source steams entering the CHOSYN design system are segregated into component flowrates defined as $F_c^{Source\ Component}$. This is provided with the following relation:

$$F_c^{Source\ Component} = \sum_{s_p} F_{s_p}^{Source} x_{s_p,c} \qquad \forall c \qquad (1)$$

These component flowrates are disaggregated further into quantities of atoms which is defined as $Atom_a^{Source}$. These quantities are determined as follows:

$$Atom_a^{Source} = \sum_c Atom\ Set_{c,a} F_c^{Source\ Component} \qquad \forall a \qquad (2)$$

where $Atom\ Set_{c,a}$ is the predefined quantity of atoms a in component c.

Similarly, the quantities of atoms a leaving the CHOSYN design system as products and unutilized byproducts are defined as $Atom_a^{Demand}$ and $Atom_a^{Leftover}$, respectively. The relations to determine these values are:

$$Atom_a^{Demand} = \sum_{c \in PRODUCT} Atom\ Set_{c,a} F_c^{Product} \qquad \forall a \qquad (3)$$

$$Atom_a^{Leftover} = \sum_c Atom\ Set_{c,a} F_c^{Unutilized} \qquad \forall a \qquad (4)$$

where $F_c^{Product}$ and $F_c^{Unutilized}$ are the component flowrates of products and unutilized byproducts leaving the CHOSYN design system, respectively.

The amounts of atoms that entering and leaving the CHOSYN design system are subject to the conservation of mass law which is provided as:

$$Atom_a^{Source} - Atom_a^{Demand} - Atom_a^{Leftover} = 0 \qquad \forall a \qquad (5)$$

The overall conversion of the component c, Θ_c, is determined as the difference between the quantities of product and unutilized byproducts leaving and the starting materials entering the CHOSYN system. A negative value for Θ_c denotes that the component c is consumed within the design system and a positive value denotes the generation of component c. The relationship determining Θ_c is given as:

$$F_c^{Product} + F_c^{Unutilized} - F_c^{Source\ Component} = \Theta_c \qquad \forall c \qquad (6)$$

The net generation or consumption of component c is also defined as the sum of the characteristic reactions that facilitate the conversion of component c into component c'. This is represented as:

$$\Theta_c = \sum_{p \in Tenant} \alpha_{p,c} \xi_p \qquad \forall c \qquad (7)$$

where $\alpha_{p,c}$ is a parameter that describes the stoichiometric coefficient of component c of the characteristic reaction representing tenant p, and ξ_p is the extent of the characteristic reaction representing tenant p.

Constraints on the supply of starting materials, demand of products and limits of exiting unutilized byproduct are defined as follows:

$$F_{s_p}^{Source} \leq F_{s_p}^{Supply} \qquad \forall s_p \qquad (8)$$

$$F_c^{Product} \leq F_c^{Demand} \qquad \forall c \in PRODUCT \qquad (9)$$

$$F_c^{Unutilized} \leq F_c^{Unutilized\ Limit} \qquad \forall c \qquad (10)$$

where $F_{s_p}^{Supply}$, F_c^{Demand} and $F_c^{Unutilized\ Limit}$ are the limiting values for supply, demand and byproduct emissions, respectively.

Equations (1) to (10) are subject to an objective function and additional constraints that are optimized in pursuit of a policy in mind. The recommended objectives include but are not limited to the maximization of the gross margin (defined as the difference of product sales and raw material costs), minimization of unutilized byproducts, and minimization of virgin raw materials. Combinations of these objectives could be pursued with an objective being defined and subject to additional constraints on other criteria.

3.3.1.2. Species Sorting Reaction Stages (SSRS) Superstructure

Following the AETPP technique in Figure 3.1 is the SSRS superstructure technique (Bao, 2011), which involves another layer of detailed targeting for determining which tenants to invite and integrate. This technique considers the multi-stage sharp separation of the involved chemical species and the allocation of those species to a set of characteristic reactions representing the tenants. The tenants are represented as reaction nodes that can accept and emit component flowrates as well as convert component c into component c'. These reaction nodes are defined to accept and emit certain components which are given in the sets $COMPONENT\ IN_p = [c_p^{in} | c_p^{in} = 1, 2, N_{Component\ In_p}]$ and $COMPONENT\ OUT_p = [c_p^{out} | c_p^{out} = 1, 2, N_{Component\ Out_p}]$. The component allocation, conversion and segregation are represented over multiple stages as seen in Figure 3.2. These stages are represented by the set $STAGE = \{m | m = 1, 2, \dots, N_{Stage}\}$.

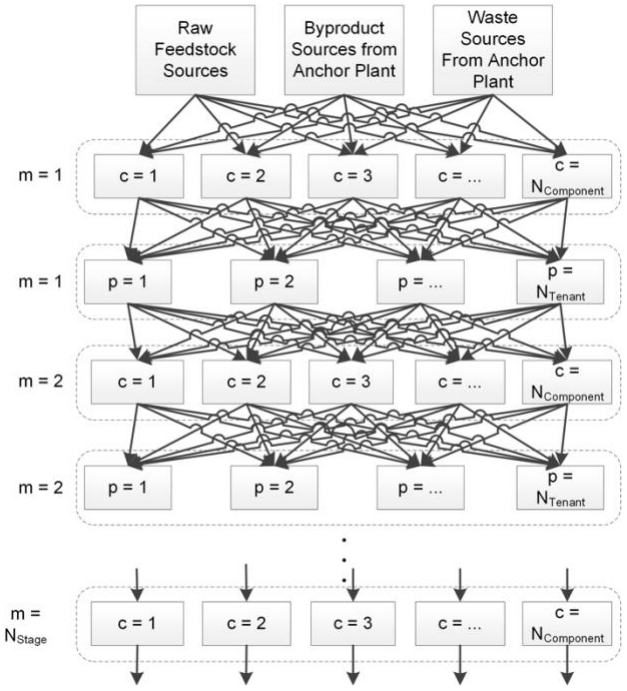

Figure 3.2: Structural Representation of the SSRS Superstructure (adapted from Topolski et al., 2018)

Material streams from anchor plant and raw material sources are discretized into a stage of chemical species sorting cells. Each sorting cell corresponds to a chemical species that is defined in the CHOSYN system. These sorting cells are followed by a stage of reaction nodes that accept and convert these chemical species. Both stages of sorting cells and reaction are defined as a processing stage m and is repeated over N_{Stage} stages in this structure.

Material streams defined in $SOURCE_p$ are divided into component flowrates, $F_{c,m}^{Stage}$, which represent the chemical species sorting cells. This is represented by the following relation where the element of m represents the first stage of the superstructure:

$$F_{c,1}^{Stage} = \sum_p \sum_{s_p} F_{s_p}^{Source} x_{s_p,c} \qquad \forall c \tag{11}$$

The component flowrates of each stage are divided further into component split flowrates $F_{c_p^{in},m}^{In}$ directed to a reaction node for tenant p on stage m. The relation for component flowrate splitting is provided as:

$$F_{c,m}^{Stage} = \sum_{p \in Tenant} F_{c_p^{in},m}^{In} \quad \forall c, \forall m \tag{12}$$

There are several methods to model the conversion of materials within a tenant. Options include modeling the throughput of tenants while considering input-output, fundamental or mechanistic methods. This study employs stoichiometric reactions to model tenants with process yield information incorporated. The relation representing the tenants receiving component split flowrate at stoichiometric ratio is:

$$F_{c_p^{in},m}^{In} = \alpha_{p,c_p^{in}} R_{p,m} \quad \forall p \in Tenant, \forall c_p^{in}, \forall m \tag{13}$$

where $R_{p,m}$ and $\alpha_{p,c_p^{in}}$ represent the conversion of the characteristic reaction representing tenant p on stage m and the stoichiometric coefficient of component c_p^{in} within said characteristic reaction, respectively.

The relationship for tenant outputs is:

$$F_{c_p^{out},m}^{Out} = Y_{p,c_p^{out}} \alpha_{p,c_p^{out}} R_{p,m} \quad \forall p \in Tenant, \forall c_p^{out}, \forall m \tag{14}$$

where $Y_{p,c_p^{out}}$ and $F_{c_p^{out},m}^{Out}$ are the yield of component c_p^{out} for the characteristic reaction representing tenant p and the exiting component split flowrate of c_p^{out} from the characteristic reaction representing tenant p on stage m, respectively.

Subsequent to the conversion of materials by the reaction node p is the mixing of the component split flowrate of component c_p^{out} on stage $m+1$. This is provided as:

$$F_{c,m+1}^{Stage} = \sum_{p \in Tenant} F_{c_p^{out},m}^{Out} \quad \forall c, \forall m \tag{15}$$

Component flowrates for component c are allocated as a product or an unutilized byproduct upon the terminal stage. This relation is given as:

$$F_{c,N_{Stage}}^{Stage} = F_c^{Product} + F_c^{Unutilized} \quad \forall c \tag{16}$$

Equations (8) to (16) are optimized to an objective function and additional constraints representing the policy for CHOSYN development. Much like the previous techniques, these equations could be optimized while using a variety of different criteria or combinations of criteria. Examples of criteria that could be included are metrics on safety, reliability and/or sustainability.

The purpose of the SSRS superstructure is to screen and evaluate numerous plant processes to invite into the CHOSYN design system. The outcome of this technique is a preliminary superstructure illustrating the main process flowrates from each plant involved in the design system as well as sized capacities of the selected tenants.

3.3.2. Energy Targeting, Utility Generation and Network Analysis

The intent of the energy integration techniques following the mass integration targeting in Figure 3.1 is to reinforce the selection of tenant plants by providing an opportunity to increase profit, reduce emissions and to operate sustainably via the reduction of utility usage. The energy integration of the screened tenants with the anchors is decomposed further into an iterative procedure shown in Figure 3.3. It is assumed in the Energy Targeting, Utility Generation and Network Analysis (ETUGNA) step that anchor

plants are internally heat integrated and will discharge low grade hot and cold streams. As tenant plants are not built and their heat exchanger networks not established, there are opportunities for economic and environmental benefits by designing tenant heat exchanger networks while considering the later interplant energy integration. Figure 3.3 illustrates the procedure for the internal tenant heat integration followed by interplant energy integration.

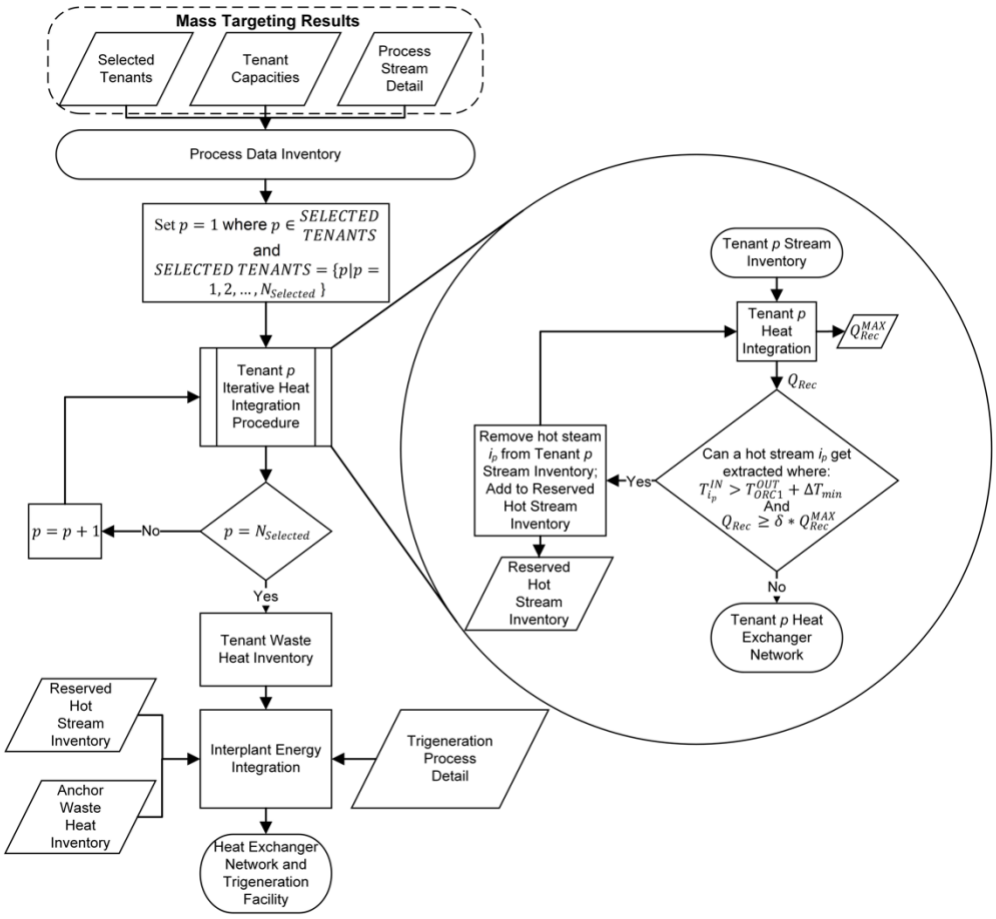

Figure 3.3: Procedure for Tenant and Interplant Heat Integration

Temperature and heat capacities of both the anchor's and screened tenant's candidate streams for integration are identified for the ETUGNA targeting step. An iterative pinch analysis procedure is applied to the heat integration of the tenants to identify opportunities to generate electricity in the interplant energy integration. This iterative process looks to extract high-grade process heat for later energy integration without significantly affecting the benefits gained from internal heat integration.

The motive to modify tenant heat exchanger network designs is to reserve high grade hot streams that could be utilized for lucrative electricity generation while also reducing cooling utilities for that tenant. This is accomplished through the iterative heat integration procedure, shown in sub-picture within Figure 3.3, where the first round of heat integration is applied to the tenant main process to determine the maximum heat recovery, Q_{Rec}^{Max}. Subsequent rounds are applied with tenant hot streams extracted to determine a nominal heat recovery, Q_{Rec}. The hot stream with the highest inlet temperature in the tenant hot stream inventory is extracted upon iteration. A hot stream is extracted when the exclusion of the hot stream does alter the nominal heat recovery such that it is sufficiently close to the maximum tenant heat recovery. The parameter δ represents the acceptable tolerance between the nominal and maximum heat recovery of which a tenant heat exchanger network design can be applied to the interplant energy integration,

After the tenant internal heat integration, interplant energy integration is applied using the waste and high-grade heat from all plants involved in the CHOSYN system to develop an interplant heat exchanger network with a centralized utility system to support anchor and tenant plant operation. The resulting intra- and inter-plant energy integration

network provides participating plants further reductions in utility usage as well as provide a sustainable means to produce electricity.

3.3.2.1. Internal Tenant Heat Integration

The heat integration superstructure shown in Figure 3.4 is used to develop the heat exchanger networks for each tenant and evaluate hot stream extraction (Yee and Grossmann, 1990) (Lira, 2014).

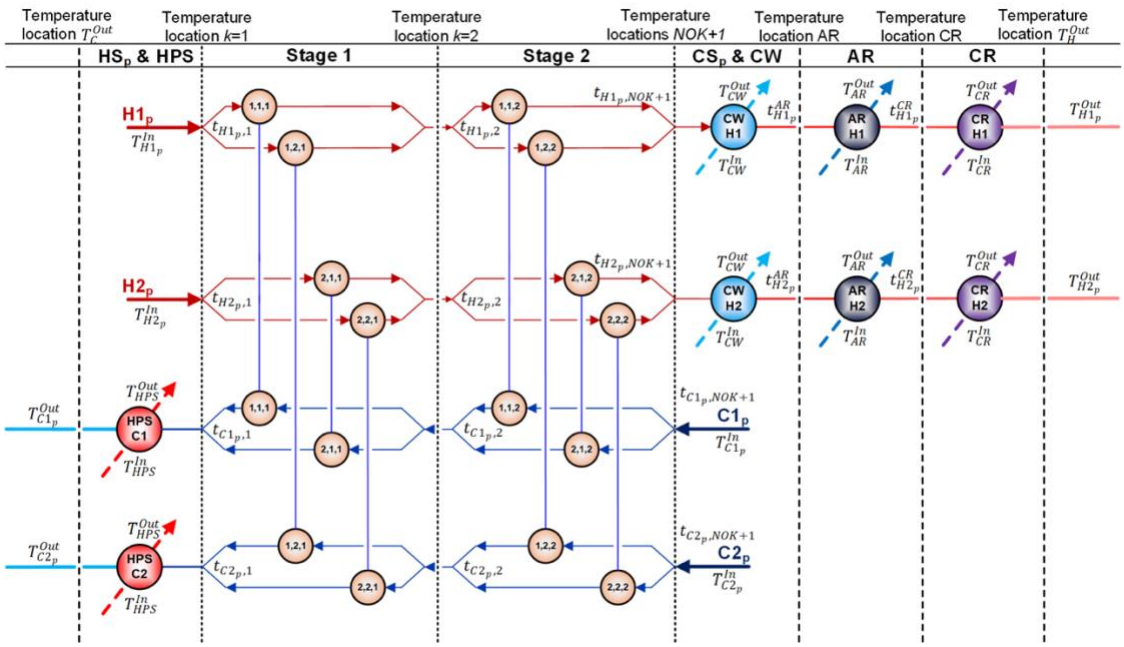

Figure 3.4: Proposed Superstructure for the Heat Integration of Tenant Plants

The proposed superstructure shown in Figure 3.4 considers the exchange of heat for any match on each stage between the hot and cold streams indicated by the sets HS_p and CS_p, respectively. After the hot streams transfer their energy to cold streams, the hot streams can transfer their remaining heat loads through coolers employing cooling water,

absorption refrigeration and compression refrigeration on the stages denoted as *CW*, AR and CR in Figure 3.4, respectively. It should be noted that the coolers in the AR and CR stages are employed when the hot streams require refrigeration below ambient temperature. Alternatively, the cold streams can complete their heating after matching with hot streams through heaters using high pressure steam on the stage denoted as HPS. The following equations in this section describe the mathematical representation of Figure 3.4 for a given tenant p. This mathematical system is optimized for each given tenant p to determine the internal heat exchanger network, recoverable high-grade heat for interplant integration and waste heat streams that would require utilities.

The heat load of hot stream i_p is equal to the sum of the heat exchanged with all cold streams in CS_p over all stages in ST and with the cooling utilities. This relation is presented as:

$$\left(T_{i_p}^{In} - T_{i_p}^{Out}\right) FCp_{i_p} = \sum_{k \in ST} \sum_{j_p \in CS_p} q_{i_p,j_p,k} + q_{i_p}^{CW} + q_{i_p}^{AR} + q_{i_p}^{CR} \quad i_p \in HS_p \qquad (17)$$

where $q_{i_p,j_p,k}$ represents the energy transferred from hot stream i_p to cold stream j_p on stage k. $q_{i_p}^{CW}$, $q_{i_p}^{AR}$, and $q_{i_p}^{CR}$ represents the energy transferred from hot stream i_p to cooling water, absorption and compression refrigeration utilities, respectively.

For any cold stream j_p, the cooling load is equal to the sum of the heat exchanged with all hot streams HS_p over all stages in ST in addition to the heat received from the high pressure steam utility. This is provided as:

$$\left(T_{j_p}^{In} - T_{j_p}^{Out}\right) FCp_{j_p} = \sum_{k \in ST} \sum_{i_p \in HS_p} q_{i_p,j_p,k} + q_{j_p}^{HPS} \qquad j_p \in CS_p \qquad (18)$$

where $q_{j_p}^{HPS}$ represents the energy transferred from high pressure steam to cold stream j_p.

The following relationships are required to determine the internal temperatures between each stage k of the proposed superstructure. For hot stream i_p, the energy balance is stated as follows:

$$\left(t_{i_p,k} - t_{i_p,k+1}\right) FCp_{i_p} = \sum_{j_p \in CS_p} q_{i_p,j_p,k} \qquad i_p \in HS_p,\ k \in ST \tag{19}$$

where $t_{i_p,k}$ is the internal temperature of hot stream i_p at the beginning of stage k.

For the cold stream j_p:

$$\left(t_{j_p,k} - t_{j_p,k+1}\right) FCp_{j_p} = \sum_{i_p \in HS_p} q_{i_p,j_p,k} \qquad j_p \in CS,\ k \in ST \tag{20}$$

where $t_{j_p,k}$ is the internal temperature of cold stream j_p at the end of stage k.

The proposed superstructure considers the use of cold utilities on hot streams over the three terminal stages. Subsequent to exchanging heat with cold streams, hot stream i_p is able to transfer heat to cooling water. This is provided as:

$$\left(t_{i_p,NOK+1} - t_{i_p}^{AR}\right) FCp_{i_p} = q_{i_p}^{CW} \qquad i_p \in HS_p \tag{21}$$

where $t_{i_p}^{AR}$ is the temperature of hot stream i_p after passing the cooling water utility.

The next stage corresponds to the heat of hot stream i_p exchanged with the absorption refrigeration utility. This is given as:

$$\left(t_{i_p}^{AR} - t_{i_p}^{CR}\right) FCp_{i_p} = q_{i_p}^{AR} \qquad i_p \in HS_p \tag{22}$$

where $t_{i_p}^{CR}$ is the temperature of hot stream i_p after passing the absorption refrigeration utility.

The option to use compression refrigeration to cool hot stream i_p to below freezing is made available on the terminal stage. This is represented as:

$$\left(t_{i_p}^{CR} - T_{i_p}^{Out}\right) FCp_{i_p} = q_{i_p}^{CR} \quad i_p \in HS_p \tag{23}$$

The option to use high pressure steam to heat cold stream j_p is included on the initial stage of the superstructure. This is provided with:

$$\left(T_{j_p}^{Out} - t_{j_p,1}\right) FCp_{j_p} = q_{j_p}^{HPS} \qquad j_p \in CS_p \tag{24}$$

A boundary condition for the proposed superstructure is given where the inlet temperature of hot stream i_p is equal to the internal temperature on the first stage of the superstructure:

$$T_{i_p}^{In} = t_{i_p,1} \qquad i_p \in HS_p \tag{25}$$

Alternatively, the inlet temperature of cold stream j_p is equal to the internal temperature on stage $NOK + 1$ of the superstructure:

$$T_{j_p}^{In} = t_{j_p,NOK+1} \qquad j_p \in CS_p \tag{26}$$

An important aspect of the proposed superstructure is the equality or decrease of temperatures upon successive stages. This behavior is modeled through the following relationships:

$$t_{i_p,k} \geq t_{i_p,k+1} \;\; i_p \in HS_p, k \in ST \tag{27}$$

$$t_{i_p,NOK+1} \geq t_{i_p}^{AR} \qquad i_p \in HS_p \tag{28}$$

$$t_{i_p}^{AR} \geq t_{i_p}^{CR} \qquad i_p \in HS_p \tag{29}$$

$$t_{i_p}^{CR} \geq T_{i_p}^{Out} \qquad i_p \in HS_p \tag{30}$$

$$T_{j_p}^{Out} \geq t_{j_p,1} \quad j_p \in CS_p \tag{31}$$

$$t_{j_p,k} \geq t_{j_p,k+1} \;\; j_p \in CS_p, k \in ST \tag{32}$$

It is significant to determine the existence of all potential heat exchange matches. A binary variable is employed to associate the existence of each match and is set to one if the match exists. Otherwise, the binary variable is zero when a match is not required. The following relation is provided for indicating matches between hot and cold streams:

$$q_{i_p,j_p,k} - Q_{i_p,j_p}^{Max} z_{i_p,j_p,k} \leq 0 \qquad i_p \in HS_p, j_p \in CS_p, k \in ST \tag{33}$$

where Q_{i_p,j_p}^{Max} and $z_{i_p,j_p,k}$ represents the maximum heat exchanged between hot stream i_p and cold stream j_p and the binary variable indicating the existence of a match between hot stream i_p and cold stream j_p on stage k, respectively.

For the coolers employing cooling water:

$$q_{i_p}^{CW} - Q_{i_p}^{Max} z_{i_p}^{CW} \leq 0 \qquad i_p \in HS_p \tag{34}$$

where $Q_{i_p}^{Max}$ and $z_{i_p}^{CW}$ represents the maximum heat exchanged by hot stream i_p and the binary variable indicating the existence of a match between hot stream i_p and cooling water.

For coolers employing absorption refrigeration:

$$q_{i_p}^{AR} - Q_{i_p}^{Max} z_{i_p}^{AR} \leq 0 \;\; i_p \in HS_p \tag{35}$$

where $z_{i_p}^{AR}$ represents the binary variable indicating the existence of a match between hot stream i_p and the absorption refrigeration utility.

For coolers employing compression refrigeration:

$$q_{i_p}^{CR} - Q_{i_p}^{Max} z_{i_p}^{CR} \leq 0 \;\; i_p \in HS_p \tag{36}$$

where $z_{i_p}^{CR}$ represents the binary variable indicating the existence of a match between hot stream i_p and the compression refrigeration utility.

For the cold streams employing high pressure steam:

$$q_{j_p}^{HPS} - Q_{j_p}^{Max} z_{j_p}^{HPS} \leq 0 \qquad j_p \in CS_p \tag{37}$$

where $Q_{j_p}^{Max}$ and $z_{j_p}^{HPS}$ represents the maximum cooling exchanged by cold stream j_p and the binary variable indicating the existence of a match between cold stream j_p and high pressure steam.

An important criterion when designing heat exchanger networks is the minimum temperature difference which directly affects the utilities cost and the capital costs of the heat exchanger network. Any exchanger of the superstructure indicated in the optimal solution must satisfy the minimum temperature difference constraints. The following logical relationships are provided to determine the temperature differences for all potential heat exchangers.

For the heat exchanger between hot stream i_p and cold stream j_p on stage k:

$$dt_{i_p,j_p,k} \leq t_{i_p,k} - t_{j_p,k} + \Delta T_{i_p,j_p}^{Max}(1 - z_{i_p,j_p,k}) \qquad i_p \in HS_p, j \in CS_p, k \in ST \tag{38}$$

$$dt_{i_p,j_p,k+1} \leq t_{i_p,k+1} - t_{j_p,k+1} + \Delta T_{i_p,j_p}^{Max}(1 - z_{i_p,j_p,k}) \qquad i_p \in HS_p,\ j_p \in CS_p,\ k \in ST \tag{39}$$

where $dt_{i_p,j_p,k}$ and $\Delta T_{i_p,j_p}^{Max}$ represents the temperature difference between hot stream i_p and cold stream j_p on stage k and the maximum temperature difference between hot stream i_p and cold stream j_p, respectively.

For the coolers employing cooling water:

$$dt_{i_p}^{CW-1} \leq t_{i_p,NOK+1} - T_{CW}^{Out} + \Delta T_{i_p}^{CWMax}\left(1 - z_{i_p}^{CW}\right) \qquad i_p \in HS_p \tag{40}$$

$$dt_{i_p}^{CW-2} \leq t_{i_p}^{AR} - T_{CW}^{Out} + \Delta T_{i_p}^{CWMax}\left(1 - z_{i_p}^{CW}\right) \qquad i_p \in HS_p \tag{41}$$

where $dt_{i_p}^{CW-1}$ and $dt_{i_p}^{CW-2}$ are the temperature differences between hot stream i_p and cooling water at the $NOK+1$ and AR temperature locations, respectively. $\Delta T_{i_p}^{CWMax}$ represents the maximum temperature difference between hot stream i_p and cooling water.

For the absorption refrigeration coolers:

$$dt_{i_p}^{AR-1} \leq t_{i_p}^{AR} - T_{AR}^{Out} + \Delta T_{i_p}^{ARMax}\left(1 - z_{i_p}^{AR}\right) \qquad i_p \in HS_p \tag{42}$$

$$dt_{i_p}^{AR-2} \leq t_{i_p}^{CR} - T_{CR}^{In} + \Delta T_{i_p}^{ARMax}\left(1 - z_{i_p}^{AR}\right) \qquad i_p \in HS_p \tag{43}$$

where $dt_{i_p}^{AR-1}$ and $dt_{i_p}^{AR-2}$ are the temperature differences between hot stream i_p and the absorption refrigeration utility at the AR and CR temperature locations, respectively. $\Delta T_{i_p}^{ARMax}$ represents the maximum temperature difference between hot stream i_p and the absorption refrigeration utility.

For the compression refrigeration coolers:

$$dt_{i_p}^{CR-1} \leq t_{i_p}^{CR} - T_{CR}^{Out} + \Delta T_{i_p}^{CRMax}\left(1 - z_{i_p}^{CR}\right) \qquad i_p \in HS_p \tag{44}$$

where $dt_{i_p}^{CR-1}$ and $\Delta T_{i_p}^{CRMax}$ are the temperature differences between hot stream i_p and the compression refrigeration utility at CR temperature location and maximum temperature difference between hot stream i_p and the compression refrigeration utility, respectively. Notice that the end of the CR stage is the boundary of the superstructure where the temperatures are known parameters ($T_{i_p}^{Out} - T_{CR}^{In}$). Therefore, this additional temperature difference constraint is not necessary.

For the hot utility:

$$dt_{j_p}^{HPS-2} \leq T_{HPS}^{Out} - t_{j_p,1} + \Delta T_{j_p}^{HPSMax}(1 - z_{j_p}^{HPS}) \qquad j_p \in CS_p \tag{45}$$

where $dt_{j_p}^{HPS-2}$ and $\Delta T_{j_p}^{HPSMax}$ are the temperature differences between cold stream j_p and the high pressure steam at stage one temperature location and maximum temperature difference between cold stream j_p and the high pressure steam, respectively. Similarly, it should be noted that the temperature difference constraint for this stage is not required because these temperatures are given by the problem statement ($T_{HPS}^{In} - T_{j_p}^{Out}$).

Finally, the temperature difference for all heat exchangers must be greater than the minimum temperature difference:

$$\Delta T_{min} \leq dt_{i_p,j_p,k} \qquad i_p \in HS_p, j_p \in CS_p, k \in ST \tag{46}$$

$$\Delta T_{min} \leq dt_{i_p}^{CW-1} \qquad i_p \in HS_p \tag{47}$$

$$\Delta T_{min} \leq dt_{i_p}^{CW-2} \qquad i_p \in HS_p \tag{48}$$

$$\Delta T_{min} \leq dt_{i_p}^{AR-1} \qquad i_p \in HS_p \tag{49}$$

$$\Delta T_{min} \leq dt_{i_p}^{AR-2} \qquad i_p \in HS_p \tag{50}$$

$$\Delta T_{min} \leq dt_{i_p}^{CR-1} \qquad i_p \in HS_p \tag{51}$$

$$\Delta T_{min} \leq dt_{j_p}^{HPS-2} \qquad j_p \in CS_p \tag{52}$$

where ΔT_{min} is the minimum temperature difference.

3.3.2.2. Interplant Energy Targeting

The superstructure employed to determine the heat exchanger network for tenants is expanded upon for the interplant energy integration. The superstructure for the interplant energy integration builds upon the previous superstructure by including the option to transfer heat to generate electricity and refrigeration. Whereas the previous

superstructure associated a cost to use absorption refrigeration as a cooling service, this superstructure allows for the transfer of low grade heat to generate below ambient cooling.

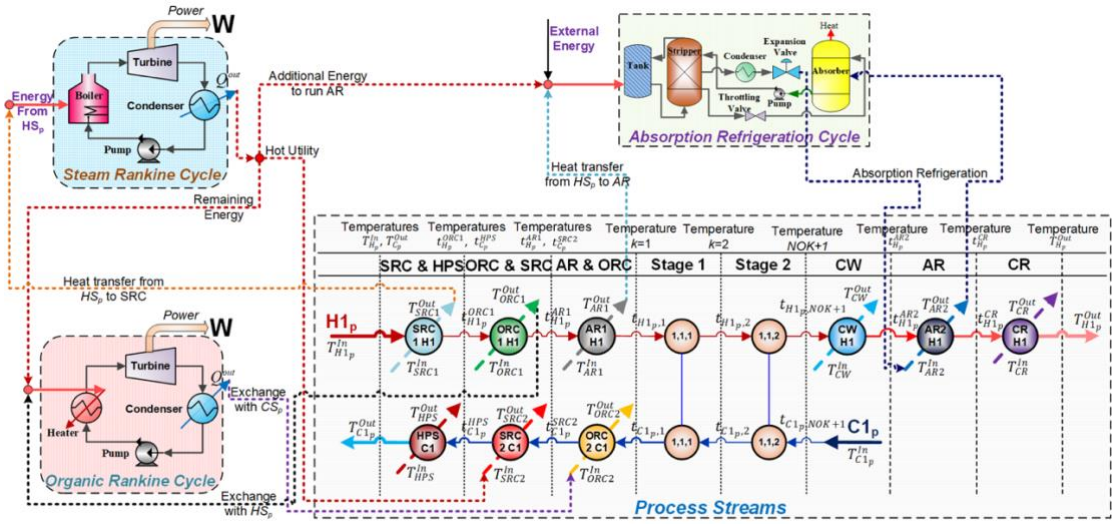

Figure 3.5: Schematic Representation of the Proposed Integrated System

The proposed superstructure shown in Figure 3.5 considers the heat exchange for any match between hot streams and cold streams on each stage as well as the heat transfer from hot streams to the AR cycle, SRC and ORC. The hot streams can satisfy their cooling demands by using cooling water and by using absorption and compression refrigeration services when they require refrigeration below ambient temperature. The cold streams have the possibility to exchange heat with the SRC, ORC and hot process streams on any stage of the superstructure. The cold streams can also satisfy their heating loads using high pressure steam as a hot utility.

The heat load of hot stream i_p is equal to the sum of the heat exchanged with all cold streams in CS_p over all stages in ST and for all plants in $PLANT$, the heat transferred to the SRC, ORC and the section of the AR cycle that accepts low grade heat, and the heat exchanged with cooling water, compression refrigeration and the section of the AR cycle that provides sub-ambient cooling. This is provided as:

$$\left(T_{i_p}^{In} - T_{i_p}^{Out}\right) FCp_{i_p} = q_{i_p}^{SRC1} + q_{i_p}^{ORC1} + q_{i_p}^{AR1} + \sum_{p'} \sum_{k \in ST} \sum_{j_{p'} \in CS_{p'}} q_{i_p, j_{p'}, k} + q_{i_p}^{CW} + q_{i_p}^{AR2} + q_{i_p}^{CR} \qquad p \in PLANT, i_p \in HS_p \tag{53}$$

where $q_{i_p}^{SRC1}$ represents the heat accepted by the SRC, $q_{i_p}^{ORC1}$ represents the heat accepted by the ORC and $q_{i_p}^{AR1}$ and $q_{i_p}^{AR2}$ represents the heating accepted and cooling provided by the AR cycle, respectively.

The cooling load of cold stream j_p is equal to the sum of heat exchanged with all hot streams in HS_p over all stages in ST and for all plants in $PLANT$ and with the heat received from the SRC, ORC and high pressure steam utility. This is given as:

$$\left(T_{j_p}^{Out} - T_{j_p}^{In}\right) FCp_{j_p} = \sum_{p'} \sum_{k \in ST} \sum_{i_{p'} \in HS_{p'}} q_{i_{p'}, j_p, k} + q_{j_p}^{ORC2} + q_{j_p}^{SRC2} + q_{j_p}^{HPS} \qquad p \in PLANT, j_p \in CS_p \tag{54}$$

where $q_{j_p}^{SRC2}$ and $q_{j_p}^{ORC2}$ represents the heat provided by the SRC and ORC.

The next relationships are used to determine the internal temperatures for each stage of the proposed superstructure. For each hot stream, the energy balances are stated as follows:

$$\left(T_{i_p}^{In} - t_{i_p}^{ORC1}\right) FCp_{i_p} = q_{i_p}^{SRC1} \qquad p \in PLANT, i_p \in HS_p \tag{55}$$

$$\left(t_{i_p}^{ORC1} - t_{i_p}^{AR1}\right) FCp_{i_p} = q_{i_p}^{ORC1} \qquad p \in PLANT, i_p \in HS_p \tag{56}$$

$$\left(t_{i_p}^{AR1} - t_{i_p,1}\right) FCp_{i_p} = q_{i_p}^{AR1} \quad p \in PLANT, i_p \in HS_p \tag{57}$$

$$\left(t_{i_p,k} - t_{i_p,k+1}\right) FCp_{i_p} = \sum_{p'} \sum_{j_{p'} \in CS_{p'}} q_{i_p,j_{p'},k} \qquad p \in PLANT, \quad i_p \in HS_p, \quad k \in ST \tag{58}$$

where $t_{i_p}^{ORC1}$ and $t_{i_p}^{AR1}$ are the internal temperatures of hot stream i_p at the beginning of the stages hosting exchangers that can accept heat to drive the ORC and AR cycle, respectively.

The hot streams can transfer their energy to cooling water at the internal stage section exit of the superstructure. This is given as:

$$\left(t_{i_p,NOK+1} - t_{i_p}^{AR2}\right) FCp_{i_p} = q_{i_p}^{CW} \qquad p \in PLANT, i_p \in HS_p \tag{59}$$

where $t_{i_p}^{AR2}$ is the internal temperature of hot stream i_p leaving the stage hosting the cooling water exchanger.

Subsequent to the cooling water stage, the hot streams that require refrigeration can be cooled exchanging their energy with the AR cycle and compression refrigeration utility. This is provided by the following:

$$\left(t_{i_p}^{AR2} - t_{i_p}^{CR}\right) FCp_{i_p} = q_{i_p}^{AR2} \quad p \in PLANT, i_p \in HS_p \tag{60}$$

$$\left(t_{i_p}^{CR} - T_{i_p}^{Out}\right) FCp_{i_p} = q_{i_p}^{CR} \quad p \in PLANT, i_p \in HS_p \tag{61}$$

where $t_{i_p}^{CR}$ is the internal temperature of hot stream i_p at the entrance of the compression refrigeration cooling stage.

For the cold streams:

$$\left(t_{j_p,k} - t_{j_p,k+1}\right) FCp_{j_p} = \sum_{p'} \sum_{i_{p'} \in HS_{p'}} q_{i_{p'},j_p,k} \qquad p \in PLANT, \quad j_p \in CS_p, \quad k \in ST \tag{62}$$

After the cold streams have exchanged heat on the inner stages of the superstructure, the cold stream target temperatures can be achieved by obtaining heat from the SRC, ORC and high pressure steam utility. These relations are given as:

$$\left(t_{j_p}^{SRC2} - t_{j_p,1}\right) FCp_{j_p} = q_{j_p}^{ORC2}, \qquad p \in PLANT, j_p \in CS_p \tag{63}$$

$$\left(t_{j_p}^{HPS} - t_{j_p}^{SRC2}\right) FCp_{j_p} = q_{j_p}^{SRC2}, \qquad p \in PLANT, j_p \in CS_p \tag{64}$$

$$\left(T_{j_p}^{Out} - t_{j_p}^{HPS}\right) FCp_{j_p} = q_{j_p}^{HPS}, \qquad p \in PLANT, j_p \in CS_p \tag{65}$$

where $t_{j_p}^{SRC2}$ is the internal temperature of cold stream j_p as it exits the stage hosting the exchanger that provides heat from the SRC.

It is significant to state that the inlet temperature for cold stream j_p is equal to the temperature of stage $NOK + 1$ in the superstructure. This is provided as:

$$T_{j_p}^{In} = t_{j_p,NOK+1}, \qquad p \in PLANT, j_p \in CS_p \tag{66}$$

The temperatures in the superstructure decrease upon successive stages. This behavior is modeled through the next relationships:

$$T_{i_p}^{In} \geq t_{i_p}^{ORC1}, \quad p \in PLANT, i_p \in HS_p \tag{67}$$

$$t_{i_p}^{ORC1} \geq t_{i_p}^{AR1}, \; p \in PLANT, i_p \in HS_p \tag{68}$$

$$t_{i_p}^{AR1} \geq t_{i_p,1}, \quad p \in PLANT, i_p \in HS_p \tag{69}$$

$$t_{i_p,k} \geq t_{i_p,k+1}, p \in PLANT, i_p \in HS_p, k \in ST \tag{70}$$

$$t_{i_p,NOK+1} \geq t_{i_p}^{AR2}, \qquad p \in PLANT, i_p \in HS_p \tag{71}$$

$$t_{i_p}^{AR2} \geq t_{i_p}^{CR}, \quad p \in PLANT, i_p \in HS_p \tag{72}$$

$$t_{i_p}^{CR} \geq T_{i_p}^{Out}, \quad p \in PLANT, i_p \in HS_p \tag{73}$$

$$T_{j_p}^{Out} \geq t_{j_p}^{HPS}, \ p \in PLANT, j_p \in CS_p \tag{74}$$

$$t_{j_p}^{HPS} \geq t_{j_p}^{SRC2}, \ p \in PLANT, j_p \in CS_p \tag{75}$$

$$t_{j_p}^{SRC2} \geq t_{j_p,1}, \ p \in PLANT, j_p \in CS_p \tag{76}$$

$$t_{j_p,k} \geq t_{j_p,k+1}, p \in PLANT, j_p \in CS_p, k \in ST \tag{77}$$

The following constraints are used to determine the existence of heat exchangers. A binary variable is employed and is equal to one if a exchanger exists. The following relationships are given for the existence of the heat exchangers that draw heat from hot stream i_p to drive the ORC and SRC:

$$q_{i_p}^{SRC1} - Q_{i_p}^{Max} z_{i_p}^{SRC1} \leq 0, \qquad p \in PLANT, i_p \in HS_p \tag{78}$$

$$q_{i_p}^{ORC1} - Q_{i_p}^{Max} z_{i_p}^{ORC1} \leq 0, \qquad p \in PLANT, i_p \in HS_p \tag{79}$$

where $z_{i_p}^{SRC1}$ and $z_{i_p}^{ORC1}$ are the binary variables indicating the existence of heat exchangers accepting heat from hot stream i_p to power the SRC and ORC, respectively.

For the heat transferred from hot stream i_p to the AR cycle:

$$q_{i_p}^{AR1} - Q_{i_p}^{Max} z_{i_p}^{AR1} \leq 0, \qquad p \in PLANT, i_p \in HS_p \tag{80}$$

Where $z_{i_p}^{AR1}$ is the binary variable indicating if the heat exchanger accepting low grade from hot stream i_p to drive the AR cycle exists.

For the heat exchanger matching hot stream i_p with cold stream j_p:

$$q_{i_p,j_{p'},k} - Q^{Max}_{i_p,j_{p'}} z_{i_p,j_{p'},k} \leq 0, p \in PLANT, i_p \in HS_p, p' \in PLANT, j_{p'} \in CS_{p'}, k \in ST \quad (81)$$

For the cooler using cooling water on hot stream i_p:

$$q^{CW}_{i_p} - Q^{Max}_{i_p} z^{CW}_{i_p} \leq 0, \qquad p \in PLANT, i_p \in HS_p \quad (82)$$

For the cooler refrigerating hot stream i_p through via the AR cycle:

$$q^{AR2}_{i_p} - Q^{Max}_{i_p} z^{AR2}_{i_p} \leq 0, \qquad p \in PLANT, i_p \in HS_p \quad (83)$$

where $z^{AR2}_{i_p}$ is the binary variable indicating if the exchanger providing sub-ambient cooling from the AR cycle to hot stream i_p exists.

For the cooler refrigerating hot stream i_p through the compression refrigeration utility:

$$q^{CR}_{i_p} - Q^{Max}_{i_p} z^{CR}_{i_p} \leq 0, \qquad p \in PLANT, i_p \in HS_p \quad (84)$$

Binary variables are employed denoting the existence of a heat exchanger for cold stream j_p receiving heat from the SRC and ORC. These are given as:

$$q^{ORC2}_{j_p} - Q^{Max}_{j_p} z^{ORC2}_{j_p} \leq 0, \qquad p \in PLANT, j_p \in CS_p \quad (85)$$

$$q^{SRC2}_{j_p} - Q^{Max}_{j_p} z^{SRC2}_{j_p} \leq 0, \qquad p \in PLANT, j_p \in CS_p \quad (86)$$

where $z^{SRC2}_{j_p}$ and $z^{ORC2}_{j_p}$ are the binary variables indicating the existence of heat exchangers providing heat to cold stream j_p from the SRC and ORC, respectively.

For the high pressure steam heater employed to heat cold stream j_p:

$$q^{HPS}_{j_p} - Q^{Max}_{j_p} z^{HPS}_{j_p} \leq 0, \qquad p \in PLANT, j_p \in CS_p \quad (87)$$

Each heat exchanger in the interplant energy superstructure shown in Figure 5 is required to maintain a minimum temperature difference if applied. However, it is not necessary to fulfill of the minimum temperature difference constraints for the heat exchangers in the superstructure that do not exist in the optimal solution. This is modeled through the following logical relationships.

For the exchanger transferring heat from hot stream i_p to the SRC:

$$dt_i^{SRC1-2} \leq t_{i_p}^{ORC1} - T_{SRC1}^{In} + \Delta T_{i_p}^{SRCMax}(1 - z_{i_p}^{SRC1}), \qquad p \in PLANT, \qquad i_p \in HS_p \tag{88}$$

where $dt_{i_p}^{SRC1-2}$ and $\Delta T_{i_p}^{SRCMax}$ are the temperature difference between hot stream i_p at the ORC temperature location and the inlet to the SRC heat exchanger and maximum temperature difference between hot stream i_p and the SRC stream inlet, respectively. Notice in Figure 5 for the other end of this heat exchanger, the temperatures are known parameters ($T_{i_p}^{In} - T_{SRC1}^{Out}$). Therefore, this constraint is not required.

For the heat exchanger transferring heat from hot stream i_p to the ORC:

$$dt_{i_p}^{ORC1-1} \leq t_{i_p}^{ORC1} - T_{ORC1}^{Out} + \Delta T_{i_p}^{ORC1Max}(1 - z_{i_p}^{ORC1}), \qquad p \in PLANT, \qquad i_p \in HS_p \tag{89}$$

$$dt_{i_p}^{ORC1-2} \leq t_{i_p}^{AR1} - T_{ORC1}^{In} + \Delta T_{i_p}^{ORC1Max}\left(1 - z_{i_p}^{ORC1}\right), \qquad p \in PLANT, \qquad i_p \in HS_p \tag{90}$$

where $dt_{i_p}^{ORC1-1}$ and $dt_{i_p}^{ORC1-2}$ are the temperature difference between hot stream i_p and the ORC stream outlets and inlets, respectively. $\Delta T_{i_p}^{ORC1Max}$ is the maximum temperature difference between hot stream i_p and the ORC streams.

For the heat exchanger withdrawing heat from hot stream i_p to power the AR cycle:

$$dt_{i_p}^{AR1-1} \leq t_{i_p}^{AR1} - T_{AR1}^{Out} + \Delta T_{i_p}^{AR1Max}(1 - z_{i_p}^{AR1}), \quad p \in PLANT, i_p \in HS_p \tag{91}$$

$$dt_{i_p}^{AR1-2} \leq t_{i_p,1} - T_{AR1}^{In} + \Delta T_{i_p}^{AR1Max}(1 - z_{i_p}^{AR1}), \quad p \in PLANT, i_p \in HS_p \tag{92}$$

where $dt_{i_p}^{AR1-1}$ and $dt_{i_p}^{AR1-2}$ are the temperature difference between hot stream i_p and the AR cycle stream outlets and inlets, respectively. $\Delta T_{i_p}^{AR1Max}$ is the maximum temperature difference between hot stream i_p and the AR cycle streams.

For the heat exchanger between hot stream i_p and cold stream $j_{p'}$:

$$dt_{i_p,j_{p'},k} \leq t_{i_p,k} - t_{j_{p'},k} + \Delta T_{i_p,j_{p'}}^{Max}(1 - z_{i_p,j_{p'},k}), \quad p \in PLANT, \quad i_p \in HS_p, \quad p' \in PLANT, j_{p'} \in CS_{p'}, k \in ST \tag{93}$$

$$dt_{i_p,j_{p'},k+1} \leq t_{i_p,k+1} - t_{j_{p'},k+1} + \Delta T_{i_p,j_{p'}}^{Max}(1 - z_{i_p,j_{p'},k}), \quad p \in PLANT, \quad i_p \in HS_p, p' \in PLANT, j_{p'} \in CS_{p'}, k \in ST \tag{94}$$

For the coolers employing cooling water for hot stream i_p:

$$dt_{i_p}^{CW-1} \leq t_{i_p,NOK+1} - T_{CW}^{Out} + \Delta T_{i_p}^{CWMax}\left(1 - z_{i_p}^{CW}\right), \quad p \in PLANT, \quad i_p \in HS_p \tag{95}$$

$$dt_{i_p}^{CW-2} \leq t_{i_p}^{AR2} - T_{CW}^{IN} + \Delta T_{i_p}^{CWMax}\left(1 - z_{i_p}^{CW}\right), \quad p \in PLANT, \quad i_p \in HS_p \tag{96}$$

For the AR cycle heat exchanger providing sub-ambient cooling to hot process stream i_p:

$$dt_{i_p}^{AR2-1} \leq t_{i_p}^{AR2} - T_{AR2}^{Out} + \Delta T_{i_p}^{AR2Max}(1 - z_{i_p}^{AR2}), \quad p \in PLANT, i_p \in HS_p \tag{97}$$

$$dt_{i_p}^{AR2-2} \leq t_{i_p}^{CR} - T_{AR2}^{In} + \Delta T_{i_p}^{AR2Max}(1 - z_{i_p}^{AR2}), \qquad p \in PLANT, i_p \in HS_p \qquad (98)$$

where $dt_{i_p}^{AR1-1}$ and $dt_{i_p}^{AR1-2}$ are the temperature difference between hot stream i_p and the AR cycle stream outlets and inlets, respectively. $\Delta T_{i_p}^{AR1Max}$ is the maximum temperature difference between hot stream i_p and the AR cycle streams.

For the compression refrigeration heat exchanger used to cool hot stream i_p:

$$dt_{i_p}^{CR-1} \leq t_{i_p}^{CR} - T_{CR}^{Out} + \Delta T_{i_p}^{CRMax}(1 - z_{i_p}^{CR}), \qquad p \in PLANT, i_p \in HS_p \qquad (99)$$

As with the tenant heat integration superstructure, the temperatures are known parameters ($T_{i_p}^{Out} - T_{CR}^{In}$). Therefore, this constraint is not required.

For the ORC heat exchanger providing heat to cold stream j_p:

$$dt_{j_p}^{ORC2-1} \leq T_{ORC2}^{In} - t_{j_p}^{SRC2} + \Delta T_{j_p}^{ORC2Max}(1 - z_{j_p}^{ORC2}), \qquad p \in PLANT, j_p \in CS_p \qquad (100)$$

$$dt_{j_p}^{ORC2-2} \leq T_{ORC2}^{Out} - t_{j_p,1} + \Delta T_{j_p}^{ORC2Max}(1 - z_{j_p}^{ORC2}), \qquad p \in PLANT, j_p \in CS_p \qquad (101)$$

where $dt_{j_p}^{ORC2-1}$ and $dt_{j_p}^{ORC2-2}$ are the temperature differences between cold stream j_p and the ORC outlets and inlets, respectively. $\Delta T_{i_p}^{ORC2Max}$ is the maximum temperature difference between cold stream j_p and the ORC streams.

For the SRC exchanger providing heat to cold stream j_p:

$$dt_{j_p}^{SRC2-1} \leq T_{SRC2}^{In} - t_{j_p}^{HPS} + \Delta T_{j_p}^{SRC2Max}(1 - z_{j_p}^{SRC2}), \qquad p \in PLANT, j_p \in CS_p \qquad (102)$$

$$dt_j^{SRC2-2} \leq T_{SRC2}^{Out} - t_{j_p}^{SRC2} + \Delta T_{j_p}^{SRC2Max}(1 - z_{j_p}^{SRC2}), \qquad p \in PLANT, j_p \in CS_p \tag{103}$$

where $dt_{j_p}^{SRC2-1}$ and $dt_{j_p}^{SRC2-2}$ are the temperature differences between cold stream j_p and the SRC stream outlets and inlets, respectively. $\Delta T_{i_p}^{SRC2Max}$ is the maximum temperature difference between cold stream j_p and the SRC streams.

For the high pressure steam heaters providing heat to cold stream j_p:

$$dt_{j_p}^{HPS-2} \leq T_{HPS}^{Out} - t_{j_p}^{HPS} + \Delta T_{j_p}^{HPSMax}(1 - z_{j_p}^{HPS}), \quad p \in PLANT, j_p \in CS_p \tag{104}$$

Notice in Figure 5 that the temperatures for the cold stream j_p outlet and the high pressure steam inlet are given by the data of the problem ($T_{j_p}^{Out} - T_{HPS}^{In}$).

All the temperature differences for the heat exchangers in the superstructure must be greater than the minimum temperature difference:

$$\Delta T_{min} \leq dt_{i_p}^{SRC1-2}, \quad p \in PLANT, i_p \in HS_p \tag{105}$$

$$\Delta T_{min} \leq dt_{i_p}^{ORC1-1}, \quad p \in PLANT, i_p \in HS_p \tag{106}$$

$$\Delta T_{min} \leq dt_{i_p}^{ORC1-2}, \quad p \in PLANT, i_p \in HS_p \tag{107}$$

$$\Delta T_{min} \leq dt_{i_p}^{AR1-1}, \quad p \in PLANT, i_p \in HS_p \tag{108}$$

$$\Delta T_{min} \leq dt_{i_p}^{AR1-2}, \quad p \in PLANT, i_p \in HS_p \tag{109}$$

$$\Delta T_{min} \leq dt_{i_p,j_{p'},k}, \quad p \in PLANT, i_p \in HS_p, p' \in PLANT, j_{p'} \in CS_{p'}, k \in ST \tag{110}$$

$$\Delta T_{min} \leq dt_{i_p}^{CW1-1}, \quad p \in PLANT, i_p \in HS_p \tag{111}$$

$$\Delta T_{min} \leq dt_{i_p}^{CW1-2}, \quad p \in PLANT, i_p \in HS_p \tag{112}$$

$$\Delta T_{min} \leq dt_{i_p}^{AR2-1}, \quad p \in PLANT, i_p \in HS_p \tag{113}$$

$$\Delta T_{min} \leq dt_{i_p}^{AR2-2}, \quad p \in PLANT, i_p \in HS_p \tag{114}$$

$$\Delta T_{min} \leq dt_{i_p}^{CR-1}, \quad p \in PLANT, i_p \in HS_p \tag{115}$$

$$\Delta T_{min} \leq dt_{j_p}^{ORC2-1}, \quad p \in PLANT, j \in CS_p \tag{116}$$

$$\Delta T_{min} \leq dt_{j_p}^{ORC2-2}, \quad p \in PLANT, j \in CS_p \tag{117}$$

$$\Delta T_{min} \leq dt_{j_p}^{SRC2-1}, \quad p \in PLANT, j \in CS_p \tag{118}$$

$$\Delta T_{min} \leq dt_{j_p}^{SRC2-2}, \quad p \in PLANT, j \in CS_p \tag{119}$$

$$\Delta T_{min} \leq dt_{j_p}^{HPS-2}, \quad p \in PLANT, j \in CS_p \tag{120}$$

This work considers efficiency factors to model the operation of both power cycles and a coefficient of performance to model the AR cycle. COP^{AR} is defined as the coefficient of performance for the AR cycle. The model defines the efficiency factors for the SRC and ORC as μ^{SRC} and μ^{ORC}, respectively. The proposed superstructure considers the interactions between the thermodynamic cycles considered and the process streams to achieve an integrated scheme.

The power generated by the SRC depends on an efficiency factor to represent the performance of this cycle. Thus, the power produced by the SRC is directly related with the external heat supplied as follows:

$$Power^{SRC} = \mu^{SRC} \sum_p \sum_{i_p \in HS_p} q_{i_p}^{SRC1} \tag{121}$$

where $Power^{SRC}$ is the power produced by the SRC.

After the external energy is used to produce power, the steam is generated at the exit of the turbine of the SRC is available to provide energy to the AR cycle, the ORC and cold streams. This is provided as:

$$Q_{SRC}^{MPS} = Q_{AR}^{MPS} + Q_{ORC}^{MPS} + \sum_p \sum_{j_p \in CS_p} q_{j_p}^{SRC2} \quad (122)$$

where Q_{SRC}^{MPS} is the heat provided by the steam generated by the exit of the SRC turbine. Q_{AR}^{MPS} and Q_{ORC}^{MPS} is the heat from the SRC allocated to the AR cycle and ORC, respectively.

The overall energy balance for the SRC is represented by the following equation:

$$Power^{SRC} = \sum_p \sum_{i_p \in HS_p} q_{i_p}^{SRC1} - (Q_{SRC}^{MPS} + Q_{SRC}^{CW}) \quad (123)$$

where Q_{SRC}^{CW} is the heat that the SRC rejects to cooling water.

The desired functionality of the AR cycle is that it supplies a cooling load below the ambient temperature to be used by hot streams. The excess heat of the hot streams as well as part of the energy provided by the SRC are used to drive the AR cycle. This energy balance is stated as follows:

$$\sum_p \sum_{i_p \in HS_p} q_{i_p}^{AR2} = COP^{AR}(\sum_p \sum_{i_p \in HS_p} q_{i_p}^{AR1} + Q_{AR}^{MPS} + Q_{AR}^{External}) \quad (124)$$

where $Q_{AR}^{External}$ denotes the supplemental heat supplied to drive the AR cycle.

The power produced by the ORC is given by the equation as follows:

$$Power^{ORC} = \mu^{ORC}(\sum_p \sum_{i_p \in HS_p} q_{i_p}^{ORC1} + Q_{ORC}^{MPS}) \quad (125)$$

where $Power^{ORC}$ is the power produced by the ORC.

The next energy balance models the performance of the ORC. This is given as:

$$Power^{ORC} = (\sum_p \sum_{i_p \in HS_p} q_{i_p}^{ORC1} + Q_{ORC}^{MPS}) - (\sum_p \sum_{j_p \in CS_p} q_{j_p}^{ORC2} + Q_{ORC}^{CW}) \quad (126)$$

where Q_{ORC}^{CW} is the heat removed from the ORC via cooling water.

3.4. Case Study

The case study developed by Topolski et al. (2018) is used to demonstrate the application of the proposed approach. This case study entails the construction of a

CHOSYN near a stranded natural gas field to efficiently produce commodity chemicals. The two plants proposed as anchor plants include those that convert methane into butadiene and benzene. Table 3.1 details the components flowrates of the identified byproduct and waste streams for mass integration.

Table 3.1: Flowrates (in kmol/h) of the Chemical Species Discharged from the Two Anchor Plants (reprinted from Topolski et al., 2018)

Species	Butadiene Plant	Benzene Plant	Total
H_2	225	300	525
CO_2	160	40	200
C_2H_2	30	0	30
C_2H_4	25	0	25
C_4H_6	25	0	25
C_6H_6	0	25	25
$C_{10}H_8$	0	80	80

Table 3.2 provides the candidate tenants and products that are considered for invitation and to manufacture, respectively. These tenants are represented by their characteristic reactions and have an associated annual capital cost, non-feedstock operating cost and process yield.

Table 3.2: Potential Products for the Tenants and Relevant Data (adapted from Topolski et al., 2018)

Tenant Index	Main Product	Basic Chemistry	Non-Feedstock Op. Cost ($/kmol product)	Annualized Fixed Cost ($/yr)*	Comments
1	Acetaldehyde	$C_2H_2 + H_2O \rightarrow CH_3CHO$	17.5	$6.8*10^5*P^{0.7}$	98% of maximum theoretical yield is obtained
2	Ethylene Oxide	$C_2H_4 + 0.5\ O_2 \rightarrow C_2H_4O$	11.1	$8.5*10^5*P^{0.65}$	95% of maximum theoretical yield is obtained
3	Methanol (via partial oxidation)	$CH_4 + ½\ O_2 \rightarrow CH_3OH$	7.6	$9.8*10^5*P^{0.6}$	90% of maximum theoretical yield is obtained
4	Methanol (via CO_2 hydrogenation)	$CO_2 + 3\ H_2 \rightarrow CH_3OH + H_2O$	13.9	$3.6*10^5*P^{0.63}$	85% of maximum theoretical yield is obtained
5	Propylene	$CH_3OH \rightarrow 1/3\ C_3H_6 + H_2O$	19.2	$1.7*10^5*P^{0.7}$	0.4 tonne of propylene and ethylene is produced per tonne of methanol.**
6	Phthalic Anhydride	$C_{10}H_8 + 4.5\ O_2 \rightarrow C_8H_4O_3 + 2\ CO_2 + 2\ H_2O$	41.3	$23.1*10^5*P^{0.6}$	93% of maximum theoretical yield is obtained
7	Styrene Butadiene Rubber	$C_6H_6 + C_2H_4 \rightarrow C_8H_{10}$ $C_8H_{10} \rightarrow C_8H_8 + H_2$ $C_4H_6 + C_8H_8 \rightarrow C_{12}H_{14}$	36.7	$17.6*10^5*P^{0.6}$	97% of maximum theoretical yield is obtained

*Based on a 10-year linear depreciation scheme with P being the flowrate of the main product in kmol/h
**Propylene and ethylene are assumed to be valued at the same price

Table 3.3, Table 3.4 and Table 3.5 provide the external raw material price and availability, the transfer pricing for components traded between plants and the candidate product prices with their respective demand.

Table 3.3: External Source Price and Availability (reprinted from Topolski et al., 2018)

Fresh Source	Purchased Price ($/kmol)	Maximum Available Supply (kmol/h)
CH4	2.1	300
O2	6.4	150
H2O (steam)	0.1	250

Table 3.4: Values* of Species in Streams Discharged from Anchor Plants (reprinted from Topolski et al., 2018)

Species	Value ($/kmol)
H_2	0.35
CO_2	0.00
C_2H_2	0.20
C_2H_4	0.15
C_4H_6	0.20
C_6H_6	0.30
$C_{10}H_8$	0.10

*The value of the species is also what another plant would pay to obtain the species from another plant

Table 3.5: Selling Prices for Main Products of Prospective Tenants with respective Market Demands (reprinted from Topolski et al., 2018)

Potential Main Products for Tenants	Selling Price ($/kmol)	Maximum Market Demand (kmol/h)
Acetaldehyde CH_3CHO	43	150
Ethylene Oxide C_2H_4O	77	100
Methanol CH_3OH	39	450
Propylene C_3H_6	69	100
Phthalic Anhydride $C_8H_4O_3$	265	75
Styrene Butadiene Rubber $C_{12}H_{14}$	278	50

Table 3.6 provides the anchor hot and cold streams that are identified for interplant energy integration. These plants are assumed to be built and internally heat integrated. Table 6 displays the hot and cold streams from those plants that are consuming utilities which could be used in later energy integration. Table 3.7 shows the types of utilities available for all the plants at this location with their respective cost.

Table 3.6: Anchor Plant Heat Stream Inventory (Abedi, 2007, Özinan and El-Halwagi, 2018, and Pérez-Uresti et al., 2017)

Anchor	Anchor Index p	Stream Index i_p, j_p	Inlet Temperature [K]	Outlet Temperature [K]	FCp [kW/K]
Methane to Butadiene Plant	A1	$H1_{A1}$	423	298	187.5
		$H2_{A1}$	273	200	118.3
		$H3_{A1}$	396.1	313	304.5
		$H4_{A1}$	365	313	393.8
		$H5_{A1}$	381	313	1580.4
		$H6_{A1}$	423	313	136.6
		$H7_{A1}$	391	322	34.9
		$C1_{A1}$	667.7	755	156.3
		$C2_{A1}$	726	755	67.8
Methane to Benzene Plant	A2	$H1_{A2}$	598.8	473	249
		$H2_{A2}$	410.9	293	158
		$C1_{A1}$	1063	1073	223

Table 3.7: Available Utilities and Service Cost

Utility	Cost ($/yr-kW)
Cooling Water	20
Absorption Refrigeration	50
Compression Refrigeration	160
High Pressure Steam	150
Absorption External Cooling	25

The following parameters were considered in the tenant heat integration. The film coefficient for all hot streams, h_{HP}, is 2 kW/m^2 K and for all cold streams, h_{CP}, is 0.5

kW/m^2 K. Additionally, the film coefficients defined for cooling water streams, absorption refrigeration streams providing sub-ambient cooling, compression refrigeration streams and for high pressure steam streams which represented by the parameters h_{CW}, h_{AR2}, h_{CR}, and h_{HPS}, respectively. The value of these coefficients are 2.5, 2.3, 0.3 and 5 kW/m^2 K, respectively The temperatures for the utilities in the proposed superstructure are the following: $T_{CW}^{In} = 293K,\ T_{CW}^{Out} = 313K;\ T_{AR2}^{In} = 263K,\ T_{AR2}^{Out} = 264K;\ T_{CR}^{In} = 180K,$ $T_{CR}^{Out} = 180K$ and $T_{HPS}^{In} = 1200K, T_{HPS}^{Out} = 1199K$.

In addition to the parameters considered for the tenant integration, the following parameters are defined for the application of interplant energy integration. An AR cycle is available for construction to convert low grade waste heat into sub-ambient cooling. The AR cycle uses hot water as heat transfer medium in conjunction with the LiBr-water system. The coefficient of performance of absorption refrigeration cycle, COP^{AR}, is 0.7. The SRC and ORC are also available for construction to convert high and medium grade heat into electricity. The efficiency factors involved in the formulation are: $\mu^{SRC} = 0.35$ and $\mu^{ORC} = 0.3$, respectively. The unitary price of the power $SuP^{Power} = \$0.14/kWh$ and the power production costs are $PPCost^{SRC} = \$0.10/kWh$ and $PPCost^{ORC} = \$0.115/kWh$ for the SRC and ORC, respectively.

The service temperatures of the exchangers relating to the trigeneration facility in the proposed superstructure are the following: $T_{SRC1}^{In} = 653\ K,\ T_{SRC1}^{Out} = 773\ K;\ T_{ORC1}^{In} = 333\ K, T_{ORC1}^{Out} = 423\ K; T_{AR1}^{In} = 323\ K, T_{AR1}^{Out} = 353\ K; T_{ORC2}^{In} = 335\ K, T_{ORC2}^{Out} = 333\ K;$ and $T_{SRC2}^{In} = 673\ K,\ T_{SRC2}^{Out} = 653\ K$. Additional film coefficients are provided for the trigeneration plant energy streams which include the AR cycle stream absorbing low grade

waste heat, the SRC stream absorbing heat, the SRC stream discharging heat, the ORC stream absorbing heat and the ORC stream discharging heat. These coefficients are denoted as h_{AR1}, h_{SRC1}, h_{SRC2}, h_{ORC1} and h_{ORC2}, respectively. The values for these are 2.5, 2.5, 5, 2.5 and 5, respectively.

The objective function used for the SSRS superstructure in the mass targeting is the maximization of the collective tenant after-tax profits. This equation is stated as follows:

$$\max Collective\ After\ Tax\ Profit = \sum_{p \in Tenants} (Tax\ Rate * (Annual\ Revenue_p - Annual\ Feedstock\ Cost_p - Annual\ Operating\ Cost_p - Annualized\ Capital\ Cost_p) + Annualized\ Capital\ Cost_p) \quad (126)$$

The conditions for a tenant to pass the mass targeting include a minimum 10%/yr return on investment for each tenant and a collective park CO_2 emission limit of 150 kmol/h. Depreciation is assumed to be linear over 10 years without salvage value. The fixed capital investment is assumed to be 85% of the total capital investment. A tax rate of 35% is assumed.

The objective function used to drive the synthesis of the heat exchanger networks for the tenants is as follows:

$$\min H_Y \left(C_{CW} \left[\sum_{i_p \in HS_p} q_{i_p}^{CW} \right] + C_{AR} \left[\sum_{i_p \in HS_p} q_{i_p}^{AR} \right] + C_{CR} \left[\sum_{i_p \in HS_p} q_{i_p}^{CR} \right] + C_{HPS} \left[\sum_{j_p \in CS_p} q_{j_p}^{HPS} \right] \right) + C_{Fix} \left(\sum_{i_p} \sum_{j_p} \sum_k z_{i_p,j_p,k} + \sum_{i_p} \left[z_{i_p}^{CW} + z_{i_p}^{AR} + z_{i_p}^{CR} \right] + \sum_{j_p} z_{j_p}^{HPS} \right) \quad (127)$$

where C_{CW}, C_{AR}, C_{CR}, and C_{HPS} are the cost per kWh for cooling water, absorption refrigeration, compression refrigeration and high-pressure steam services. H_Y and C_{Fix} represents the annual hours of operation and fixed cost to build a heat exchanger. The annualized fixed cost, C_{Fix}, is assumed to be \$4,186 per heat exchanger placement. The parameter H_Y is 8,760 h/year. The heat recovery tolerance, δ, is set as 90%

The objective function used to drive the synthesis of the interplant energy network is as follows:

$$\max Power\ Sale - Fixed\ Cost - Utilities\ Cost \tag{128}$$

where $Power\ Sale$ is the annual revenue created by generating electricity, $Fixed\ Cost$ is the fixed cost associated with building a heat exchanger and $Utilities\ Cost$ is the cost associated with using hot and cold utilities. In turn, $Power\ Sale$ is represented as follows:

$$Power\ Sale = H_Y D_{SH}\big((SuP^{Power} - PPCost^{SRC})Power^{SRC} + (Su^{Power} - PPCost^{ORC})Power^{ORC}\big) \tag{129}$$

where D_{SH} is the conversion factor from kW to kWh and is equal to 3600.

$Fixed\ Cost$ is represented by the following relation:

$$Fixed\ Cost = C_{Fix}\left(\sum_p \sum_{i_p}\left(z_{i_p}^{SRC1} + z_{i_p}^{ORC1} + z_{i_p}^{AR1} + z_{i_p}^{CW} + z_{i_p}^{AR2} + z_{i_p}^{CR}\right) + \sum_p \sum_{i_p} \sum_{p'} \sum_{j_{p'}} \sum_k z_{i_p,j_{p'},k} + \sum_p \sum_{j_p}\left(z_{j_p}^{ORC2} + z_{j_p}^{SRC2} + z_{j_p}^{HPS}\right)\right) \tag{130}$$

and $Utilities\ Cost$ is represented as:

$$Utilities\ Cost = H_Y\left(C_{CW}\left(\left(\sum_p \sum_{i_p} q_{i_p}^{CW}\right) + Q_{SRC}^{CW} + Q_{ORC}^{CW}\right) + C_{CR}\left(\sum_p \sum_{i_p} q_{i_p}^{CR}\right) + C_{HPS}\left(\sum_p \sum_{j_p} q_{j_p}^{HPS}\right) + C_{AR}^{External} Q_{AR}^{External}\right) \tag{131}$$

where $C_{AR}^{External}$ is the external cooling cost for the AR cycle.

It could be observed that both objective functions for the tenant heat integration and the interplant energy integration lack economies of scale capital cost term relating to the sizing the heat exchangers. These objective functions do indirectly account for reducing the capital costs by minimizing the fixed costs involved to build exchangers. It decided that this was sufficient in optimizing the tenant and interplant energy heat exchanger networks and thus demonstrating the overall EIP approach without having the difficulties involved with optimizing large scale MINLPs. To compensate for this, the heat exchanger capital costing was included in the post processing of the tenant heat and interplant energy integration optimization results. The exponent to consider the scale economies for all heat exchangers is 0.86. The exchanger area cost coefficient is assumed as \$322/m^2. The minimum temperature difference for both the tenant heat integration and interplant energy integration is 10 K.

3.5. Results and Discussion

3.5.1. Mass Targeting

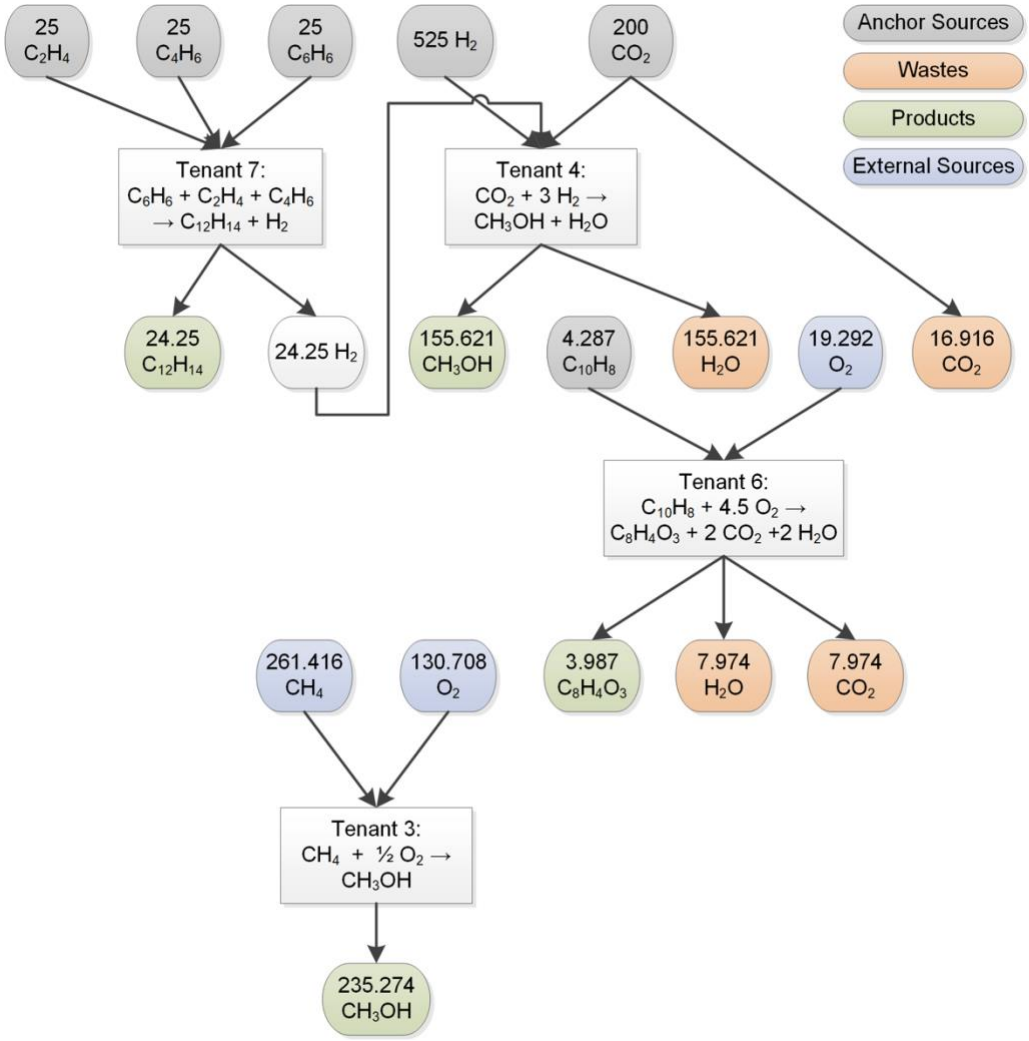

Figure 3.6: Preliminary Superstructure of Screened Tenants with Primary Component Flowrates (adapted from Topolski et al., 2018)

It is shown in Figure 3.6 that the tenants manufacturing methanol, phthalic anhydride and styrene-butadiene rubber are screened for invitation into the EIP. This

figure highlights significant mass integration between the anchors and Tenants 4, 6 and 7. Cooperation among tenants is observed as byproduct hydrogen from the Tenant 7 is sold to the Tenant 4. Alternatively, competition is observed between tenants as the Tenant 6 and Tenant 3 compete for the same raw material, oxygen.

Table 3.8: Anchor and Screened Tenant Economic Summary from Mass Targeting (adapted from Topolski et al., 2018)

Plant	Sales (MM$/ yr)	Feedstock Cost (MM$/yr)	Annualized Fixed Cap. (MM$/yr)	Annualized Non-Feedstock Op. Cost (MM$/yr)	After-tax Profit ($MM/ yr)	Return on Investment (%)
Anchor 1	0.77	--	--	--	0.50	--
Anchor 2	0.99	--	--	--	0.64	--
Tenant 3	80.35	12.13	25.95	15.66	43.24	14.17
Tenant 4	53.17	1.68	8.66	18.95	24.18	23.74
Tenant 6	9.28	1.09	5.31	1.45	6.24	10.00
Tenant 7	59.13	0.14	11.92	7.80	37.45	26.70

Table 3.8 illustrates the opportunities presented from the mass targeting application. Both anchor plants see modest gains from the sale of their byproducts at this stage of screening. However, the sale of these byproducts serves as a benefit for the construction of tenants as their feedstock costs are significantly reduced. This allows the tenants to be profitable despite having lower plant capacities and the external market conditions. The tenants observed in Table 3.8 and Figure 3.6 also pass the screening for

the additional constraints placed in the screening which include maintaining a minimum 10% ROI and a maximum park process-related CO_2 emission rate.

3.5.2. Internal Tenant Heat Integration and Stream Reservation

The tenant screening from the mass targeting section of the approach alleviates the user's expense for data collection of hot and cold streams by excluding potentially uneconomic tenants. As these tenants are screened, further evaluation is made via heat integration to increase the profitability and sustainability of each tenant. The iterative heat integration procedure is applied to each tenant to determine the internal heat exchanger network as well as which hot streams are reserved for the later interplant energy integration. Each heat integration iteration is performed by optimizing Eqn (127) subject to Eqns (17) – (52). Following the iterative heat integration of each tenant, waste heat and reserved heat from hot streams are consolidated into a park stream inventory of which interplant energy integration is conducted upon.

Tenant 3. Stream data is assembled from the methanol plant process design put forth by Ehlinger et al. (2013). Heat capacity flowrates are scaled down to match the capacity determined in the mass targeting steps. Table 3.9 describes the stream inventory for this tenant.

Table 3.9: Tenant 3 Stream Inventory (Ehlinger et al., 2013)

Stream Index i_p, j_p	Inlet temperature [K]	Outlet temperature [K]	FCp [kW/K]
$H1_{T3}$	597	313	6.5
$H2_{T3}$	420	318	13.2
$H3_{T3}$	1544	313	8.3
$H4_{T3}$	513	423	17.0
$C1_{T3}$	299	473	1.6
$C2_{T3}$	313	573	6.3

The iterative heat integration procedure is applied to this tenant and results in the heat exchanger network observed in Figure 3.7. The first iteration of heat integration with all streams in Table 3.9 included results in a maximum observed heat recovery of 1916.4 kW. The extraction of hot streams $H3_{T3}$ and $H4_{T3}$, and subsequent heat integration results in a heat exchanger network where the nominal heat recovery is equal to the maximum heat recovery. The extraction of $H1_{T3}$, $H3_{T3}$ and $H4_{T3}$ leads to heat exchanger network design where nominal heat recovery is 1475.4 kW. This design violates the 90% maximum heat recovery tolerance and so this heat exchanger network design is discarded.

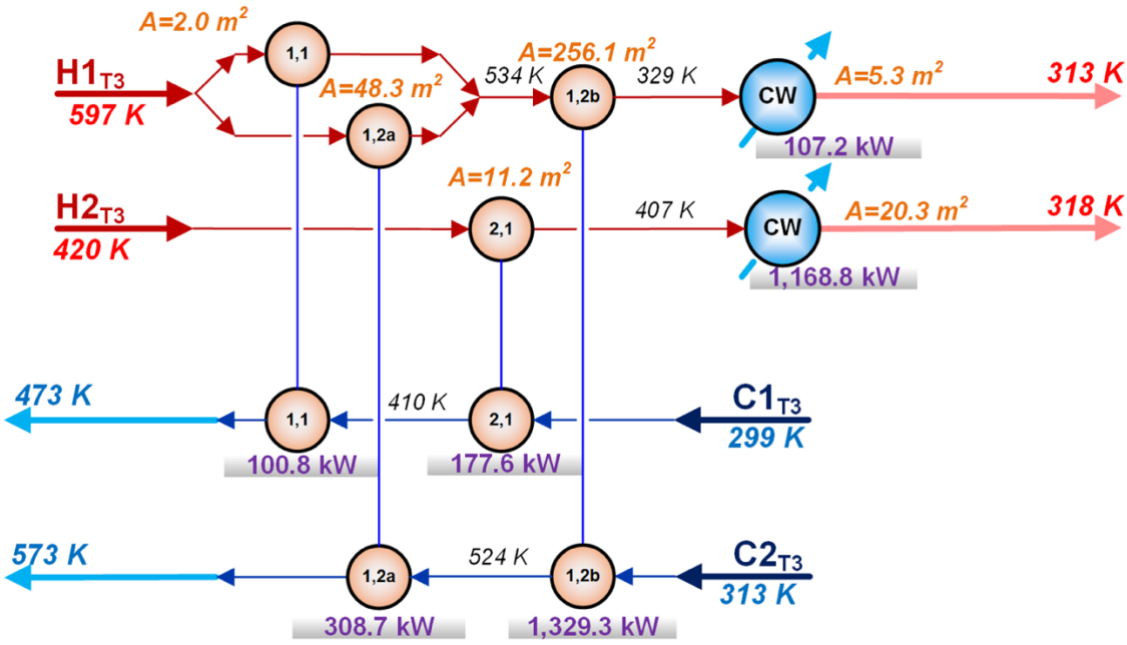

Figure 3.7: Tenant 3 Heat Exchanger Network

Tenant 4. The stream inventory in Table 10 is developed from Perez-Fortes et al. (2016). The capacity from this study is reduced from 1719 kmol/hr to 157 kmol/hr to match the capacity of Tenant 4 determined in the mass targeting.

Table 3.10: Tenant 4 Stream Inventory (Perez-Fortes et al., 2016)

Stream Index i_p, j_p	Inlet Temperature [K]	Outlet Temperature [K]	FCp [kW/K]
$H1_{T4}$	413	303	1.7
$H2_{T4}$	409	302	1.7
$H3_{T4}$	383	301	1.8
$H4_{T4}$	349	308	46.7
$H5_{T4}$	340	337	529.3
$H6_{T4}$	352	313	42.6
$H7_{T4}$	349	308	46.7
$H8_{T4}$	561	503	3.2
$H9_{T4}$	1473	519	1.5
$C1_{T4}$	372	374	562.6
$C2_{T4}$	314	335	25.4

Of the streams in Table 3.10, $H8_{T4}$ and $H9_{T4}$ are extractable to produce electricity. Upon the first iteration of the iterative heat integration procedure, the maximum amount of heat recovery is determined to be 1658.6 kW. Extracting $H9_{T4}$ reduces Tenant 4's heat recovery by 51%. However, extracting $H8_{T4}$ shows to have no effect in reducing the tenant heat recovery when compared to the maximum heat recovery. It was resolved to split $H9_{T4}$ into the two hot streams $H9_{T4}$ and $H9'_{T4}$ where $H9_{T4}$ is the higher-grade temperature stream with new target temperature of 1092.8 K and $H9'_{T4}$ is the lower-grade temperature stream with a new supply temperature of 1092.8 K. This stream is split in a way such that the higher-grade hot stream is reserved for the possibility of producing electricity while the lower-grade hot stream is heat integrated to meet internal heating needs while satisfying the minimum 90% of max heat recovery tolerance. Figure 3.8

illustrates the final design of Tenant 4's heat exchanger network with $H8_{T4}$ and $H9_{T4}$ extracted.

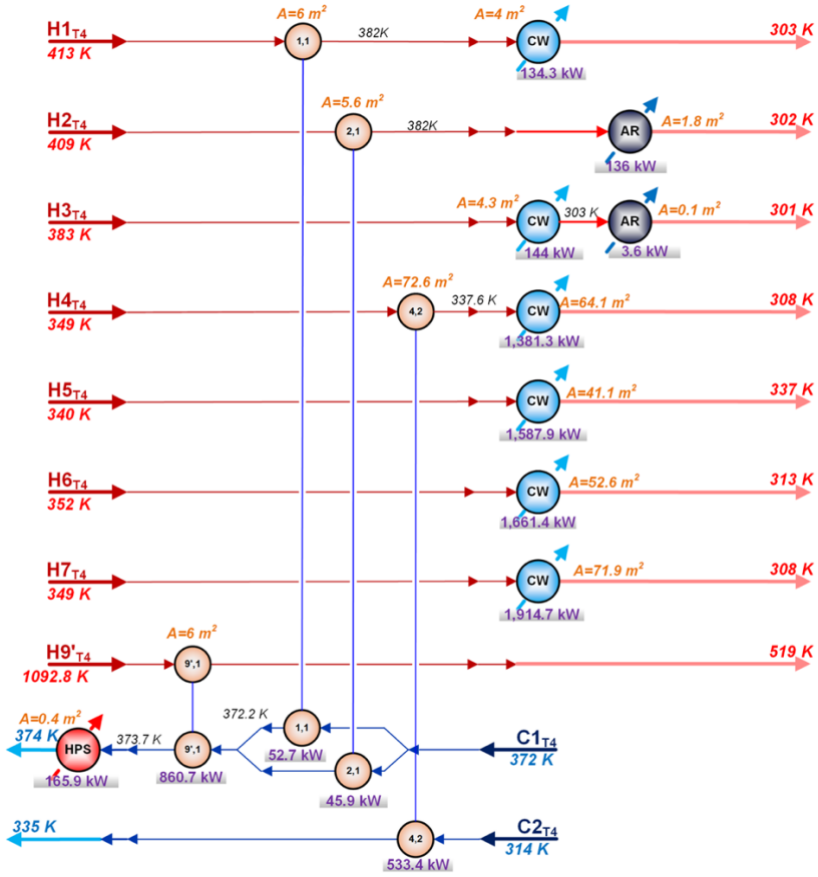

Figure 3.8: Tenant 4 Heat Exchanger Network

Tenant 6. The data in Table 3.11 is taken from Perez-Uresti et al. (2017) and adjusted for to meet the capacity of Tenant 6 determined from the mass targeting section of the approach.

Table 3.11: Tenant 6 Stream Inventory (Perez-Uresti et al., 2017)

Stream Index i_p, j_p	Supply temperature [K]	Target temperature [K]	FCp [kW/K]
$H1_{T6}$	633	433	2.9
$H2_{T6}$	464	463	264.8
$C1_{T6}$	437	513	2.4
$C2_{T6}$	513	514	250.33

The candidate hot streams from Tenant 6 that usable for interplant energy integration are $H1_{T6}$ and $H2_{T6}$. The initial heat integration determined that the maximum heat recovery that Tenant 6 could achieve is 432.73 kW. Subsequent iterations entailed extracting either hot process stream and performing the heat integration. It was found that by extracting $H1_{T6}$, the heat recovery potential is reduced by 90%; extracting $H2_{T6}$ had no impact on the heat recovery potential. Figure 3.9 illustrates the Tenant 6 heat exchanger network with $H2_{T6}$ extracted.

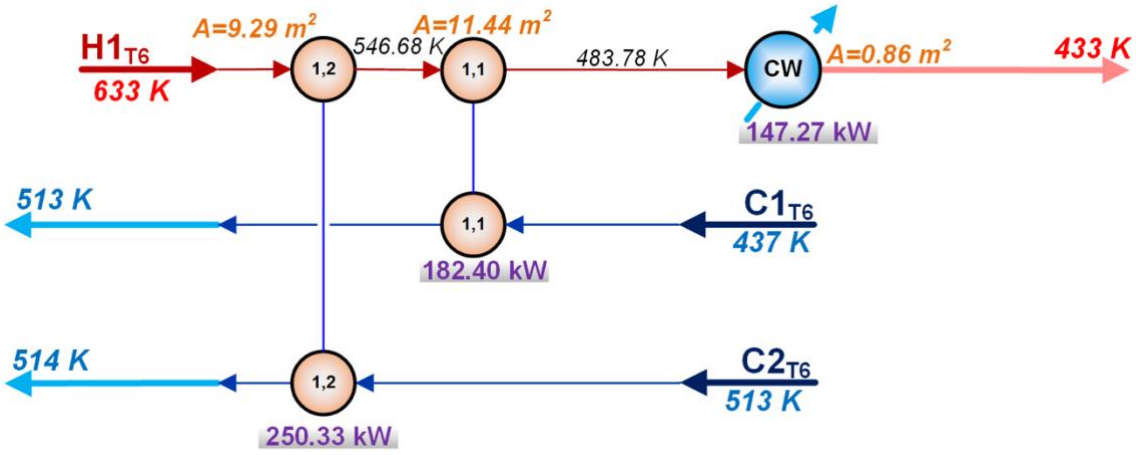

Figure 3.9: Tenant 6 Heat Exchanger Network

Tenant 7. Tenant 7 was modeled as a combination of different processes. Data for the ethylbenzene and styrene and styrene butadiene production processes are taken from Yen (1967) and Schwaar (1976). The heat capacity flowrates from these data are scaled to meet the capacities of the mass targeting section of the approach.

Table 3.12: Tenant 7 Stream Inventory (Yen, 1967) (Schwaar, 1976)

Stream Index i_p, j_p	Supply temperature [K]	Target temperature [K]	FCp [kW/K]
$H1_{T7}$	298	294	34.9
$H2_{T7}$	355	328	4.8
$H3_{T7}$	356	355	63,373.70
$H4_{T7}$	378	377	9027.8
$H5_{T7}$	377	259	8.6
$H6_{T7}$	353.2	352.6	193.6
$H7_{T7}$	369.8	369.3	338.8
$H8_{T7}$	369.8	313.7	2.6
$H9_{T7}$	408.2	407.6	810.7
$H10_{T7}$	354.3	353.7	1415.8
$H11_{T7}$	366.5	365.9	1815.1
$H12_{T7}$	320.9	320.4	2805.9
$H13_{T7}$	330.4	329.8	635.3
$C1_{T7}$	301	302	249.1
$C2_{T7}$	259.0	289	11.8
$C3_{T7}$	375	376	2162.3
$C4_{T7}$	416	417	7742.4
$C5_{T7}$	354.9	355.4	387.2
$C6_{T7}$	354.8	369.8	7.2
$C7_{T7}$	472.6	473.2	968.1
$C8_{T7}$	413.2	413.7	1742.5
$C9_{T7}$	432.6	433.2	907.5
$C10_{T7}$	369.3	369.8	291.2
$C11_{T7}$	389.3	389.8	211.8
$C12_{T7}$	360.4	360.9	1985.3
$C13_{T7}$	360.4	360.9	661.8

As seen in Table 3.12, no hot process streams meet the criteria for reservation and so the iterative heat integration procedure is not conducted. Heat integration is applied to the streams in Table 3.12 to give the results shown in Figure 3.10.

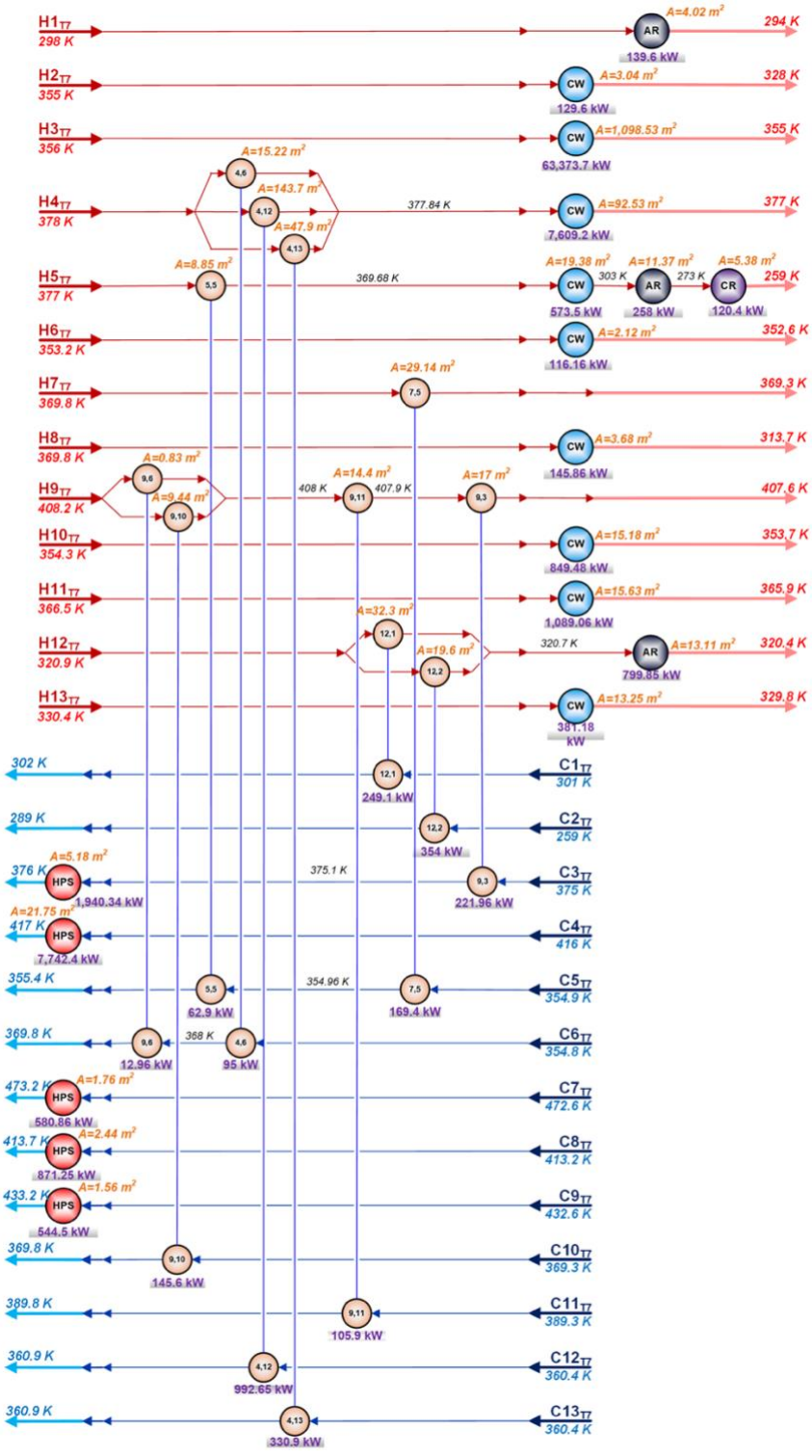

Figure 3.10: Tenant 7 Heat Exchanger Network

3.5.3. Interplant Energy Integration

Prior to performing the interplant energy integration, Figure 3.7, Figure 3.8, Figure 3.9 and Figure 3.10 are analyzed to inventory instances of waste heating and cooling. Waste heating and cooling is defined in this study as any energy stream or energy stream section that employs any form of utilities to satisfy its heating/cooling needs. Data on the tenant stream temperatures and their residual heat content are collected and considered in the interplant energy integration section of the approach. This data is complemented by the data describing the anchor plant energy streams that are available for integration and the tenant energy streams that were reserved in the iterative tenant heat integration procedure. Table 3.13 provides an inventory of anchor plant energy streams, tenant waste energy streams and tenant reserved energy streams.

Table 3.13: Park Stream Inventory

Plant p	Stream Index i_p, j_p	Supply Temperature [K]	Target Temperature [K]	FCp [kW/K]
$A1$	$H1_{A1}$	423	298	187.5
	$H2_{A1}$	273	200	118.3
	$H3_{A1}$	396.1	313	304.5
	$H4_{A1}$	365	313	393.8
	$H5_{A1}$	381	313	1580.4
	$H6_{A1}$	423	313	136.6
	$H7_{A1}$	391	322	341.9
	$C1_{A1}$	667.7	755	156.3
	$C2_{A1}$	726	755	67.8
$A2$	$H1_{A2}$	598.8	473	249
	$H2_{A2}$	410.9	293	158
	$C2_{A2}$	1063	1073	223
$T3$	$H1_{T3}$	329	313	6.5
	$H2_{T3}$	407	318	13.2
	$H3_{T3}$	1544	313	8.3
	$H4_{T3}$	513	423	17.0

Table 3.13: Park Stream Inventory (Continued)

Plant p	Stream Index i_p, j_p	Supply Temperature [K]	Target Temperature [K]	FCp [kW/K]
$T4$	$H1_{T4}$	382	303	1.7
	$H2_{T4}$	382	302	1.7
	$H3_{T4}$	383	301	1.8
	$H4_{T4}$	337.6	308	46.7
	$H5_{T4}$	340	337	529.3
	$H6_{T4}$	352	313	42.6
	$H7_{T4}$	349	308	46.7
	$H8_{T4}$	561	503	3.2
	$H9_{T4}$	1473	1092.8	1.5
	$C1_{T4}$	373.7	374	562.6
$T6$	$H1_{T6}$	483.7	433	2.9
	$H2_{T6}$	464	463	264.8
$T7$	$H1_{T7}$	298	294	34.9
	$H2_{T7}$	355	328	4.8
	$H3_{T7}$	356	355	63,373.7
	$H4_{T7}$	377.8	377	9027.8
	$H5_{T7}$	369.7	259	8.6
	$H6_{T7}$	353.2	352.6	193.6
	$H8_{T7}$	369.8	313.7	2.6
	$H10_{T7}$	354.3	353.7	1415.8
	$H11_{T7}$	366.5	365.9	1815.1
	$H12_{T7}$	320.7	320.4	2805.9
	$H13_{T7}$	330.4	329.8	635.3
	$C3_{T7}$	375.1	376	2162.3
	$C4_{T7}$	416	417	7742.4
	$C7_{T7}$	472.6	473.2	968.1
	$C8_{T7}$	413.2	413.7	1742.5
	$C9_{T7}$	432.6	433.2	907.5

Eqns (53) to (126) are optimized subject to Eqns (128) to (131) of which the capital costing of the heat exchangers is omitted to reduce computational complexity and expense. The interplant energy integration mathematical model is solved as a MILP with CPLEX used as the optimization solver. This model consists of 3,236 equations and 3,377 variables with 867 of those variables are binary. The program took 628 second to achieve an optimal solution with negligible tolerance. The value for the objective function is -$2,113,746.53/yr which includes the terms for the revenue generated from selling electricity, fixed capital costs and the cost of utilities needed to satisfy the heating and cooling needs of all plants that the interplant energy integration cannot meet.

Figure 3.11 displays the result of the interplant energy integration. This figure shows a significant reduction in cooling water and high-pressure steam use as well as significant energy integration among anchors, tenants and the trigeneration facility. It is important to highlight the heat integration between anchors and tenants as well as between tenants. Tenant 7 is especially focused upon as it possesses medium grade cooling streams and therefore, provides numerous opportunities for heat integration among the other plants. All plants illustrated in this figure are energy integrated in various extents with the trigeneration facility. Streams that were reserved from the previous iterative tenant heat integration procedures are allocated to the SRC and ORC to produce electricity with the exception of stream $H8_{T4}$ which is used to further satisfy the internal heat requirements of Tenant 4 and Tenant 7. Much of the waste heat from the involved plants is used to drive the AR cycle to provide sub-ambient cooling in the energy integration network. Tenant 7

sees much integration for its possession of medium grade cooling which serves as a major sink of the park's waste heat.

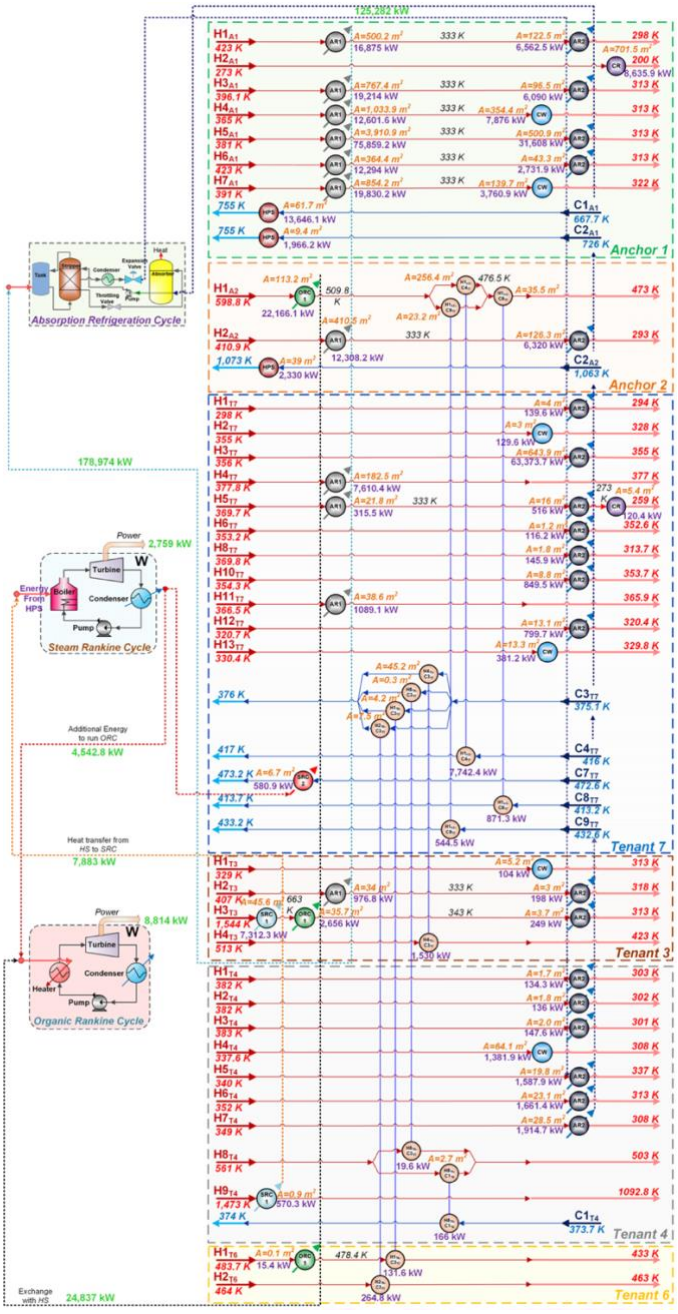

Figure 3.11: Interplant Energy Exchanger Network

It is observed that Anchor 1 is not included in any integration between other plants with the exception of the trigeneration facility. This is attributed to Anchor 1 possessing lower grade hot and cold streams which limits the extent of heat integration. There are opportunities that exist in this model to transfer high-grade heat from other plants to Anchor 1's cold streams but it is more economical to utilize that high-grade heat to produce electricity. Alternatively, cooling utility savings are gained in Anchor 2's operation as heat from Anchor 2's hot streams are transferred to Tenant 7 cold streams. The one cold stream within Anchor 2 is of low quality and will need high-pressure steam to meet its target temperature.

Tenant 7 is significantly integrated among the other tenant plants as well due to the high heat capacities of $C3_{T7}$ and $C4_{T7}$, and their low supply and target temperatures. It is significant to highlight that the inclusion of this tenant brings a significant reduction of cooling water use when paired with other plants. Integrating this tenant with other plants with medium grade hot streams leads to the reduction of high-pressure steam use for Tenant 7 when compared to the internal tenant heat integration. Further heat integration among partners could be achieved if other plants with a multitude of cold streams available for integration.

The trigeneration facility serves as a significant part of the energy integration network due to its abilities to manufacture electricity from high and medium grade heat and to produce refrigeration from low grade waste heat. As seen in Figure 3.11, significant amounts of low-grade waste heat are allocated to the AR cycle to produce sub-ambient cooling which displaces the use of cooling water in the previous internal tenant heat

exchanger networks. In this mathematical model, it is determined that it is cheaper to pay for the infrastructure to provide this refrigeration rather than pay the external cost for cooling water. There are many instances in the energy integration superstructure when low grade heat from a hot stream is used to produce refrigeration to cool that said hot stream.

Figure 3.11 shows that the streams reserved in the previous iterative tenant heat integration procedure are allocated for electricity generation with the exception of $H8_{T4}$, which is used to meet an internal tenant heating requirement. 33 MWh is extracted from the anchor and tenant plants to drive the SRC and ORC to produce 12 MWe. The reservation of high and medium grade heat during the tenant heat integration in this case study confirms the benefits that can be obtained from applying this approach as that high- and medium-grade heat may be improperly used if the hot streams were not reserved in this approach. The effect of implementing the iterative tenant heat integration procedure is the heat exchanger network design where the anchor/tenant plant experiences a reduction of cooling utility cost and the trigeneration plant obtains a free carbonless source of fuel to generate electricity for sale.

Table 3.14: Economic Summary of Plant Participation in Park through Energy Targeting

Plant	Utility Cost: Internal Integration ($MM/y)	Utility Cost: Interplant Integration ($MM/y)	Annualized Capital Cost: Interplant Integration ($MM/y)	Savings ($MM/y)
Anchor 1	8.06	3.96	0.03	4.07
Anchor 2	1.38	0.35	0.015	1.02
Tenant 3	0.26	0.0021	0.009	0.25
Tenant 4	0.18	0.028	0.013	0.14
Tenant 6	0.0082	0	0.0076	0.0006
Tenant 7	3.32	0.029	0.017	3.27

In order to determine the magnitude of the shared costs of the heat exchangers, this study employs a method that balances capital cost through using a proportional relationship of the utility prices of a plant that would pay for heating/cooling a given stream if unintegrated. This is represented in this work by the following equations:

$$Capital\ Cost_{i_p}^{Shared} = \left(\frac{C_{CW}}{C_{CW}+C_{HPS}}\right) * Exchanger\ Capital\ Cost_{i_p,j_p'} \quad (132)$$

$$Capital\ Cost_{j_p}^{Shared} = \left(\frac{C_{HPS}}{C_{CW}+C_{HPS}}\right) * Exchanger\ Capital\ Cost_{i_p',j_p} \quad (133)$$

Table 3.14 illustrates the benefits that each plant enjoys if participating in the interplant energy integration. The benefactors that have the most to gain their participation are both anchors and Tenant 7. Although Tenant 6 has eliminated their heating and cooling cost for its participating streams, its annualized capital cost is at parity with its annual utility costs prior to integration and so sees little benefit in participating. The remaining tenants see modest gains in their participation and the high relative savings may validate their participation.

Table 3.15: Economic and Sustainability Summary of Trigeneration Facility Targeting

Total Power Sale (MM$/yr)	14.19
ORC Production Costs (MM$/yr)	2.78
SRC Production Costs (MM$/yr)	2.42
AR Production Costs (MM$/yr)	0.70
Net Income (MM$/yr)	8.30
Avoided Natural Gas Consumption (kton/yr)	141.79

The costing of all the trigeneration-related exchangers that are trading heat with the anchor and tenant plants are included in the economic evaluation of the trigeneration facility. As seen in Table 3.15, the trigeneration appears to be a profitable enterprise at this level of screening. It is important to highlight that the circumstances of the screening include linear correlations to determine production costs of electricity as well as the direct access to free waste heat that would drive the equipment. Utilizing the waste heat as a fuel to generate electricity avoids the use of 140 kton/yr of natural gas use, assuming a natural gas heating value of 13.1 kWh/kg. It is recommended to proceed into the detailed design of the facility in this case study.

Table 3.16: Percent Reduction of Utilities Use of the Participating Streams from Each Plant in the Interplant Energy Integration (in %)

Plant	CW	CR	HPS
Anchor 1	94.6	0	0
Anchor 2	100	0	0
Tenant 3	99.2	0	0
Tenant 4	81.8	0	100
Tenant 6	100	0	0
Tenant 7	99.3	0	100

The interplant energy integration network succeeds in converting the tenant waste heat into valuable utilities as well as reducing their respective cooling duty and reducing the expensive heating duty for tenants. As seen in Table 3.16, there were no opportunities to reduce the utility use of compression refrigeration as there are no high-quality cold streams that could accept that low grade heat. Few opportunities are available to reduce the high-pressure steam use as seen in Figure 3.11 for Tenant 4 and Tenant 7. Much of the cost saving is driven by the reduction of cooling water use and the production of absorption refrigeration from waste heat to supplement the need for hot stream cooling.

3.5.4. Combined Economic Assessment of Mass and Energy Targeting

It is significant to iterate that although potential tenants are screened, and mass and energy superstructures are developed, the user of this approach has the final decision on what tenants to invite. As seen in in Figure 3.1, the user can decide to reiterate the approach with updated criteria if it is determined if the result(s) deem unsatisfactory. For this study,

a decision on which tenants to invite for the next stage of design is made based on their economic merits.

Table 3.17: Economic Assessment of Mass and Energy Targeting in the Approach for Selecting Tenants to Invite and Integrate

Plant	Sales (MM$/yr)	Feedstock Cost (MM$/yr)	Annualized Fixed Cap. (MM$/yr)	Annualized Op. Cost (MM$/yr)	After Tax Profit ($MM/yr)	Return on Investment (%)
Anchor 1	0.767	--	0.029	-4.073	3.156	929.65
Anchor 2	0.989	--	0.015	-1.016	1.309	719.19
Tenant 3	80.348	12.132	25.955	15.408	43.409	14.22
Tenant 4	53.166	1.684	8.669	18.806	24.273	23.80
Tenant 6	9.28	1.088	5.313	1.445	6.245	9.99
Tenant 7	59.13	0.142	11.939	4.525	39.579	28.18

* Negative values indicate savings

With Table 3.8, Table 3.14 and Table 3.17, it is observed that different participants benefited from different sections of the approach. Tenants 3 and 4 benefited from the mass targeting section of the approach while both anchors benefited from the energy targeting section of the approach. Tenant 7 is the only screened plant to enjoy benefits from both sections of the approach. In Table 17, anchor participation in the park integration is rewarded with the payback periods of 1.29 and 1.67 months for Anchors 1 and 2, respectively. This is driven by the energy targeting step of the approach. When comparing Table 3.8 with Table 3.17, a small uptick of ROI observed for Tenants 3 and 4 due to relatively low impact of the energy targeting. Tenant 3 is especially highlighted as it is involved in the park through a low degree integration among other park participants as

seen in Figure 3.6 and Figure 3.11. Also seen in Figure 3.6 and Figure 3.11 is that the benefits that Tenant 7 reaped are mirrored in its level of integration with other plants.

All tenants previously screened in the mass targeting section of the approach would be recommended for invitation into the EIP with the exception of Tenant 6. When comparing Table 3.8 with Table 3.17, it is observed that the ROI of Tenant 6 decreases when applying the park energy targeting. Also, whereas a minimum 10% ROI is deemed necessary for consideration to be included into the EIP in the mass targeting section of the approach, it may not be a sufficient condition for invitation into the EIP. The impact of excluding Tenant 6 on other participating plants is predicted to be minimal as seen in Figure 3.6 and Figure 3.11 where there is little energy integration and that Tenant 6 is a benefactor in obtaining its raw materials from the Anchor 2. Tenants that are excluded are done so on the basis that they should possess stable economic health as the invited tenants may feature as anchor plants in future park expansion projects. Unstable economic health of one plant may compromise the health of other participating plants in the park.

The demonstration of the approach to this case study illustrates the richness of solutions that could be obtained when considering additional tenants for invitation. This demonstration shows that despite the limited benefits that are accrued by some participating plants from the mass targeting section of the approach, these benefits could be bolstered significant through additional energy targeting. A limitation of this approach is that tenants that rely heavily on utilities rather than raw materials for operation may be unnecessarily ruled out as the tenants did not meet the criteria established in the mass targeting section of the approach. The development of alternative approaches in selecting

tenants are necessary when addressing the invitation of tenants that rely on utility usage for operation. This may be accomplished via developing a sequential approach that considers energy targeting for tenant selection first followed by mass targeting or a simultaneous approach that selects tenants to invite while considering both mass and energy characteristics.

3.6. Conclusion

This chapter has addressed the problem of designing CHOSYNs with mass and energy considerations. A hierarchical approach has been introduced to establish performance benchmarks, to guide the selection of tenants to invite, and to create synergistic opportunities for integrating mass and energy among the participating plants. Atomic targeting and multi-scale optimization approaches are coupled with multi-plant heat and power integration. The proposed approach decomposes the CHOSYN design task of selecting tenants to invite into a series of sub-problems that address high level decisions before proceeding into the detailed network designs. Decisions on screening potential tenants are first through mass targeting techniques and then is followed with energy targeting techniques. The mass targeting techniques employ fundamental chemical processing information to screen tenants. The energy targeting techniques apply superstructures to reserve high grade heat streams for the subsequent interplant energy integration where the production of utilities is considered. The culmination of this approach is a set of tenant plants that are sized and integrated among themselves and the anchors. A case study is solved to demonstrate the application of this approach. The results of the case study illustrate each participating plant gaining significant benefits from

different sections of the approach. These results also illustrate that among the selected set of screened tenants, invitation of certain tenants might be withheld and therefore, excluded from further detailed design.

3.7. References

Abedi, A. A. (2007). Economical analysis of a new gas to ethylene technology (Doctoral dissertation, Texas A&M University).

Al-Fadhli, F. M., Mukherjee, R., Wang, W., & El-Halwagi, M. M. (2018). Design of multiperiod C–H–O symbiosis networks. ACS Sustainable Chemistry & Engineering, 6(7), 9130-9136. doi:10.1021/acssuschemeng.8b01462

Alves, J. J., & Towler, G. P. (2002). Analysis of refinery hydrogen distribution systems. Industrial & Engineering Chemistry Research, 41(23), 5759-5769. doi:10.1021/ie010558v

Aviso, K. B., Tan, R. R., & Culaba, A. B. (2010a). Designing eco-industrial water exchange networks using fuzzy mathematical programming. Clean Technologies and Environmental Policy, 12(4), 353-363.

Aviso, K. B., Tan, R. R., Culaba, A. B., & Cruz Jr, J. B. (2010b). Bi-level fuzzy optimization approach for water exchange in eco-industrial parks. Process Safety and Environmental Protection, 88(1), 31-40.

Bagajewicz, M., & Rodera, H. (2000). Energy savings in the total site heat integration across many plants. Computers & Chemical Engineering, 24(2-7), 1237-1242.

Bagajewicz, M., & Rodera, H. (2002). Multiple plant heat integration in a total site. AIChE Journal, 48(10), 2255-2270.

Bao, B., Ng, D. K., Tay, D. H., Jiménez-Gutiérrez, A., & El-Halwagi, M. M. (2011). A shortcut method for the preliminary synthesis of process-technology pathways: An

optimization approach and application for the conceptual design of integrated biorefineries. Computers & Chemical Engineering, 35(8), 1374-1383.

Boix, M., Montastruc, L., Pibouleau, L., Azzaro-Pantel, C., & Domenech, S. (2012). Industrial water management by multiobjective optimization: from individual to collective solution through eco-industrial parks. Journal of Cleaner Production, 22(1), 85-97.

Chertow, M., & Ehrenfeld, J. (2012). Organizing self-organizing systems. Journal of Industrial Ecology, 16(1), 13-27.

Chertow, M. R. (2007). "Uncovering" industrial symbiosis. Journal of Industrial Ecology, 11(1), 11-30.

Chew, I. M. L., Tan, R., Ng, D. K. S., Foo, D. C. Y., Majozi, T., & Gouws, J. (2008). Synthesis of direct and indirect interplant water network. Industrial & Engineering Chemistry Research, 47(23), 9485-9496.

Chew, I. M. L., Tan, R. R., Foo, D. C. Y., & Chiu, A. S. F. (2009). Game theory approach to the analysis of inter-plant water integration in an eco-industrial park. Journal of Cleaner Production, 17(18), 1611-1619.

Dhole, V. R., & Linnhoff, B. (1993). Total site targets for fuel, co-generation, emissions, and cooling. Computers & chemical engineering, 17, S101-S109.

Ehlinger, V. M., Gabriel, K. J., Noureldin, M. M., & El-Halwagi, M. M. (2013). Process design and integration of shale gas to methanol. ACS Sustainable Chemistry & Engineering, 2(1), 30-37.

Ehrenfeld, J., & Gertler, N. (1997). Industrial ecology in practice: the evolution of interdependence at Kalundborg. Journal of Industrial Ecology, 1(1), 67-79.

El-Halwagi, M. M., Gabriel, F., & Harell, D. (2003). Rigorous graphical targeting for resource conservation via material recycle/reuse networks. Industrial and Engineering Chemistry Research, 42(19), 4319-4328. doi:10.1021/ie030318a

El-Halwagi, M. M. (2017). A shortcut approach to the multi-scale atomic targeting and design of C–H–O symbiosis networks. Process Integration and Optimization for Sustainability, 1-11. doi:10.1007/s41660-016-0001-y

Gibbs, D., & Deutz, P. (2007). Reflections on implementing industrial ecology through eco-industrial park development. Journal of Cleaner Production, 15, 1683-1695. doi:10.1016/j.jclepro.2007.02.003

Hasan, M. M. F., Karimi, I. A., & Avison, C. (2011). Preliminary synthesis of fuel gas networks to conserve energy and preserve the environment. Industrial & Engineering Chemistry Research, 50(12), 7414-7427.

Hu, C. W., & Ahmad, S. (1994). Total site heat integration using the utility system. Computers & Chemical Engineering, 18(8), 729-742. doi.org/10.1016/0098-1354(93)E0019-6

Juárez-García, M., Ponce-Ortega, J. M., & El-Halwagi, M. M. (2018). A disjunctive programming approach for optimizing carbon, hydrogen, and oxygen symbiosis networks. Process Integration and Optimization for Sustainability. doi:10.1007/s41660-018-0065-y

Klemeš, J., Dhole, V. R., Raissi, K., Perry, S. J., & Puigjaner, L. (1997). Targeting and design methodology for reduction of fuel, power and CO_2 on total sites. Applied Thermal Engineering, 17(8), 993-1003. doi.org/10.1016/S1359-4311(96)00087-7

Lira-Barragán, L. F., Ponce-Ortega, J. M., Serna-González, M., & El-Halwagi, M. M. (2014). Optimal design of process energy systems integrating sustainable considerations. Energy, 76, 139-160.

Lovelady, E. M., & El-Halwagi, M. M. (2009). Design and integration of eco-industrial parks for managing water resources. Environmental Progress and Sustainable Energy, 28(2), 265-272. doi:10.1002/ep.10326

Lowe, E. A. (2001). Eco-industrial park handbook for Asian developing countries. Report to Asian Development Bank.Mukherjee, R. and M. M. El-Halwagi, **"**Reliability of C-H-O Symbiosis Networks under Source Streams Uncertainty", Smart and Sustainable Manufacturing Systems Vol. 2, No. 2, (2018) DOI: 10.1520/SSMS20180022

Mukherjee, R., & El-Halwagi, M. M. (2018). Reliability of CHO Symbiosis Networks under Source Streams Uncertainty. SMART AND SUSTAINABLE MANUFACTURING SYSTEMS, 2(2), 132-153.

Noureldin, M. M. B., & El-Halwagi, M. M. (2015). Synthesis of C-H-O symbiosis networks. AIChE Journal, 61(4), 1242-1262. doi:10.1002/aic.14714

Özinan, E., & El-Halwagi, M. M. (2018). Techno-Economic Analysis of Monetizing Shale Gas to Butadiene. Natural Gas Processing from Midstream to Downstream, 403.

Pérez-Fortes, M., J. C. Schöneberger, A. Boulamanti and E. Tzimas (2016). Methanol synthesis using captured CO 2 as raw material: Techno-economic and environmental assessment. Applied Energy 161: 718-732.

Pérez-Uresti, S., J. Adrián-Mendiola, M. El-Halwagi and A. Jiménez-Gutiérrez (2017). Techno-economic assessment of benzene production from shale gas. Processes 5(4).

Roddy, D. J. (2013). A syngas network for reducing industrial carbon footprint and energy use. Applied Thermal Engineering, 53(2), 299-304. doi.org/10.1016/j.applthermaleng.2012.02.032

Rodera, H., & Bagajewicz, M. J. (1999). Targeting procedures for energy savings by heat integration across plants. AIChE Journal, 45(8), 1721-1742.

Rodera, H., & Bagajewicz, M. J. (2001). Multipurpose heat-exchanger networks for heat integration across plants. Industrial & engineering chemistry research, 40(23), 5585-5603.

Rubio-Castro, E., Ponce-Ortega, J. M., Nápoles-Rivera, F., El-Halwagi, M. M., Serna-González, M., & Jiménez-Gutiérrez, A. (2010). Water integration of eco-industrial parks using a global optimization approach. Industrial & Engineering Chemistry Research, 49(20), 9945-9960.

Rubio-Castro, E., Ponce-Ortega, J. M., Serna-Gonzalez, M., Jimenez-Gutierrez, A., & El-Halwagi, M. M. (2011). A global optimal formulation for the water integration in eco-industrial parks considering multiple pollutants. Computers and Chemical Engineering, 35(8), 1558-1574. doi:10.1016/j.compchemeng.2011.03.010

Schwaar, R. H. (1976). Process Economics Program (PEP) Report 104: Thermoplastic Elastomers, SRI Consulting, California.

Song, R., Feng, X., & Wang, Y. (2016). Feasible heat recovery of interplant heat integration between two plants via an intermediate medium analyzed by Interplant Shifted Composite Curves. Applied Thermal Engineering, 94(Supplement C), 90-98. doi.org/10.1016/j.applthermaleng.2015.10.125

Song, R., Tang, Q., Wang, Y., Feng, X., & El-Halwagi, M. M. (2017a). The implementation of inter-plant heat integration among multiple plants. Part I: A novel screening algorithm. Energy, 140(Part 1), 1018-1029. doi.org/10.1016/j.energy.2017.09.039

Song, R., Chang, C., Tang, Q., Wang, Y., Feng, X., & El-Halwagi, M. M. (2017b). The implementation of inter-plant heat integration among multiple plants. Part II: The mathematical model. Energy, 135(Supplement C), 382-393. doi.org/10.1016/j.energy.2017.06.136

Spriggs, D., Lowe, E., Watz, J., El-Halwagi, M. M., & Lovelady, E. (2004). Design and development of eco-industrial parks. Paper presented at the AIChE Spring Meeting, New Orleans.

Stijepovic, M. Z., & Linke, P. (2011). Optimal waste heat recovery and reuse in industrial zones. Energy, 36(7), 4019-4031.

Topolski, K., Noureldin, M. M. B., Eljack, F. T., & El-Halwagi, M. M. (2018). An anchor-tenant approach to the synthesis of carbon-hydrogen-oxygen symbiosis networks.

Computers & Chemical Engineering. doi.org/10.1016/j.compchemeng.2018.02.024

Varbanov, P. S., Fodor, Z., & Klemeš, J. J. (2012). Total Site targeting with process specific minimum temperature difference (ΔTmin). Energy, 44(1), 20-28.

Wang, Y., Chang, C., & Feng, X. (2015). A systematic framework for multi-plants Heat Integration combining Direct and Indirect Heat Integration methods. Energy, 90, 56-67.

Yee, T. F., & Grossmann, I. E. (1990). Simultaneous optimization models for heat integration—II. Heat exchanger network synthesis. Computers & Chemical Engineering, 14(10), 1165-1184.

Yen, Y. (1967). Process Economics Program (PEP) Report 33: Styrene, SRI Consulting, California.

4. CONCLUSIONS

In this study, methodological approaches are proposed for the synthesis of EIPs. These approaches are inspired by the Anchor-Tenant Model for EIPs synthesis where Tenants are screened prior to selection for construction and integration with the Anchors. Process systems engineering techniques are incorporated into these approaches where performance benchmarking is used to determine the viability of a Tenant being included into the EIP. Chapter II addressed the screening of Tenants based on the material throughputs of both Anchors and Tenants in a multi-scale process systems approach. Chapter III expanded process systems approach introduced by Chapter II to include the consideration of the Anchor and Tenant energy throughputs within in the screening of Tenants. The culmination of the approach application indicates unique plant synergies and significant economic and sustainable benefits.

The multi-scale process systems approach introduced in Chapter II addresses Tenant screening through employing multiple mass integration techniques. Products to manufacture are screened by optimizing the overall atom balance of the EIP design system. Product screening is followed by optimizing a preliminary superstructure that screens Tenants as well as determines the flowrates of significant chemical species transferred between plants. These techniques are presented as flexible frameworks where the objective function being optimized could include considerations for economics, safety, pollution prevention and etc. The approach applied to the case study in Chapter II considered economics in the objective functions and constraints with an emissions limit placed on carbon dioxide. The demonstration of the approach on the case study indicates

the potential interaction between EIP participants as examples of synergism and competition being present. The case study results also showed the potential profitability of lower capacity Tenants as their raw material costs are substantially lower when compared to their unintegrated counterparts.

It is also significant to consider the energy throughput characteristics of each plant participating in the EIP as additional interactions could be accounted for. The approach in Chapter III expands the approach from Chapter II by including energy integration techniques to screen tenants subsequent to the screening performed by mass integration techniques. This approach extension recognizes that there are opportunities to convert Tenant high grade heat into profitable electricity. This extension establishes the heat exchanger networks for the screened Tenants such that high grade hot streams are extracted without compromising the extent of heat integration for the said Tenants. These hot streams along with the residual hot and cold streams are applied in an interplant energy integration technique to determine the allocation of heat in an interplant heat exchanger network and the sizing of a trigeneration facility that provides electricity, steam and refrigeration. The case study from Chapter II is extended to demonstrate the application of this approach extension. The results of the case study elucidate additional areas for EIP participant interaction as well as increased economic and sustainable benefits.

This work has generated new ideas of interest to pursue for further investigation. Chapter III elucidates the deficiencies of the proposed approach when it comes to evaluating the fit of Tenants in an EIP when the Tenants rely heavily on energy for their operation. These Tenants may be excluded from the mass integration section of the

approach but would serve as a good fit in situations where there is a bountiful source of waste energy. One research direction to approach this is to modify the approach such that energy targeting is conducted first, followed by mass targeting. The emissions determined from the energy targeting could be used as an input for the subsequent mass targeting. Another direction could be the development of a process systems engineering technique that addresses the screening of tenants via simultaneous mass and energy targeting. This technique should also consider the option to use byproduct and waste material streams as a fuel gas to supply energy to EIP participants. Likewise, burning fuel gas results in carbon dioxide as a waste product which should also be considered.

The question of EIP participant reliability is also significant to the formation of the EIP complex. What participating plants in the EIP will experience adverse economic effects if another EIP participant shuts down for maintenance? In light of these situations, would it make economic sense to retrofit the participating plant or EIP to provide a material stream that the plant in shutdown would otherwise provide? Could flexibility be enabled through the invitation of additional tenants that provides key byproduct material streams that other EIP participants can use to continue operation?

These questions could be addressed through the development of a mass targeting technique that considers the reliability of each plant via the on-stream factor. The mass targeting superstructure of the SSRS technique could be complemented with a targeting formulation for developing a gantt chart. Certain tenants could be invited to enable better EIP operation flexibility by taking this approach. Possible tenants may be a process that provides a single byproduct stream or processes that can provide different byproducts

depending on its mode of operation. An example of the latter is an ethane steam cracker which could maximize its production of ethylene or maximize the generation of byproducts such as propylene and butadiene. Any excess byproduct hydrocarbons not utilized in park operation could be delivered to a furnace to generate steam in order to generate an energy credit for the material source plant.

An analog to the iterative heat integration procedure in Chapter III that addresses the selection of material sinks of tenants to participate in the mass integration could be developed. Heuristic rules assessing the cost/benefit of including given material sink from a plant could be used to determine that sinks participation in the subsequent mass integration. The consideration of material sinks rather than material source is significant as not meeting the requirements of the sinks will have negative effects on the participating plants on-stream factor and economic performance. The intent on reserving material sinks is to improve sustainable outcomes from sharing byproduct and waste streams while maintaining a given on-stream factor or economic performance.

Lastly, it may be of interest to extend the application of fundamental chemical processing information in Chapter II to include energetic phenomena such as the heats of reaction. It is recognized as the heat of reaction is not an accurate indicator of the energy characteristic of a plant. However, this could be used as a high-level method to screen possible tenants to invite into the EIP. This method could also be used to screen potential reactor combinations to generate novel intensified processes. Smaller process system scales would be of interest to determine synergistic mass and energy phenomena between reactions to identify novel chemical processes to investigate further in detail.